FIELD SWCC MODELING AND SOIL WATER STORAGE EVALUATION THROUGH GEOPHYSICAL TESTING

By

LINKAN SARKER

Presented to the Faculty of the Graduate School of

The University of Texas at Arlington in Partial Fulfillment

of the Requirements

for the Degree of

MASTER OF SCIENCE IN

CIVIL ENGINEERING

THE UNIVERSITY OF TEXAS AT ARLINGTON

DECEMBER 2018

Acknowledgements

First, I would like to express my sincere gratitude to my advisor, Dr. Sahadat Hossain, for continuously providing me inspiration, assistance and guidance throughout my research works. Dr. Hossain has been a true mentor, and his patience and constructive comments have helped me to become a better researcher. The completion of this work would not have been possible without his continuous guidance, valuable suggestions and ever-present encouragement.

I would like to express my gratitude to Dr. Xinbao Yu and Dr. Nur Yazdani for sharing their precious time and valuable suggestions, and for participating as members of my committee.

I wish to acknowledge the City of Denton, Texas Municipal Solid Waste (MSW) Landfill authority for their assistance in sample collection, field instrumentation and field investigation throughout the study period.

I would further like to extend my sincere appreciation to my colleagues and friends for their constant cooperation and assistance throughout my graduate studies. Special thanks to Dr. Jobair Bin Alam, Dr. Asif Ahmed, Rakib Ahmed, Sangeeta Bhattacharjee and Farnaz Seraj for continuously supporting me in my research.

Infinite gratitude goes to my family - my parents, siblings for their endless support and encouragement. My mother has been a constant source of inspiration to me; everything I am today, I owe it to her.

December 04, 2018

Abstract

FIELD SWCC MODELING AND SOIL WATER STORAGE EVALUATION THROUGH GEOPHYSICAL TESTING

Linkan Sarker

The University of Texas at Arlington, 2018

Supervising Professor: MD. Sahadat Hossain

Evapotranspiration (ET) landfill cover is an emerging final cover system and offers several benefits over conventional landfill closure system. It is a cost-effective green solution for the sustainability of a landfill as its performance enhances with time compared to the conventional solution where low hydraulic conductivity soil barrier deteriorates with time. ET cover system relies on the water store-release principle and its performance depends on the site-specific factors such as on-site climatological conditions, soil hydraulic properties and native vegetation. To effectively monitor the performance of this type of cover system, its unsaturated behavior, field capacity, available moisture for plant growth, soil water storage (SWS) and moisture retention capacity need to be assessed in a continuous manner. In previous studies, those monitoring parameters were observed through installed sensors and data logger system. But the main disadvantages associated with those sensors, are, they damage with time and exhibit poor performance in the long run which demands replacement of the sensors after a certain time. In this study, electrical resistivity imaging (ERI) technique was employed as an alternative tool to measure the unsaturated behavior of the ET cover system.

The study was conducted on test section ET cover (Lysimeter) on different types of vegetation in the City of Denton landfill. Three types of vegetated soil; covering Native trail grass, Switchgrass and Bermuda grass, were considered for the current study. Moisture content and matric suction of the cover soil were measured by installed sensors in the lysimeter at different depths. ERI

test was performed in the field at regular interval across the positions of the sensors. Based on the field instrumentation and geophysical measurement, the change in electrical resistivity with moisture content and matric suction was investigated at two different depths (12-inch and 30-inch) from the surface. The results indicated a significant relationship between soil resistivity and field unsaturated soil behavior. Field capacity, permanent wilting point and plant available water were also estimated from ERI technique.

Average SWS was determined simultaneously from the installed sensors during the ERI test. Unit cross sectional area resistance (ρ_a) was introduced and concurrent values were extracted from the obtained resistivity profile. An inverse relationship between SWS and ρ_a was observed. Existing soil moisture retention capacity (ESMRC) was also observed in terms of ρ_a. Average SWS and ESMRC were analyzed for three different assumed thicknesses of ET cover soil (4 ft, 3.5 ft and 3 ft) which showed that with decreasing ET cover thickness, its moisture holding capacity also decreases.

The field investigation results showed the ERI technique to be a potential non-destructive geophysical method to quantify and evaluate the field unsaturated behavior of ET cover and hence, it is an effective alternative way to monitor the ET cover performance.

Table of Contents

List of Illustrations

List of Tables

Chapter 1

Introduction

1.1 Background

The primary purpose of a landfill final closure system is to isolate the municipal solid waste (MSW) from the environment and restrict the entrance of water into the waste underlying it. The conventional method for waste confinement involves the use of low hydraulic conductivity soil barrier which is prone to deteriorate with time due to the change in the environmental condition thus reduction in the cover performance (Dwyer 2000; Hauser et al. 2001). Evapotranspiration (ET) cover system is a cost-effective green solution for the long-term viability of any landfill as its performance improves with time (Albright et al. 2004; Hauser 2009; EPA 2003; Benson et al. 2001; ITRC 2003). This type of cover system relies on the water store-release principle and has greater potential for long-term successful performance comparative to traditional final cover performance (Benson et al. 2002).

Performance of ET cover largely depends on the hydrologic behavior of the soil. One of the major purposes of the ET cover system is to store precipitation and minimize percolation which is the drainage of the stored water from the bottom of the cover into the underlying waste mass. Thus, percolation is one of the major performance indicators of any ET cover system. Hydraulic characteristics of cover soil such as hydraulic conductivity, soil water characteristic curve (SWCC) and soil water storage (SWS) capacity affect percolation significantly (Khire et al. 1997; Ogorzalek et al. 2008; Bohnhoff et al. 2009). Since the final cover is exposed to the environment, the hydraulic properties of the soil change substantially due to the natural wet-dry cycling and freeze-thaw effect (Chamberlain and Gow 1979, Beven and Germann 1982, Suter et al. 1993, Albrecht and Benson 2001). Therefore, continuous monitoring of soil moisture-suction behavior (SWCC) and soil water storage (SWS) is essential to preserve the consistency of the ET cover system, thus maintain the long-term successful performance.

1.2 Problem Statement

Typical methods available for performance monitoring and evaluation of ET cover are drainage lysimeter and soil moisture monitoring devices such as capacitance sensors, thermal dissipation sensors, psychrometers, tensiometers, and time domain reflectometer (USEPA 2011). In the Alternative Cover Assessment Program (ACAP), time domain reflectometry (TDR) probes (Campbell Scientific Inc, Model 615) (Campbell and Anderson, 1998) and thermal dissipation sensors (Campbell Scientific Inc, Model 229) (Phene et al., 1992) were utilized to measure the soil moisture and matric potential in the sites. Alam et al. (2017) compared the percolation rate of flat and slope section lysimeter using moisture and temperature sensors and tensiometers from Decagon devices. Fredlund also developed thermal conductivity sensors to predict the field SWCC (Fredlund 2004). DeVries (2016) monitored the water balance cover performance using moisture and temperature sensors and tensiometers. However, the existing methods available to monitor the unsaturated behavior of field scale lysimeter equipped with instrumentation provide discrete information. These methods are unable to provide an accurate spatial or depth-wise variation of unsaturated soil characteristics. Moreover, sensors installation is expensive and sometimes they are not durable enough to last ET cover design life.

1.3 Research Objectives

The overall objective of the current study is to evaluate the efficacy of the ERI technique to determine the unsaturated behavior of the ET cover soil. In order to accomplish this objective, following tasks were undertaken:

- Selection of the study area.
- Soil Characterization.
- ET cover performance analysis through installed sensors.
- ET cover performance analysis through ERI technique.
- Statistical analysis of the unsaturated soil parameters.

1.4 Thesis Organizations

The thesis is divided into five chapters that can be summarized as follows:

- Chapter 1 provides a background for the current study, identification of the related problems and corresponding research objectives to address the problems.
- Chapter 2 presents the literature review on the unsaturated behavior of the ET cover system and the changes of related unsaturated parameters with changing electrical properties of the soil. It contains description of the unsaturated soil behavior, previous methods to evaluate unsaturated soil properties, previous studies on ERI technique and finally the advantages of ERI technique over conventional methods to address the ET cover performance.
- Chapter 3 describes the research methodologies of the study including the selection of the study area, characterization of the in-situ soil, field monitoring and geophysical investigation of the instrumented study area, selection of a statistical software and procedures to establish best fitted relations among soil electrical properties and unsaturated soil parameters.
- Chapter 4 presents the results obtained from the laboratory tests and statistical observations of the ERI technique to measure field unsaturated soil behavior.
- Chapter 5 summarizes the results obtained from the field observations and statistical determinations. It also includes the conclusions drawn from the obtained results and future aspects of the current study.

Chapter 2

Literature Review

2.1 Landfill Evapotranspiration (ET) Cover

The primary purpose of a landfill final cover system is to isolate the underlying Municipal Solid Waste (MSW) from the surrounding environmental exposure and to minimize the amount of leachate generation by restricting the water percolation through the waste in addition with controlling fugitive gas emissions. In a conventional landfill, final cover, there are several layers consisting of compacted clays with low saturated hydraulic conductivity, geomembrane overlain by a drainage layer and a topsoil layer to fulfil the final cover requirements per Texas Commission on Environmental Quality (TCEQ) regulatory guidance 2017. But evapotranspiration (ET) cover is an updated landfill final cover system (EPA 2003; Benson et al. 2005; ITRC 2003) which provides a cost-effective green solution for the long-term performance of landfill final cover system and has certain advantages over traditional landfill final cover system. In addition, with the traditional final cover features, ET cover has a vegetative top soil layer underlying by a storage layer which acts as a sponge or a reservoir rather than a barrier (Zornberg et al. 2003) that functions to store precipitation during the rainfall season and release it into the environment during the dry period by means of evaporation from the top cover soil and transpiration from the vegetation. Thus, an ET cover generally follows a water balance concept meaning that the water enters the system will be balanced by the water that exits from the system which can be described by the following equation (Alam 2017).

$$P = R + S + P_r + E + T$$

Where, P = Precipitation; R = Surface Runoff; S = Soil Water storage (SWS); P_r = Percolation; E = Evaporation; T = Transpiration.

Rainfall, snowmelts and other irrigation applications are the forms of precipitation (P) whose magnitude and distribution significantly vary with time. Surface Runoff (R) is defined by

that portion of precipitation which does not infiltrate through the cover soil rather flows over the surface. Soil Water storage (SWS) is the volume of moisture that retains throughout the pore spaces of the cover soil and percolation (P_r) means the amount of precipitation that infiltrates into the cover soil. Again, the portion of precipitation which transforms into gaseous state from liquid phase due to atmospheric temperature variation and returns into the atmosphere is called Evaporation (E) which is also a function of relative humidity of the surrounding atmosphere. Transpiration (T) is related to surface vegetation and is defined by the process of moisture movement through plants from roots to small pores on the underside of leaves, where it changes to vapor and is released to the atmosphere which is basically a form of evaporation of water from plant leaves.

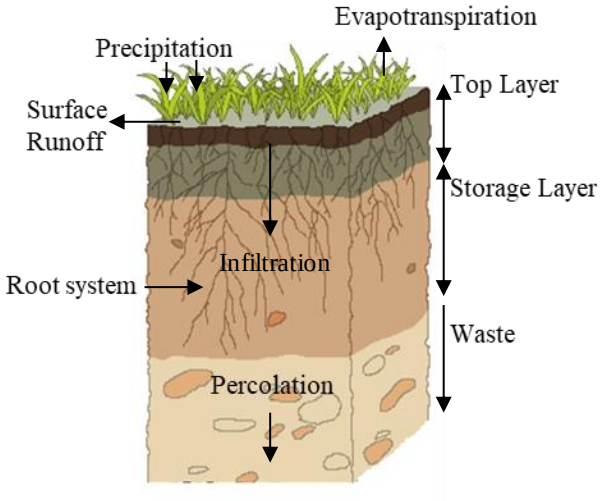

Figure 2.1 Different layers of ET cover with different water balance components

In a traditional landfill final cover system, geomembrane and compacted clay liner are usually used to prevent the percolation of water through it. But a certain amount of moisture is needed to be maintained throughout the whole solid waste mass underneath the final cover to accelerate the degradation process and to produce maximum amount of gas in a shorter period. To assist on this phenomenon, a landfill ET cover system functions to minimize the percolation but not

to stop it completely in an engineered way that helps maintaining proper moisture distribution throughout the waste mass and attaining maximum gas generation in an earliest possible time. Therefore, in advance with the traditional resistive barrier, an ET cover has some additional monitoring features like evapotranspiration and soil water storage that are needed to be assessed for proper performance analysis of an ET cover (Zornberg et al. 2003).

2.2 Unsaturated Behavior of Evapotranspiration (ET) Cover Soil

Soil particles have intergranular voids in between and those spaces are filled with air and water. At a complete dry state, those intergranular voids are only filled with air but when the soils are fully saturated, those air voids are completely replaced by water. When partial saturation or unsaturation condition exists, both air and water will be present in the scenario. In case of landfill ET cover soil, it remains unsaturated for most of the time in a year. For performance monitoring of an unsaturated cover soil, its water retention properties, matric suction, soil water storage capacity, surrounding weather, vegetation types and hydraulic conductivity need to be assessed in a continuous manner (Zornberg et al. 2003).

2.2.1 Soil Suction

The pressure of groundwater that is held in gaps between the soil or rock particles is termed as pore water pressure. Porewater pressure is positive below the phreatic level of groundwater which indicates the soil zone to be saturated, but it shows negative value above the saturation line specifying unsaturated soil zone. This negative value of porewater pressure is usually called soil suction. It happens due to the combination of several forces like molecular, physical-chemical forces acting at the boundary between the soil particles and the water, evaporation and transpiration acting at and close to the surface and so on which cause the water to be drawn into the upward empty void space. If the water contained in the voids of a soil was subjected to no other force than that due to gravity, the soil above the water table would be completely dry causing zero suction. Soil suction can be described by capillary tube pressure concept provided by Albright et al. (2004).

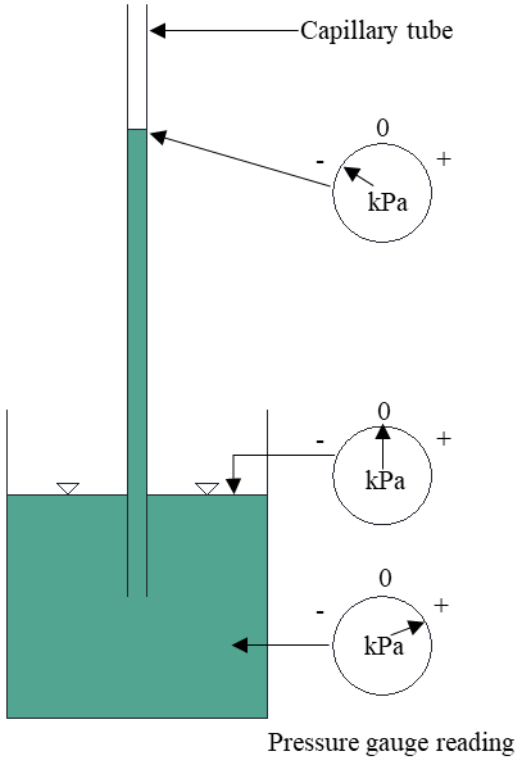

Figure 2.2 Soil Suction Concept (Albright et al. 2004)

Figure Figure 2.2.2 illustrates the soil suction (also known as capillary rise) concept with the water pressure in a capillary tube where the rise of water in the capillary tube above the free water surface indicates the negative pressure or suction head. Pressure at the phreatic level is zero and positive below that level. Suction stress (ψ) is a function of radius (r) of the capillary tube which can be expressed by the following equation.

$$\psi = \frac{2\sigma \cos \beta}{r}$$

Where, σ is the surface tension between the water perimeter and capillary tube material and β is the angle of contact. Similarly, for the unsaturated soil, its intergranular void spaces act as capillary tubes and water is retained in the soil pores due to the action of capillary forces which

develop suction in the soil. In landfill ET cover or water balance cover, these capillary forces are the adsorptive forces between the water molecules and the surface of the solid particles which contribute to retaining water in the unsaturated soil. Thus, soil suction is a function of volumetric water content (θ) and is inversely proportional to it as with the increase of moisture content, the related gravimetric forces become large enough to overcome the capillary forces resulting the decrease in soil suction. Therefore, soil suction has been a prime concern while designing a water balance cover or ET cover system.

2.2.2 Soil Water Storage (SWS)

Soil water storage is defined as the equivalent depth of water stored in a certain soil depth. One of the primary purposes of an ET cover system is to store maximum amount of moisture in its soil body and minimize the percolation. Thus, continuous monitoring of the ET cover SWS is necessary for its performance analysis. Again, soil water storage capacity is another term which refers to the maximum amount of water that a soil can hold without having any percolation. SWS can be explained by the sponge concept (shown in Figure 2.3) given by Albright et al. (2009). Soil acts like a sponge material that can absorb and release water. There are voids in between the soil particles which are filled with air at completely dry condition. When water enters the soil body, those air voids are replaced by that water. Thus, the soil body drives into unsaturated condition from completely dry condition. Due to the gravity force acting on the water mass, water particles try to drain away from the soil body. Soil suction created among the soil particles attempts to restrain that water mass from draining away from the soil.

However, water can be stored in the soil body up to a certain amount corresponding to a limiting soil suction depending on the soil texture. That limiting point of soil suction refers to the SWS capacity beyond which water will try to percolate from the bottom of the soil body. The primary purpose of any landfill final cover system is to restrict the precipitation from turning into percolation. In order to achieve this objective, ET cover system follows water store release principal

to limit the percolation to an acceptable limit. Again, for an advanced ET cover system over a bioreactor landfill, moisture recirculation in a certain interval is proved to be a supportive factor to expedite the MSW degradation underneath (Alam, 2016). Thus, for performance analysis of an advanced ET cover system, continuous monitoring of SWS is obligatory.

Figure 2.3 Schematic illustration of sponge concept for soil water storage (Albright et al., 2009)

2.2.3 Soil Moisture Retention Capacity (SMRC)

Soil moisture retention capacity is one of the most significant performance indicators for landfill ET cover soil as it gives the idea about how much the soil can store the precipitation and minimize the percolation through the bottom of the cover. Moisture retention in unsaturated soil can be explained by the following Campbell's equation (Campbell 1974).

$$h = a\left(\frac{\theta}{\theta_s}\right)^{-b}$$

Where, h = suction head; θ = volumetric moisture content; θ_s = saturated volumetric water content; a and b are constants. Soil moisture retention capacity mainly depends on the grain size distribution and organic matter content of the soil (Gupta et al. 1979). Soil with fine particles has higher moisture retention capacity compared to soil with granular particles.

Field capacity (FC) is another term which refers to the SMRC and typically measured by the amount of SWS at 33 kPa soil suction. If the water entering the soil body exceeds its FC, the excess amount of water will be drained away in the form of percolation. Permanent wilting point (PWP) refers to the minimal amount of SWS that is needed by the plant not to wilt. If the SWS up to the plant root zone goes below that point, plants in the surface zone will die. Conventionally, PWP is measured by the SWS at 1500 kPa soil suction. However, the corresponding value of the soil suction changes with the fluctuations in the surrounding environment and soil texture. A schematic diagram is shown in the following figure to illustrate the FC and PWP concept.

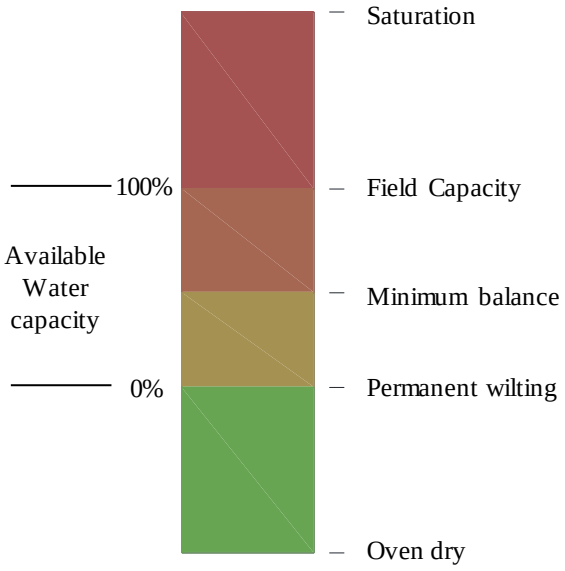

Figure 2.4 Schematic illustration of field capacity and wilting point

2.2.3.1 Effect of Vegetation on SMRC

Surface vegetation plays a significant role in the evaluation of SMRC. In vegetated soil, the root system of plants removes the additional water via the transpiration process under ambient temperature and surrounding humidity until PWP is reached. Evaporative demand is a term defined by the measure of the extent to which the environment continues striving to evaporate water. SWS

below PWP plant can no longer maintain its cell turgidity against evaporative demand created by the surrounding atmosphere. Plant available water (PAW) refers to the amount of water that plant can release to the atmosphere in the form of transpiration. It is the difference between FC and PWP. Again, the root distribution in the soil creates void spaces between the soil particles which can store an additional amount of precipitation. If the evaporative demand is high and the soil is comparatively less permeable, the surface vegetation can release a significant amount of water to the environment before percolation occurs. Thus, surface vegetation has a positive effect on the SMRC.

2.2.4 Soil Water Characteristics Curve (SWCC)

Soil-water characteristic curve (SWCC) plays an important role in the assessment of unsaturated soil property functions (Fredlund 2002). Previously, Williams (1982) defined SWCC for a soil as the relationship between water content and suction for the soil and it shows different trends corresponding to different grain size distributions. Figure 2.5 illustrates the concept of SWCC in terms of capillary rise over a phreatic surface. At low moisture content, suction head or negative pore water pressure is higher compared to the suction head at high moisture content. Thus, the soil with high void ratio generates low suction head compared to any dense soil.

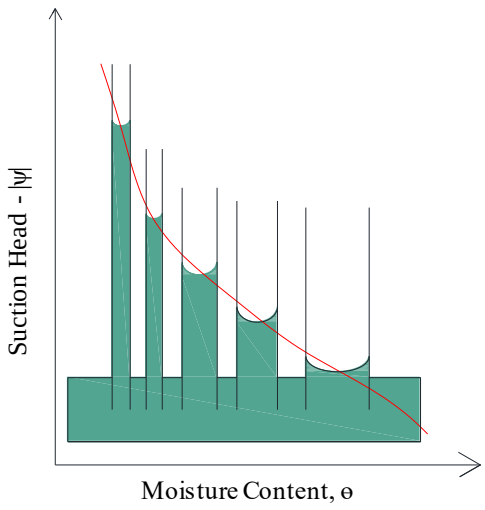

Figure 2.5 Variation of suction head with different pore size distribution (Alam, 2017)

Moisture content is the key element for any SWCC and can be expressed in various ways shown on the following.

Gravimetric Moisture Content

Gravimetric moisture content is defined by the mass of water (m_w) in the soil volume divided by the mass of soil solids (m_s).

$$w = \frac{m_w}{m_s}$$

Volumetric Moisture Content (VMC)

Volumetric moisture content is defined by the volume of water (V_w) over any soil volume (V).

$$\theta = \frac{V_w}{V_s + V_v}$$

Where, Soil Volume, V = Volume of Soil Solid (V_s) + Volume of Void (V_v)

Normalized Moisture Content on Volumetric Basis

Normalized moisture content (Θ_d) establishes relationship between initial saturated moisture content and residual moisture content and is defined by the following relation.

$$\Theta_{dv} = \frac{\theta - \theta_r}{\theta_s - \theta_r}$$

Where, Θ_{dv} = Volumetric normalized moisture content, θs = saturated volumetric moisture content and θr = residual volumetric moisture content.

Normalized Moisture Content on Gravimetric Basis

Normalized moisture content can also be expressed in terms of gravimetric moisture content in the following way.

$$\Theta_{dg} = \frac{w - w_r}{w_s - w_r}$$

Where, Θ_{dg} = Gravimetric normalized moisture content, w_s = saturated gravimetric moisture content and w_r = residual gravimetric moisture content.

Residual Moisture Content

Residual moisture content is defined by the water content where a large suction change is required to remove additional water from the soil. Fredlund (2002) developed a consistent way to define the residual water content shown on Figure 2.6.

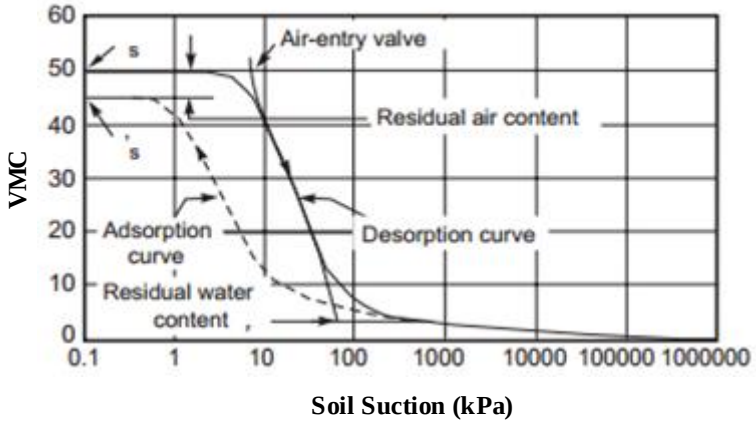

Figure 2.6 Typical Soil Water Characteristics curve for silty soil (Fredlund, 2002)

Fredlund experimented on silty soil in laboratory setup and observed it unsaturated behavior. It was found that volumetric moisture content (VMC) is subjected to a sharp decrease after the air entry suction up to a certain point where soil suction is substantially high. After that high suction point is reached, the slope of the curve gets reduced and no significant amount of change in VMC is observed with increasing suction, therefore, an inflection point is initiated. A tangent line is drawn from the inflection point. The curve in the high suction range can be approximated by another line. The residual water content θ_r can be approximated as the ordinate of the point at which the two lines intersect.

Previously numerous empirical equations have been developed to simulate the SWCC. Brooks and Corey (1964) proposed the following equation in the form of power-law relationship:

$$\Theta = \left(\frac{\psi_b}{\psi}\right)^{\lambda}$$

Where, Θ is the normalized water content, ψ_b is the air-entry suction, ψ is suction and λ is pore size distribution parameter. Another term, effective degree of saturation (S_e) has also been used in place of the normalized water content which is defined by the following equation.

$$S_e = \frac{S - S_r}{1 - S_r}$$

Where, S = degree of saturation and S_r = residual saturation.

Van Genuchten (1980) established a most functional relationship between normalized water content and suction which is given by the following equation.

$$\Theta = \left[\frac{1}{1 + (\alpha\psi)^n}\right]^m$$

Where, α, n and m are Van Genuchten fitting parameters and m = 1-(1/n). In some cases, more accurate results can be obtained by leaving m and n parameters with no fixed relationship (Fredlund et al., 1994).

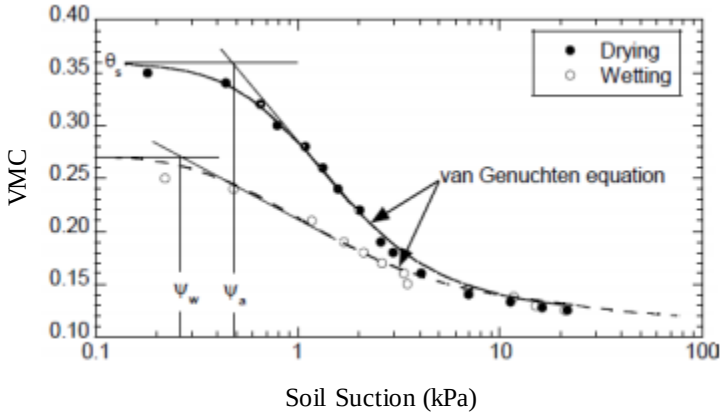

Figure 2.7 Drying and Wetting phase of SWCC showing fit to Van Genuchten equation (Fredlund et al., 1994)

Fredlund et al. (1994) also proposed an equation to predict the volumetric water content (θ) as a function of matric suction and three fitting parameters which is shown below.

$$\theta(\psi, a, n, m) = C(\psi)\left[\frac{\theta_s}{\left\{\ln\left[e + \left(\psi/a\right)^n\right]\right\}^m}\right]$$

Where, C(ψ) is a correction factor defined as

$$C(\psi) = \frac{\ln(1 + \psi/\psi_r)}{\ln[1 + (10^6/\psi_r)]}$$

Where, ψ_r is the suction corresponding to the residual water content θ_r.

2.2.4.1 Factors Affecting SWCC

SWCC depends on several factors like grain size distribution, temperature, soil density, initial void ratio or volume change property of the soil, field stress history, wetting and drying phenomenon or hysteresis effect etc (Fredlund 2002). Capillary rise on the in-situ soil can be a measure of the in-situ soil suction. Smaller grain size results in high capillary rise which gives a high suction value in the field.

Soil water characteristics curve depends on the onsite stress history and wetting-drying phenomenon of the soil. There is a difference in soil suction with corresponding moisture content depending on the drying or wetting of the soil specimen. Plastic deformation of the soil also occurs during this wetting drying phenomenon which indicates a plastic settlement in the unsaturated soil. This wetting drying phenomenon of the soil over soil suction is called hysteresis and it has a significant effect on clay soils.

When soil sample is collected from the field, it is difficult to know whether the sample is on the drying path or wetting path. Slight changes in soil nature can cause a lateral shift in the SWCC which makes it extremely difficult to predict the in-situ soil suctions from the lab constructed SWCC. It has been found that the field soil suction is somewhere between the corresponding wetting and drying suctions found from the SWCC constructed in lab.

To measure the hysteresis effect on the clayey soil effectively, high suction value is required during the test. Fredlund et al. (2007) showed the hysteresis effect on clayey soil using

dew-point Water Potential Meter, WP4-T, and an air-tight chamber, ATC. Different saturated salt solutions with known osmotic suction were prepared and the suction value was measured using the WP4-T and it has been found that the theoretical value of soil suction and the measured suction using WP4-T are nearly similar.

According to Likos et al. (2003), total suction value depends on the relative humidity of the surrounding environment. The theoretical value of the soil suction with relative humidity is measured using the following Kelvin's equation (Sposito, 1981; Likos et al., 2003).

$$\Psi = -\frac{RT}{V_{wo}\omega_v} ln\left(\frac{u_v}{u_w}\right)$$

Where, Ψ = soil suction (kPa), R = universal gas constant (8.31432 $Jmol^{-1}K^{-1}$), T = absolute temperature in kelvin, V_{w0} = specific volume of water (kg/m^3), ω_v = molecular mass of the water vapor (18.016 kg/kmol), u_v/u_w = Relative humidity (RH).

2.2.4.2 Lab scale measurement of SWCC

Previously many researches have been done to predict the soil suction behavior with numerous variables like soil density, temperature, pre-consolidation pressure, degree of saturation, swelling-shrinkage potential, grain size distribution etc. In lab, SWCC has been developed by using Tempe pressure Cell and other pressure plate apparatus, Double walled triaxial cell, thermocouple psychrometer, filter paper etc. Fredlund used thermal conductivity sensors in both field and lab to predict the SWCC. Kong et al., (2017) used DZD-6 DC resistivity meter and 15 bar pressure plate extractors in lab to conduct electrical resistivity test on soil and developed SWCC based on ERI technique which is an indirect method of estimating SWCC.

Soil physics and agronomy disciplines have played a dominant role in the development of testing equipment and procedures for the SWCC. The testing method and procedures depend on the type of soil whether it is clay, silt or sand. In lab, SWCC can be established by using one of the following methods.

2.2.4.2.1 Tempe pressure cell apparatus

This type of testing is mainly useful for porous material like sand. It utilizes the axis-translation technique (Hilf 1956) and have a measuring range between 0 and 100 kPa (1 bar) depending on the ceramic disk placed in the device. The moisture characteristics of the field soil is readily and very accurately measured by weighing the complete cell at pressure equilibrium points.

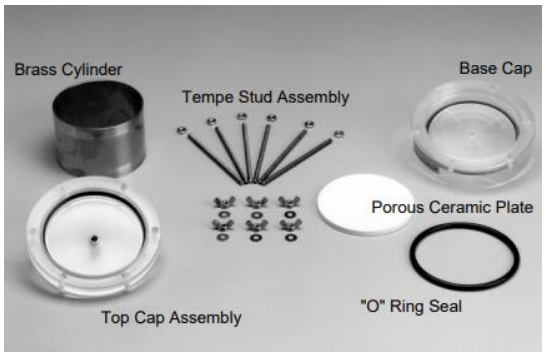

Figure 2.8 Different Parts of the Tempe Pressure Cell Apparatus

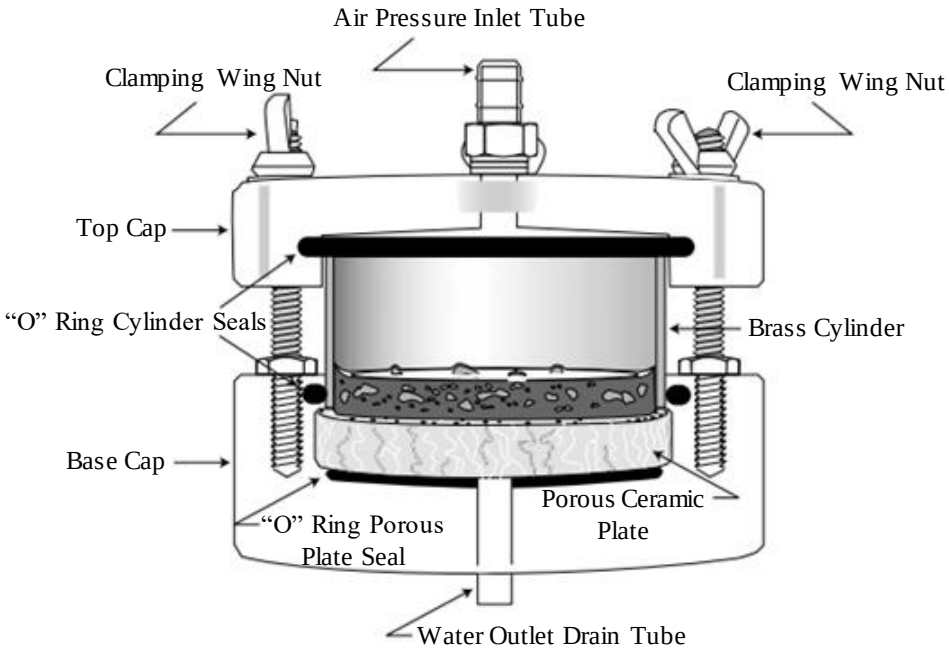

Figure 2.9 Setup of the Tempe Pressure Plate Apparatus (Soil Moisture Equipment Corp., 2003)

When soil samples are placed on the porous ceramic plate of the Tempe Cell and are saturated with water, and the air pressure inside the Tempe Cell is raised above atmospheric pressure, water will flow from around each of the soil particles and out through the pores of the Porous Ceramic Plate until the curvature of the water films at the junction of each of the soil particles is the same as in the pores of the porous ceramic plate and corresponds to the curvature associated with that pressure.

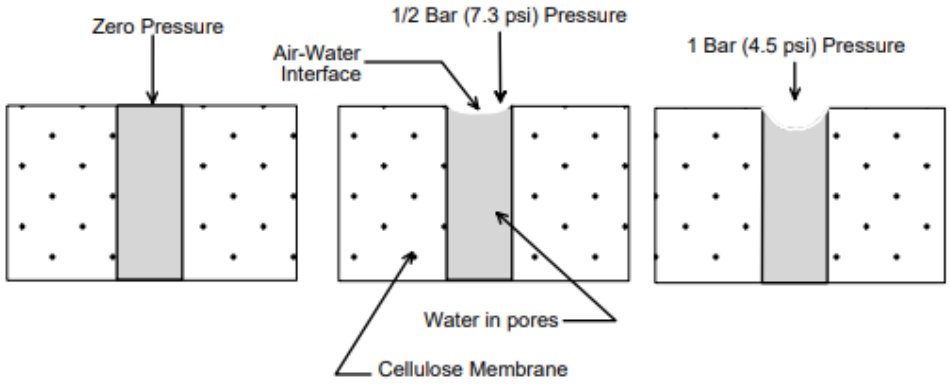

Figure 2.10 pore water curvature due to applied air pressure

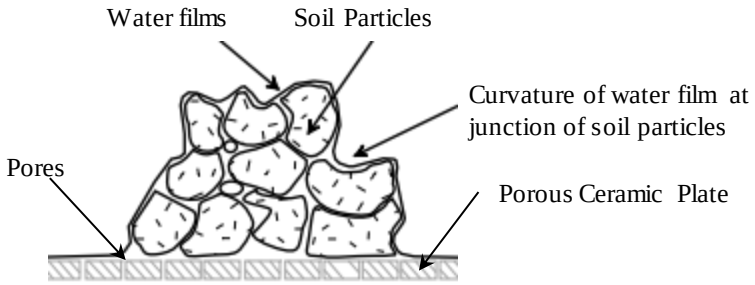

Figure 2.11 Curvature equilibrium of water film for the soil particles and porous ceramic plate

The bar value of the porous plate influences the flow of moisture and therefore the time required to reach equilibrium. Higher bar value indicates more required time for the system to reach equilibrium because of their relatively small pore size. Thus, it indicates high suction value for clay or silty clay soil compared to the sandy soil with larger intergranular void spaces.

2.2.4.2.2 Suction controlled double walled triaxial cell

Suction controlled double walled triaxial cell has been developed to measure small overall and pore water volume change with the control or measurement of small values of suction using axis translation technique and it shows good performance on unsaturated sand. It consists of a double walled triaxial cell, a modular loading frame including the axial power unit and a computer for controlling and data logging. The shear strength, hydraulic conductivity along with the SWCC of unsaturated soil can be determined using this device.

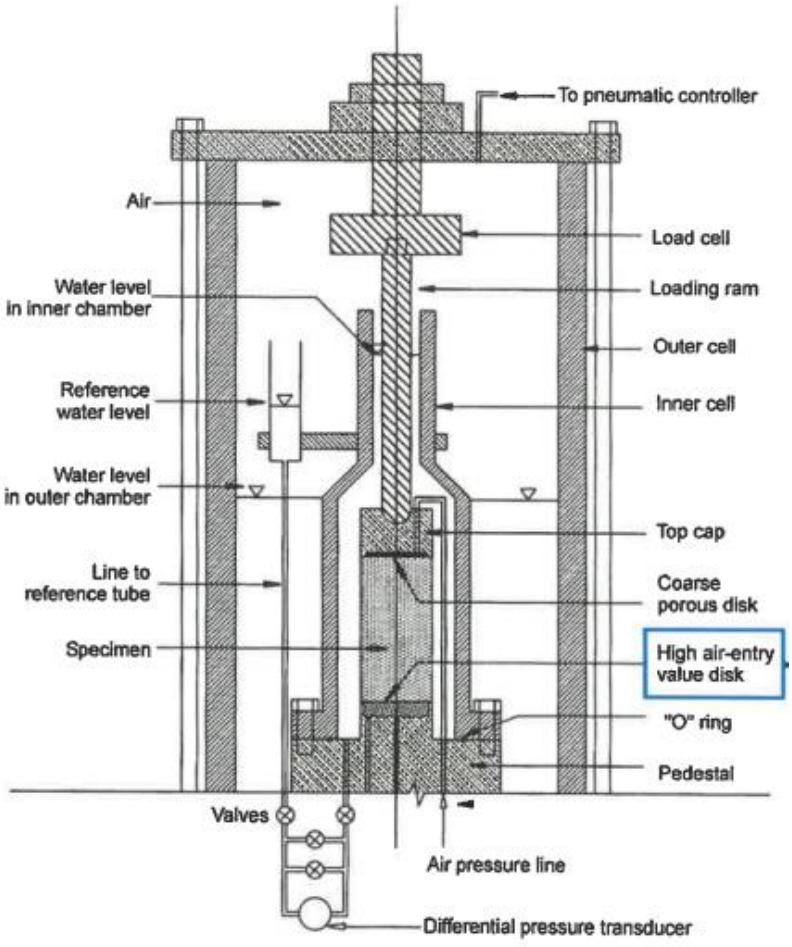

Figure 2.12 Experimental setup for the suction controlled double walled triaxial cell (Ng et al., 2002)

In this device air pressure is controlled to increase or decrease the suction value. The range of suction value that the device can measure depends on the properties of the air-entry value disk. Porous disk with high air entry value requires more time for equilibrium with the corresponding air pressure. This device can measure suction up to a range of 0 to 1500 kPa while 15 bars air- entry value disk is used.

2.2.4.2.3 Thermocouple psychrometer

The thermocouple psychrometer was first introduced by Spanner (1951). The device makes use of Peltier and Seebeck effects. The Peltier effect is a temperature drop induced by an electrical current passing across a junction made of two different metal wires, which is a function of relative humidity of vapor space where measurement is conducted (Figure 2.13).

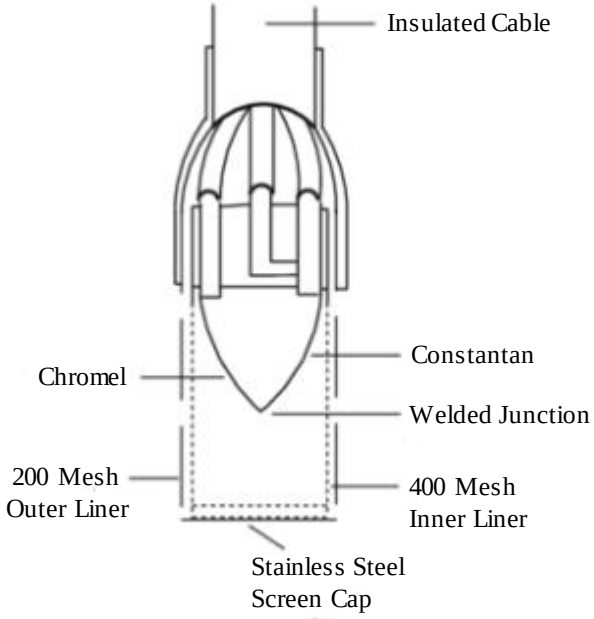

Figure 2.13 Schematic illustration of a thermocouple psychrometer (Fredlund et al., 1993)

2.2.4.2.4 Transistor psychrometer

The thermistor or transistor psychrometer was developed by Richards (1965). Transistor psychrometer consists of a thermally insulated container that holds the psychrometer probes and a

data logger for measurement and recording of output. The transistor psychrometer is an electronic wet and dry bulb thermometer in which a wet and dry transistor probe is used instead of wet and dry thermometer bulbs as in thermistor psychrometers. Evaporation takes place as both bulbs are exposed tovapor space in the soil, which results in an electromotive force being generated. The temperature depression of the wet transistor, which holds a standard-size water drop, is measured with the sensors in the probe. The wet and dry transistors are employed as heat sensors and the voltage output from the probe is used to infer total suction. Improvements in performance have been made that allow the device to measure a much wider range of total suction, from about 100 kPa to about 10,000 kPa. Much of the improvement is due to calibration procedure and advances in micro-chip technology (Woodburn et al.1993). The range and accuracy in measurements are also attributed to sensitivity of the transistors to changes in temperature. It has practically replaced thermocouple psychrometers in many laboratory soil suction measurements.

2.2.4.2.5 Chilled Mirror Hygrometers

A chilled-mirror hygrometer uses the chilled mirror dew point technique to infer total suction under isothermal conditions in a sealed container. Measurement of total suction with the chilled-mirror hygrometer is based on equilibrating the liquid phase of the water in a soil sample with the vapor phase of the water in the air space above the sample in a sealed chamber. The chilled-mirror hygrometer measures dew point and temperature of the headspace above the specimen. The specimen is contained in a special closed chamber to minimize drying of the specimen. Water vapor from the soil specimen is allowed to condense on the mirror and a photoelectric cell is used to detect the exact point at which condensation first appears on the mirror. The temperature of specimen which is considered to be equal to the temperature of vapor space is measured via an infrared thermocouple. The relative humidity or the water activity of the specimen is computed from the measured dew point and temperature. A small fan is also employed to circulate the air in the sensing chamber and speed up vapor equilibrium. The soil samples and device were kept at the same location

for at least several hours for temperature equilibrium prior to the testing. The chilled mirror technique offers a fundamental characterization of humidity in terms of the temperature at which vapor condenses. Temperature control is very important. The measured difference between dew point and sample temperatures must be kept small. It is important to avoid contamination of the instrument. Leong et al. (2003) reported that the technique could be used to quantify total suction as low as about 150 kPa.

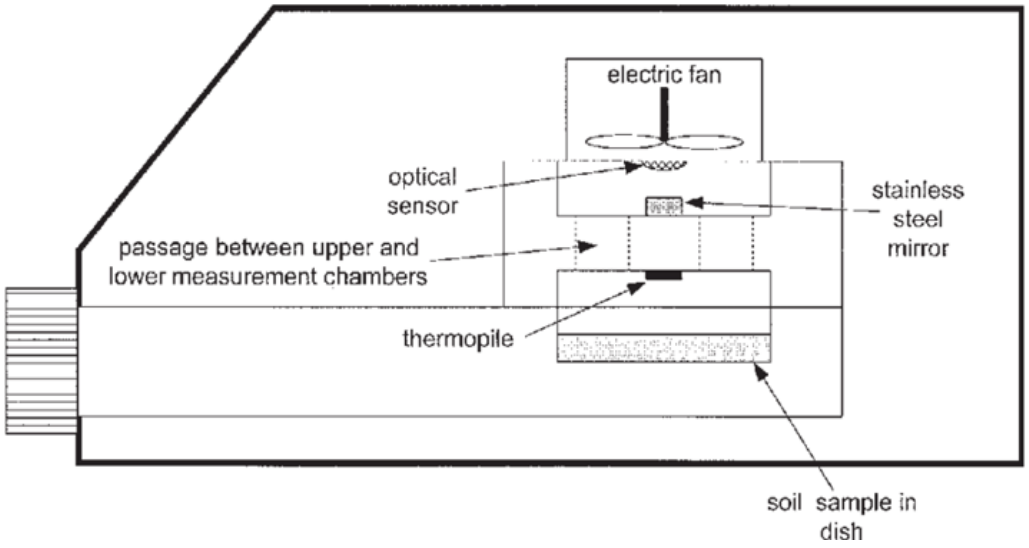

Figure 2.14 Schematic of Chilled Mirror Hygrometer (Albrecht et al., 2003)

2.2.4.2.6 Filter paper methods

The filter paper covers a wide range of suction measurements. For the non-contact technique, a dry filter paper was suspended above a soil specimen in a sealed container for water vapor equilibrium between the filter paper and the soil specimen at a constant temperature. The vapor space above the soil specimen acts as a true semi-permeable membrane which is only permeable to water vapor but not to ions from the pore-water. The separation between the filter paper and the soil by a vapor barrier limits water exchange to the vapor phase only and prevents solute movement. Therefore, in this technique, total suction is measured. Having achieved equilibrium condition, the filter paper is removed, and water content of the filter paper determined

as quickly as possible. Then, by using the appropriate filter paper calibration curve, the suction of the soil is estimated.

2.2.4.3 Field scale measurement of SWCC

Tensiometers, suction probe, thermal conductivity sensors etc. are more commonly used in the field for the direct measurement of the soil suction.

2.2.4.3.1 Tensiometer

Tensiometer is normally used for directly measuring the negative pore-water pressure of soil. The basic principle is that the pressure of water contained in a high air entry material will come to equilibrium with the soil water pressure making it possible to measure negative soil water pressures. Since a true semi-permeable membrane for soluble salts does not exist in tensiometer, the effect of osmotic component of suction is not measured. Thus, the measurement only provides the value of matric suction component in the soil. In a typical tensiometer, a small ceramic cup is attached to a tube filled with deaired water which is connected to a pressure measuring device.

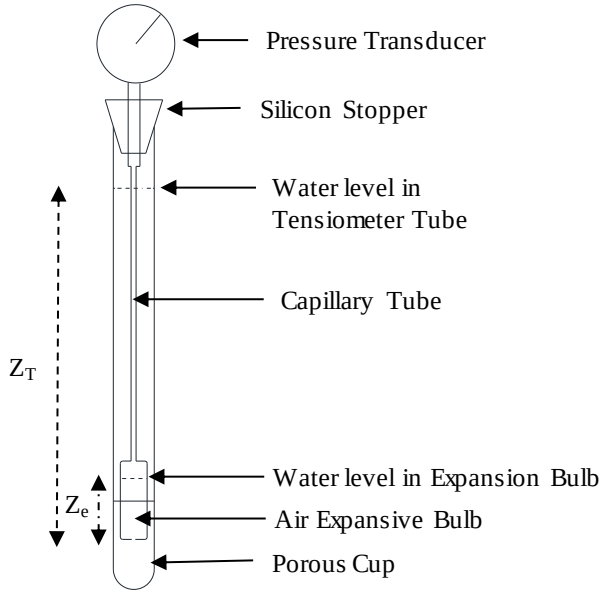

Figure 2.15 Schematic illustration of different components of tensiometer

Figure 2.15 illustrates the construction of a typical tensiometer. Saturation of the ceramic cup and tube is ensured by filling the cup with water and applying a vacuum to the tubing. The ceramic tip is allowed to dry to reduce the water pressure in the sensor and air bubbles are removed. Due to the cavitation problem, the use of a ceramic cup with a higher air entry value will not increase the measurement range of the tensiometer. However, improvements have been made to the tensiometer technique to enable measurements of matric suction greater than 100 kPa to be performed.

2.2.4.3.2 Thermal conductivity sensors

Fredlund (2004) developed a thermal conductivity sensor for both laboratory testing and field monitoring. It was digitally designed which proved to be accurate for all soil types and also unaffected by the effects of soil water salinity. As an updated version, it can also support solar panel system through which continuous power supply can be provided.

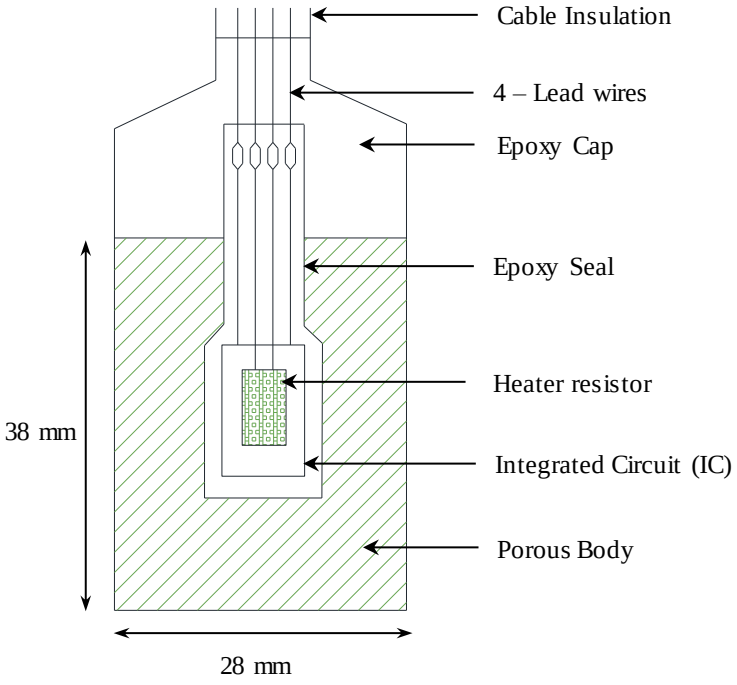

Figure 2.16 Thermal Conductivity Sensor (Fredlund, 2004)

Though the sensor performed well in many ways, however, several drawbacks were identified. One of the main drawbacks was the failure of the sensor in moist environment due to ceramic cracking leading to moisture penetration in the electronics. Again, sensitivity of the readings depends on the surrounding temperature gradient and length of the cable used in the setup. Later the equipment was further developed using moisture barrier around the electronics which solved the cracking and moisture penetration problem. Also, implementation of the state-of-the-art digital signals in the design increased the sensitivity of the data reducing the effect of surrounding temperature.

The digital temperature sensor has a resolution of 0.004^{o} C which contributes to the accuracy of the suction measurements even in the low ranges. The maximum possible accuracy of suction measurements is less than 0.2 kPa in the lowest range of 1-10 kPa, less than 0.5 kPa for 10-100 kPa and less than 6 kPa for the range of 100-1000 kPa. That means it can give the possible accurate measurements within the 5% of the measured suction. Tan et al. (2003) also implemented the idea of thermal conductivity sensors over a highway slope to address its performance in terms of unsaturated behavior.

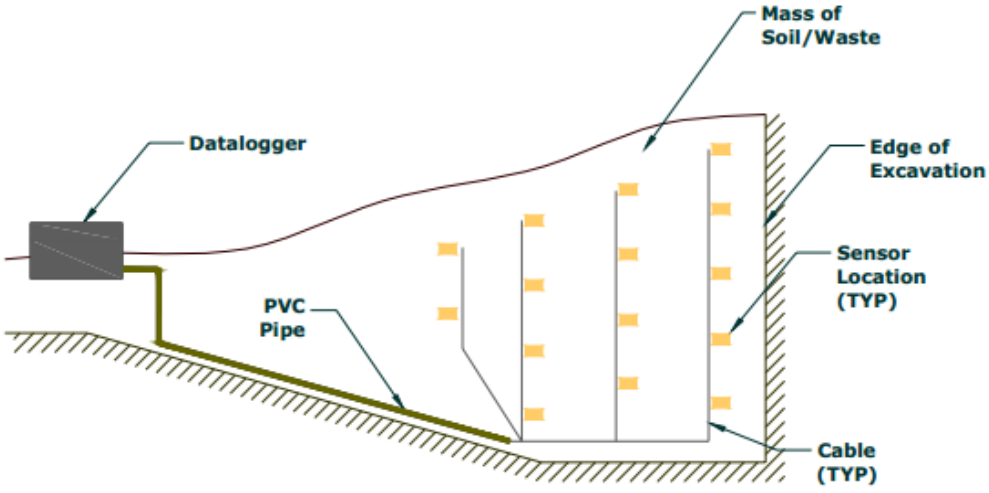

Figure 2.17 Layout of thermal conductivity sensors in the field (Tan et al., 2003)

Conventionally, the idea of field implementation of thermal conductivity sensors includes the installation of multiple sensors in unsaturated soil masses or waste piles by excavating trenches, installing the sensors on trench walls, running cables to the datalogger and backfilling the excavation simulating the preexisted condition. Typical layout of the sensors in the field are shown in Figure 2.17.

The datalogger should be housed in a weather proof enclosure where hardware and software must be available for monitoring the sensors. A temperature calibration curve should be predetermined in the laboratory. Sensors take the reading of the initial temperature by sending electrical current to the heating element for a specific period and records the peak temperature. The corresponding suction is then obtained by entering the calibration curve with the maximum temperature rise.

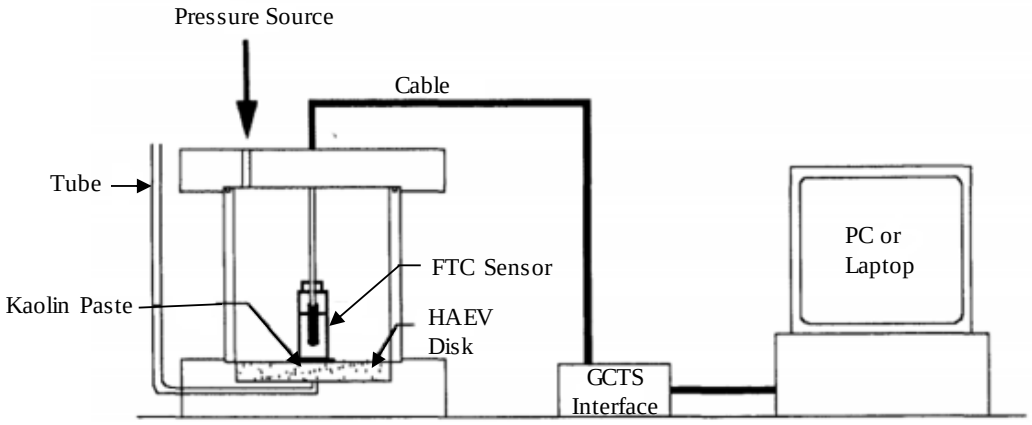

Figure 2.18 Temperature Calibration setup for Fredlund thermal conductivity sensors

2.3 Drawbacks of Different Soil Suction Measuring Methods

Several direct and indirect techniques were introduced in previous studies to measure the soil suction at both laboratory and field setup. However, the selection of the proper method depends on the required accuracy, time limitations and available range of the study area. Table 2.1 describes the constrains that each method generally faces.

Table 2.1: Principal Constraints for different suction measuring device (Perera et al. 2004)

Device	Method	Suction Measured	Range (kPa)	Principal constraints
Thermocouple psychrometers	Indirect (Relative Humidity)	Total	100 to 7500	Affected by temperature fluctuations and gradients. Sensitivity deteriorates with time.
Thermistor psychrometers	Indirect (Relative Humidity)	Total	100 to 10000	Poor sensitivity in the low suction range. Frequent re-calibration is required.
Transistor psychrometers	Indirect (Relative Humidity)	Total	100 to 71000	Frequent re-calibration is required. Specimens must be tested in order of increasing suction to avoid hysteresis.
Filter paper (non-contact)	Indirect (Water content)	Total	400 to 30000	Calibration is sensitive to the equilibration time.
Filter paper (in-contact)	Indirect (Water content)	Matric	Entire range	Automation of the procedure is difficult.
Pressure plate (Null Technique)	Direct	Matric	0 to 1500	Range of suction limited by the air-entry value of the plate (laboratory usage).
Standard tensiometer	Direct	Matric	0 to 90	Requires daily maintenance. Temperature fluctuations affect readings.
Osmotic tensiometer	Direct	Matric	0 to 1500	Reference pressure can deteriorate with time. Temperature dependent.
Imperial College tensiometers	Direct	Matric	0 to 1800	Range in suction is limited by the air-entry value of the ceramic. Cavitation problems with time.
Porous block (Gypsum, nylon, fiberglass)	Indirect (Electrical resistance)	Matric	30 to 3000	Observations need to be corrected for temperature. Blocks are subjected to hysteresis and changes in calibration due to salt. Response to suction can be slow.
Original heat dissipation sensors	Indirect (Thermal conductivity)	Matric	0 to 1000+	High failure rate. Fragile ceramic.
Fredlund thermal conductivity sensors	Indirect (Thermal conductivity)	Matric	0 to 1500+	Range in suction is controlled by the pore size distribution of the ceramic.

Previously, Benson et al. (2004) used thermal dissipation sensors (Campbell Scientific Inc, Model 229) (Phene et al. 1992) for monitoring soil water matric potential in field for the assessment of field water balance of landfill final covers, Alam et al. (2017) used moisture content and temperature sensors with tensiometers at varying depth in ET cover soil to evaluate the soil water storage, Brett DeVries (2016) also used same kind of sensors for monitoring the hydraulic performance of ET cover systems. Fredlund also developed thermal conductivity sensors to predict the field SWCC (Fredlund, 2004). But the main drawbacks associated with those sensors are that they damage with time and for tensiometers, soil needs to be relatively wet for better operation and below freezing temperature they lose sensitivity. Again, air in the tensiometer sensor may result in bad or less negative measurements of the pore water pressure for the following reasons: a) water vaporizes as the soil water pressure approaches the vapor pressure of water at the ambient temperature; b) air in soil can diffuse through the ceramic material and c) air comes out of solution as the water pressures decrease (Pan et al. 2010).

2.4 Performance Monitoring of ET Cover Soil Using Electrical Resistivity Imaging (ERI)

Soil moisture has been a vital issue to predict the soil geotechnical properties, numerous researchers have developed various strategies and techniques with different equipment to measure the soil moisture and correlate it with different hydraulic and geotechnical properties of soil. Among those techniques, Electrical Resistivity imaging (ERI) has been a vital concept and easy method for depicting soil profiles and characteristics for the recent past few years. The main advantage of that test is that it is non-destructive and less time consuming.

2.4.1 Background of Electrical Resistivity Imaging (ERI)

The idea of electrical Resistivity or specific electrical resistance comes from the Ohm's law which states that the current through a conductor between two points is directly proportional to the voltage across the two points and it can be shown by the following equation.

$$I \propto \Delta V \; or \; I = \frac{\Delta V}{R}$$

Again, for a cylindrical soil section resistivity can be expressed as,

$$\rho = R\left(\frac{A}{L}\right)$$

Where, R = Resistance in ohms, ρ = Electrical Resistivity in ohm-m, A = Cross sectional area, L = Soil sample length, ΔV = Potential difference and I = Electrical Current.

Again, electrical conductivity is the measure of the amount of electrical current a material can carry which is reciprocal to the electrical resistivity.

$$Electrical\ Conductivity, C = \frac{1}{R}$$

For a homogeneous soil, electrical equipotential lines are hemispherical (Scollar et al., 1990; Kearey et al., 2002; Sharma, 1997; Reynolds, 1997) as shown in the following figure.

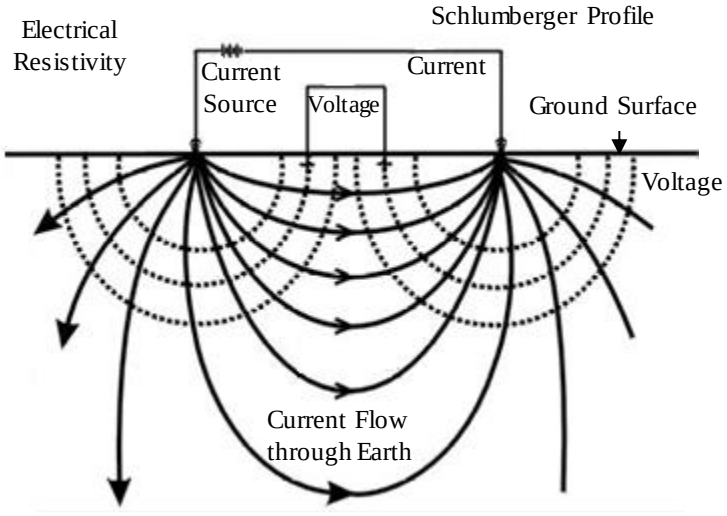

Figure 2.19 Distribution of current flow through homogeneous soil

Electrical resistivity survey basically measures the soil resistivity distribution of sounding in soil volume. Electric streams are supplied through electrodes to the soil underneath and subsequent potential contrasts are measured which gives the data on the type of subsurface heterogeneities and of their electrical properties. For unsaturated condition, clay soil has the affinity to store some moisture in itself because of its negative pore water pressure above the saturation zone

and low permeability whereas soil with greater particle size like sand is relatively dry. So electrical conductivity of clay soil will be higher than that of sandy soil. Thus, electrical resistivity survey helps to identify the grain size and soil type which can be a crucial indicator for selecting the location of boring and hence can become a dramatic breakthrough in foundation analysis and design field.

There are certain factors like soil salinity, clay content, cation exchange capacity, clay mineralogy, grain size distribution, moisture content and temperature upon which resistivity value depends and can be in different range as shown in Figure 2.20.

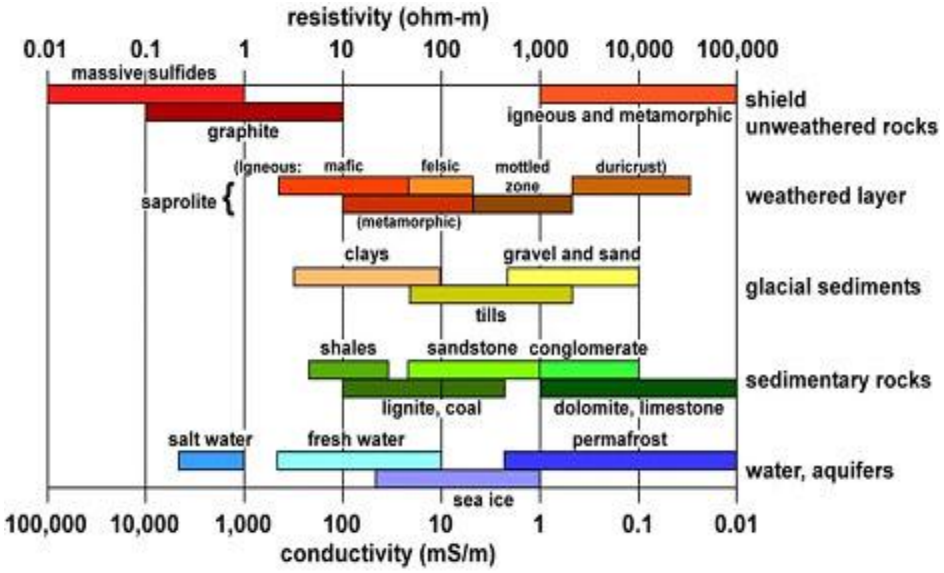

Figure 2.20 Different Values of resistivity with different types of soil (Ley-Cooper et al., 2015)

2.4.2 Field measurement of Soil resistivity

To investigate the sub-surface geology, electrical resistivity measurements have been being used since the early 20th century. Among several methods there are two methods named Wenner four pin method and Schlumberger method which have been widely used in case of field measurement of soil resistivity. Electrodes are hammered into the ground for a certain distance and relate to wires and resistivity measuring toolbox. The whole system is powered up by a battery and resistivity data are saved in the toolbox as shown in Figure 2.21.

Figure 2.21 Field measurement of soil resistivity

According to Wenner four pin method, the apparent soil resistivity value is,

$$\rho_E = \frac{4\pi a R_W}{1 + \frac{2a}{\sqrt{a^2 + 4b^2}} - \frac{a}{\sqrt{a^2 + b^2}}}$$

Where, ρ_E = measured apparent soil resistivity (ohm-m), a = Electrode spacing (m), b = depth of the electrodes (m), R_W = Wenner resistance measured as V/I according to the following figure.

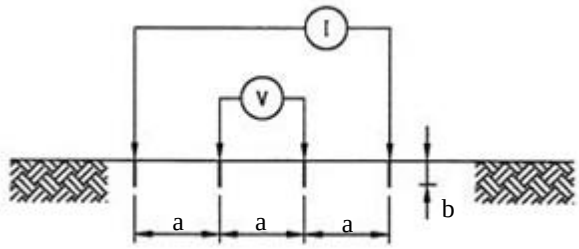

Figure 2.22 Wenner method for field soil resistivity test

According to Schlumberger method, if the distance between the voltages probe is a and the distances from voltages probe and currents probe are c as shown on the figure below and if b is small compared to a and c, and c>2a, the apparent soil resistivity value is,

$$\rho_E = \pi \frac{c(c+a)}{a} R_s$$

Where, ρ_E = measured apparent soil resistivity (ohm-m), a,c = Electrode spacing (m), b = depth of the electrodes (m), R_s = Schlumberger resistance measured as V/I according to the following figure.

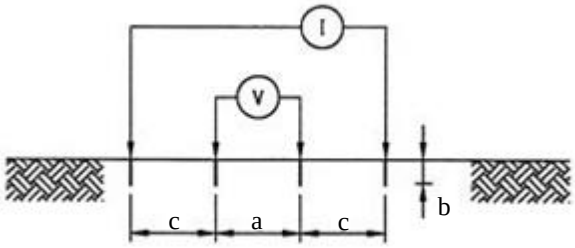

Figure 2.23 Schlumberger method for field soil resistivity test

2.4.3 Effect of Moisture on Electrical Resistivity

As electrical resistivity is the inverse measurement of electrical conductance through a specified medium, its value depends on the inherent electrical properties of that medium. Conductivity of a medium is the measure of its capacity to pass electrical flow through it and water shows a strong affinity towards electrical conductance. As a result, presence of moisture in soil mass increases its electrical conductance and therefore, decreases electrical resistivity. Jusoh & Osman (2017) established a numerical relationship between moisture content and soil resistivity for all type of soil through laboratory work with a coefficient of determination 0.8168 which indicates a strong correlation between them. This relation is given by,

$$w = 123.93 r_s^{-0.252}$$

Where, r_s = resistivity (Ω-m), w = water content (%)

Kibria (2014) performed several laboratory tests on four types of soil, such as, high plastic clay (CH), low plastic clay (CL), Ca-bentonite and kaolinite and developed correlation between electrical resistivity and moisture content using Statistical analysis software SAS (2009) at different

compaction. An inverse relationship between resistivity and moisture content was observed for all cases. But a significant difference was observed in the relationship due to the variation of dry density. At a certain moisture content, an inverse trend was observed between electrical resistivity and dry density.

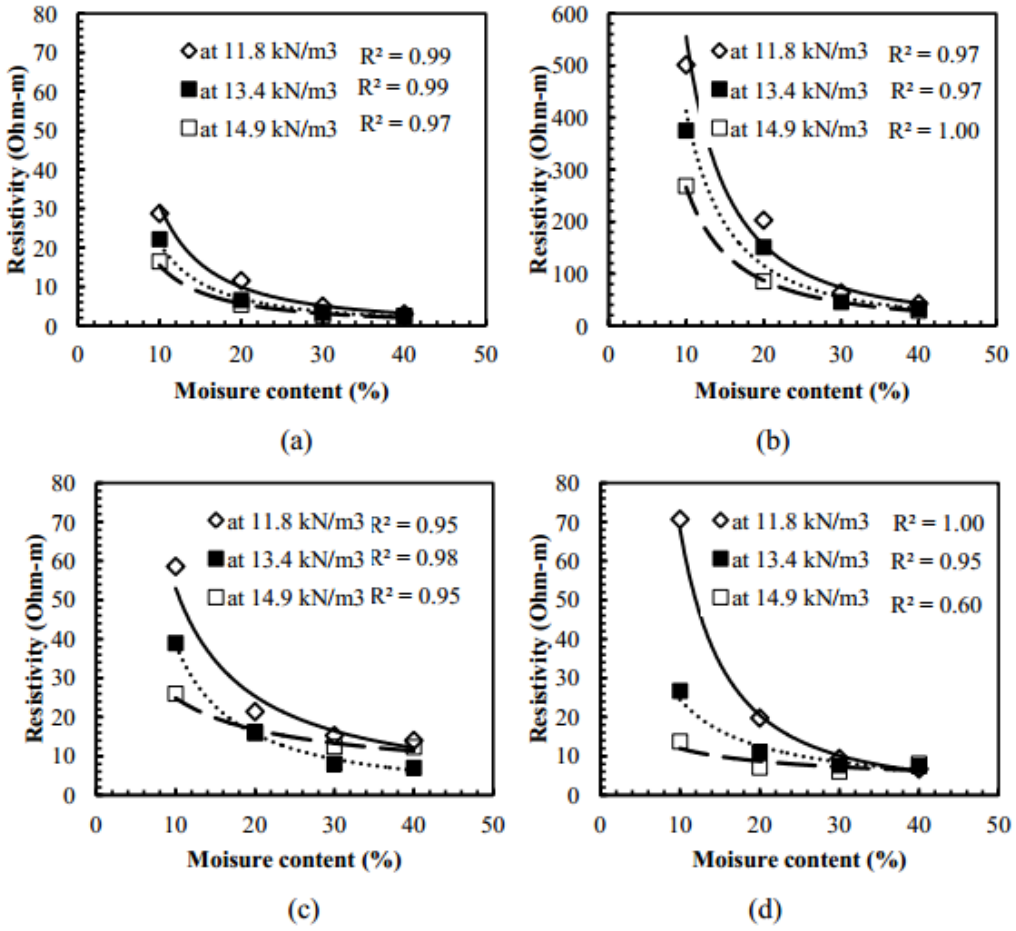

Figure 2.24 Relation between gravimetric moisture content and Resistivity at different dry unit weights for (a) Ca-bentonite (b) Kaolinite (c) Low plastic clay and (d) High plastic clay.

The developed correlation between electrical resistivity and gravimetric moisture content by Kibria (2014) followed a linear trend in log-log scale (Figure 2.25). The combined observations for Ca-bentonite, CH and CL were utilized to develop the correlation.

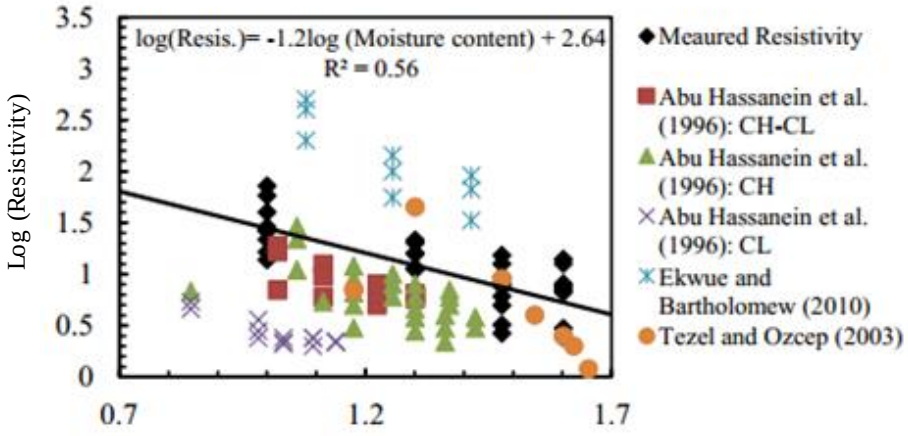

Figure 2.25 Development of correlation between electrical resistivity and moisture content for Ca-bentonite, CH, and CL (Kibria 2014)

Kalinski et al. (1993) also conducted a laboratory investigation to determine volumetric moisture content from electrical conductivity of soil and developed the following regression equation assuming surface conductivity of 0.24 mho/cm (EC_s = 0.24 mho/cm).

$$EC_0 = EC_s + EC_w\theta(1.04\theta - 0.09)$$

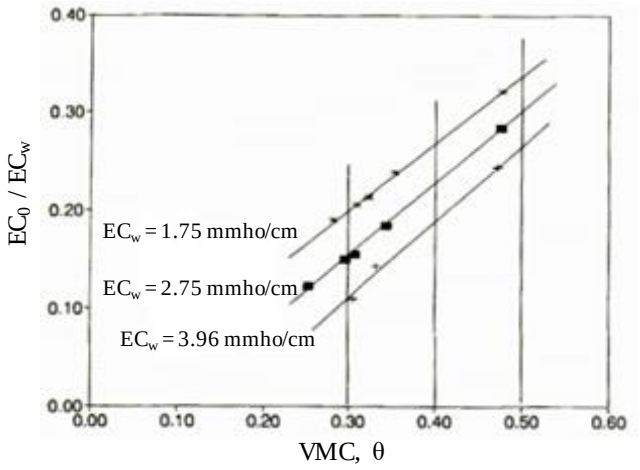

Figure 2.26 Relationship between ratio of bulk soil and pore water conductivity with volumetric moisture content (Kalinski et al., 1993)

2.4.4 Effect of Soil Suction on Electrical Resistivity

As soil suction and electrical resistivity both depend on the degree of soil saturation, there has been a strong correlation between them. Kong et al., (2017) measured the variation of soil suction with resistivity and found that with increasing soil suction, resistivity also increases. It was also observed that at a particular matric suction, loose soil shows higher resistivity than compared to more compacted soil.

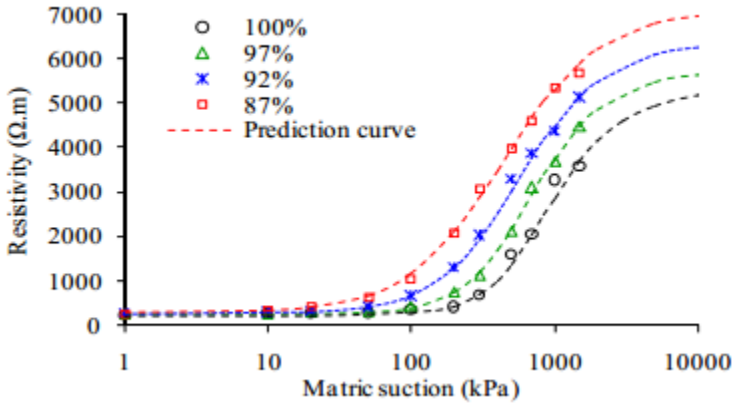

Figure 2.27 Variation of electrical resistivity with matric suction at different compaction (Kong et al., 2017)

2.4.5 Effect of Temperature on Electrical Resistivity

The electrical conductivity increases with increasing temperature and decreases with temperature decrease. Bai et al. (2013) have conducted several tests on lateritic soil and found that the relationship between electrical conductivity and temperature is non-linear as shown on Figure 2.28 and the corresponding numerical relationship is given by the following equation.

$$\rho_T = \frac{\rho_{20}}{1 + \rho_{20}\alpha e^{[\beta(T-20)]}}$$

Where, ρ_T and ρ_{20} = Resistivity at temperature T° C and 20° C respectively, α and β are tested constants with α = 0.0012 and β = 0.1562.

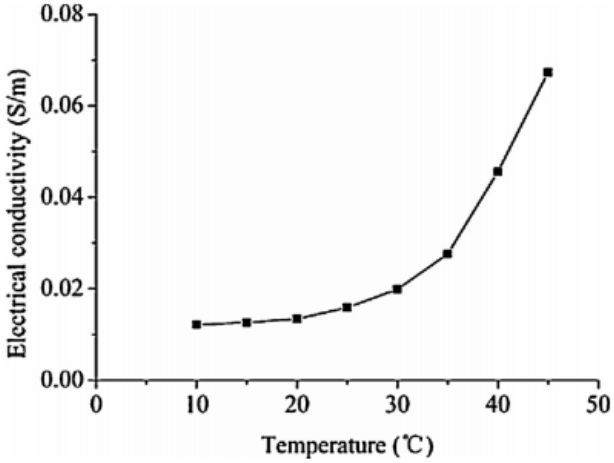

Figure 2.28 Relationship of Electrical Conductivity with temperature for lateritic soil (Bai et al., 2013)

As electrical resistivity changes with temperature, temperature correction is necessary at a certain reference point to compare the ERI test outcomes at different conditions. Samouelian et al. (2005) proposed the following relationship between field resistivity and temperature assuming 25°C as the reference point.

$$\rho = \rho T \times \{1 + \alpha(T - 25)\}$$

Where, ρ is the corrected resistivity at a reference temperature of 25°C in Ohm-m, ρT is the raw resistivity at field temperature in Ohm-m, T is the field soil temperature in °C and α is a correction factor equals to 0.0202.

2.4.6 Effect of Dry Density on Soil Resistivity

As the density of the soil depends on the degree of saturation, soil resistivity also varies with different soil dry densities. According to Kong et al. (2017), the electrical resistivity of compacted residual soil (at water content of about 22.35%) decreases with increasing dry density and tends to constant at higher dry density. They established a numerical correlation between dry density and electrical resistivity which is described by the following equation.

$$R = 170.64 + 2.65 \times 10^9 \times e^{-9.934\rho_d}$$

Where, R = resistivity (Ω-m), ρ_d = Dry density (gm/cm^3)

An inverse relationship between dry density and electrical resistivity was observed because with increasing dry density at certain water content, soil particles get closer resulting increasing degree of saturation which means higher electrolytic water content in unit intergranular open space and thus this electrolytic water can increase electrical conductivity.

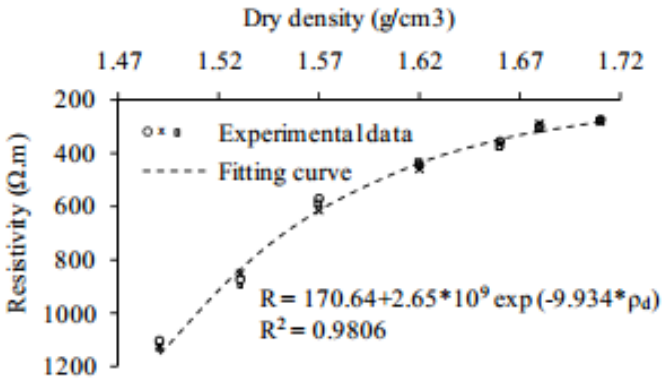

Figure 2.29 Variation of soil resistivity with dry density (Kong et al., 2017)

2.4.7 ERI Technique as an Alternative Way to Measure SWCC

Since, Electrical resistivity and soil suction both deal with the soil moisture, there can be a strong relation between them. Previously, Kong et al. (2017) have established a correlation between electrical resistivity and matric suction of soil in laboratory scale which is a modification of the van Genuchten SWCC equation and showed that the fitting parameters change with different dry densities. The experiment was done on compacted granite residual soils using DC Resistivity meter to measure electrical resistivity of the soil specimen and 15 bars pressure plate extractor for the measurement of matric suction (Figure 2.30). Soil suction has been measured from volumetric water content using proposed equation by van Genuchten (1980). The mathematical equation is,

$$\theta = \theta_r + \frac{\theta_s - \theta_r}{[1 + (\alpha\Psi)^n]^m}$$

Where, Ψ is the suction pressure (kPa) i.e (u_a-u_w), θs is the saturated water content, θr is the residual water content and α, n & m are soil parameters. Parameter m is defined in terms of n by the following equation.

$$m = 1 - \frac{1}{n}$$

(a) (b)

Figure 2.30 (a) DZD-6 DC Resistivity Meter and (b) 15 bar Pressure Plate Extractor

Again, the relationship between resistivity and volumetric water content for different density compacted soil can be described by the van Genuchten (1980) SWCC model (Kong et al. 2017) and the model equation is-

$$R_\theta = R_r + \frac{R_s - R_r}{[1 + (a/\theta)^b]^c}$$

Where, R_θ is the resistivity with respect to volumetric water content, R_s and R_r are saturated and residual resistivity, respectively, a is the x-value of the sigmoid's midpoint, b is the structural factor which depends on the compaction, porosity and particle size distributions of the solid phase and c is a curve shape factor.

Kong et al. (2017) found that the shapes of the soil-water characteristic curve (SWCC) and electrical resistivity-water characteristic curve (RWCC) of the investigated soils are very similar.

Both can be well described by the van Genuchten model with a better correlation and the fitting parameters of RWCC and SWCC are linearly proportional to each other. Based on the numerical analysis, they also proposed a modification on the van Genuchten model for directly correlating the matric suction and electrical resistivity and determined values of the related fitting parameters with a good correlation. They proposed the following equation,

$$R_\Psi = R_r + \frac{R_s - R_r}{[1 + (a_1\Psi)^{b_1}]^{c_1}}$$

Where, Rψ resistivity with respect to matric suction ψ; Rs saturated resistivity; Rr residual resistivity and a_1, b_1 & c_1 are empirical constants implicitly containing the solid phase characteristics. Again, Piegari et al. (2013) established a correlation between soil suction and electrical resistivity (shown on following equation) based on laboratory tests on pyroclastic soils found at the northern slope of Mt Pizzo d'Alvano, Italy and later based on field resistivity data on a study section, a soil suction map of that area has been developed. The study area was divided in three horizons; B is denoted for very loose pyroclastic horizons subjected to highly pedogenetic processes with dense root apparatuses (silty sand), Bb is denoted for buried soil or palaeosoil (silty sand) and Bb_{basal} is denoted for basal buried palaeosoil (silty sand). The established relations are presented on the following.

For B and Bb horizons;

$$s\,(\rho) = \frac{1}{\alpha}\left\{\left[\frac{(\rho/a)^{\frac{1}{b}} - \theta_r}{\theta_s - \theta_r}\right]^{\frac{n}{1-n}} - 1\right\}^{\frac{1}{n}}$$

For Bb_{basal} horizon;

$$s\,(\rho) = \frac{1}{\alpha}\left\{\left[\frac{((\rho - a)/b) - \theta_r}{\theta_s - \theta_r}\right]^{\frac{n}{1-n}} - 1\right\}^{\frac{1}{n}}$$

Where, s = matric suction; ρ = electrical resistivity; α, a, b and n are fitting parameters.

2.5 Advantages of ERI Technique to Monitor ET Cover System

For effective monitoring of the ET cover system, the moisture retention capacity of the soil, available soil water storage at a particular time and soil suction need to be assessed continuously. According to the conventional method, these soil parameters are measured by means of installed sensors under the surface. But the main disadvantage associated with those sensors, is, they damage in the long run and their performance get deteriorate with time. Again, sensors only provide the point measurement of the scenario and their field instrumentation is also costly and time consuming. On the other hand, ERI technique is a non-destructive technique that can capture the whole scenario by providing a numerous amount of measurements in a particular area up to a significant depth. Soil water storage, possibility of percolation, variation of soil suction etc. can be measured through the ERI technique.

Chapter 3

Methodology

3.1 Introduction

The objective of this study is to observe the unsaturated behavior of the soil in field condition and to achieve this goal an extensive laboratory program was conducted to determine the geotechnical properties of the in-situ soil. All the laboratory investigations were done on the disturbed soil samples collected from the study area during the initial stages of the study period. Laboratory investigation program included grain size distribution tests, standard proctor compaction tests, specific gravity determination and Atterberg limits tests.

To observe the effects of different types of vegetation on field unsaturated soil properties, a total of six (6) lysimeters were constructed with three (3) different types of locally available vegetation. Soil samples were collected from each of the six lysimeters before the vegetation plantation to observe in-situ soil geotechnical properties. Two different depths were selected for observing the variation in unsaturated behavior with depth; one is 12-inch from the ground surface where root effects were prevalent, and another is 30-inch where there were no significant effects of root system.

Moisture and temperature sensors along with tensiometers were installed at different depths in each lysimeter for continuous monitoring of the soil water storage and corresponding soil suctions. Electrical resistivity tests were conducted on a monthly basis throughout the study period to investigate the moisture and suction variation with resistivity and to evaluate the performance of electrical resistivity imaging method in quantification of soil water storage. The obtained data from the laboratory investigations and field monitoring was used to develop the field soil water characteristic curve (FSWCC). A statistical software Minitab was used to determine the FSWCC parameters along with its statistical variables to measure the competency of the model in predicting

field condition. Figure 3.1 summarizes the test methodologies involved in this study in an organized fashion.

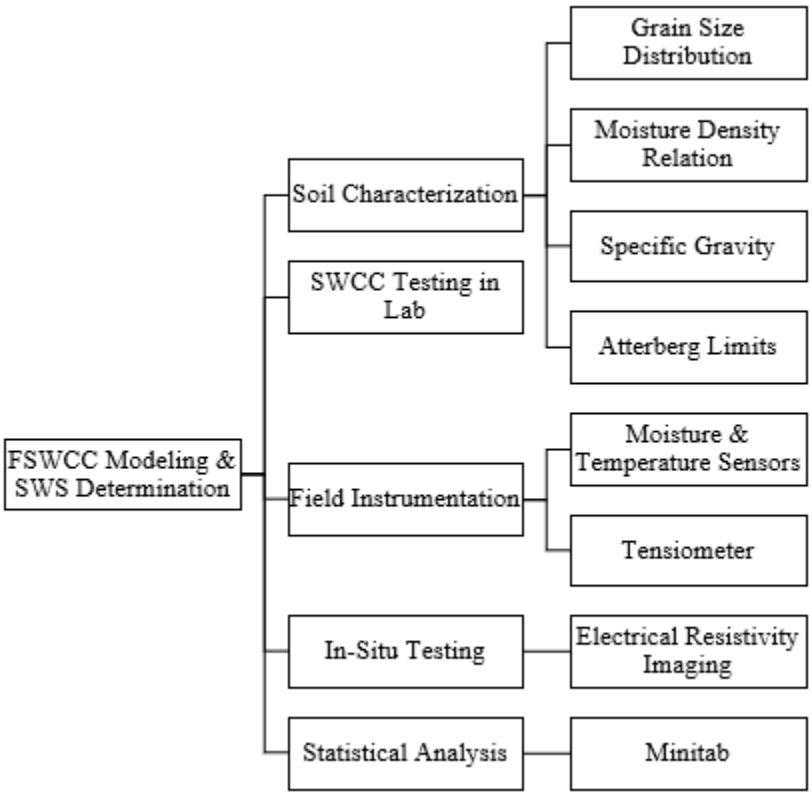

Figure 3.1 Flow chart describing the organization of Test Methodology

3.2 City of Denton Landfill

The City of Denton Municipal Solid Waste (MSW) landfill is located on the southern side of Denton, Texas at 1527 South Mayhill Road. It started its operation in 1983 and received its permit to start accepting waste on March 7, 1983 (permit number of 1590). Initially the landfill started with 32 acres and then expanded in 1998. The expanded landfill covers a total of 252 acres, with 152 acres for solid waste and 100 acres for offices, buffer zone, compost and extra rented land. At present there are six cells in the landfill and it receives approximately 550 tons of MSW a day. In 2009, the landfill transitioned to an enhanced leachate recirculation landfill to increase the gas production and

capacity of landfill space. Figure 3.2 presents the aerial view of the landfill area with surrounding facilities.

Figure 3.2 Top view of the City of Denton MSW Landfill area

3.2.1 Selection of Study Area

There are three climatic regions in Texas. One is arid region located at the western part of the Texas, second is humid region located at the eastern part of the Texas and the third one is semi-arid area which is the middle part of the Texas. City of Denton MSW landfill is located on that semi-arid region where the annual average rainfall ranges between 36 to 50-inches (Alam, 2017).

Figure 3.3 Positioning of the lysimeters

A total of six (6) lysimeters were constructed with a dimension of 40 ft × 40 ft × 4 ft over Cell 1 at the top of an intermediate cover where lysimeter 1, 2 and 3 were on the flat side with 2% slope and 4, 5 and 6 were on 25% slope side. A buffer zone of three (3) meter was reserved all around the lysimeter perimeter to reduce the effect of boundary. The arrangements of the lysimeters are shown in Figure 3.3.

3.2.2 Construction of Different Lysimeters

The construction period continued for four and a half months which was started on the mid of June 2014 and completed on the 1st week of November 2014. As the construction was performed over the landfill intermediate cover, to avoid the interference with the underlying MSW, an earthen embankment of 4 ft height was constructed over the intermediate cover using locally available clay soil. Once the embankment was completed, a total of six (6) 40 ft by 40 ft areas with 4 ft depth were excavated along the designated lysimeter locations in a way that a three (3) meters of buffer zone existed all around the excavated areas.

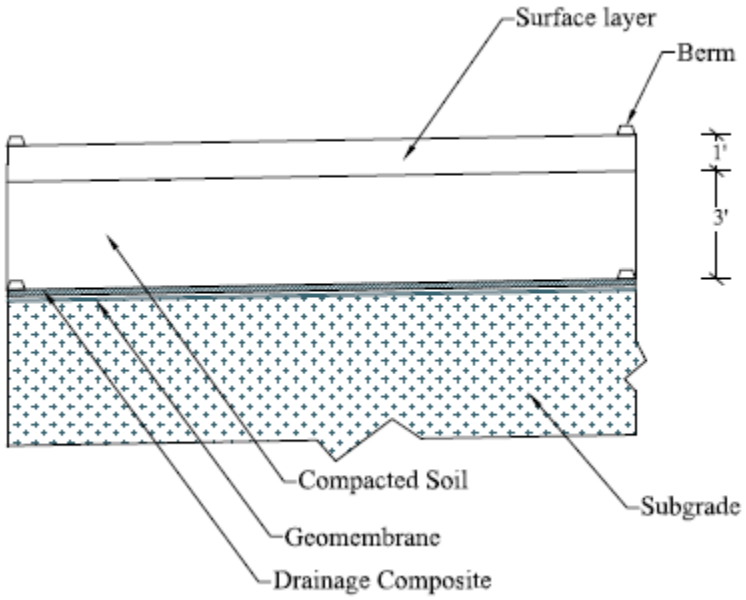

Figure 3.4 Construction details of ET cover (lysimeter)

The bottom of the excavation was compacted, and a 60-mil geomembrane was placed over that compacted subgrade and extended along the side walls. Geo-composite drains were placed over the geomembrane and at the low elevation side of each lysimeter, a HDPE pipe was installed to collect the percolation. Geotextiles were placed along the side walls of the excavation after the geomembrane. After the placement of all geosynthetic materials, clay soil was placed up to 3 ft height in approximately 12-inch lift and compacted to achieve 95% of maximum dry density (MDD) using sheep foot rollers. The compaction was done at dry of optimum to ensure the maximum amount of soil water storage due to the lower initial saturation. A nuclear density gauge was used during the construction of storage layer to monitor the field compaction state at required level. Once the construction of compacted storage layer of 3 ft was completed, a relatively less compacted 1 ft topsoil was placed over it to ensure the proper growth of vegetation. Clay berms were constructed along the periphery of each lysimeter to restrict the runoff from flowing into or out of the lysimeter. Figure 3.4 illustrates the construction details of the ET cover soil.

3.2.3 Installation of Moisture and Temperature Sensors along with Tensiometers

Once all the lysimeters were constructed, a total of eight (8) moisture and temperature sensors were installed in each lysimeter where half of them were at the east nest with another half at the west nest of the lysimeter. The spacing between two consecutive moisture sensors were 9 inches (228.6 mm). The top sensor was located 12 inches (304.8 mm) from the surface. Two tensiometers were also installed at the site co-located with the moisture sensors. The tensiometers were 18 inches (457.2 mm) apart. Tensiometers were arranged from immediately below the surface layer. The schematic locations of the installed sensors along with tensiometers are shown on Figure 3.5.

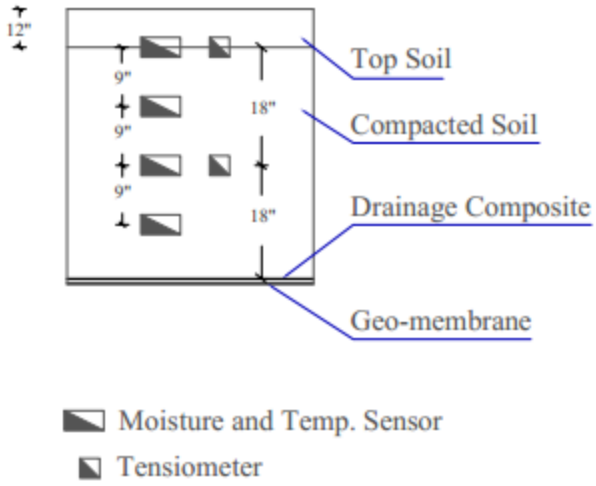

Figure 3.5 Schematic of the arrangement of the installed sensors

3.2.4 Vegetation of the ET Cover

Surface vegetation plays a significant role in evapotranspiration; thus, aids to release moisture to the surrounding environment from the ET cover soil. Three (3) types of locally available vegetation were planted on the lysimeters. Among them, Native Trail grass was planted on lysimeter 1 and 4, Switchgrass was planted on lysimeter 2 and 5 and Bermuda grass was planted on lysimeter 3 and 6. Perennial wildflower and caliche grasses were also mixed with those grasses, but the amount of their presence was not significant. Table 3.1 represents the vegetation details for all of the lysimeters.

Table 3.1 Vegetation on different lysimeters

Lysimeters	Vegetation Type
1 & 4	Native Trail grass
2 & 5	Switchgrass
3 & 6	Bermuda grass

3.3 Soil Characterization

To classify the studied soil, grain size distribution analysis, specific gravity, standard proctor compaction test and Atterberg limit tests were done on the laboratory. All the tests were performed as per ASTM International standard.

3.3.1 Soil Sample Collection

All of the lysimeters were constructed with three (3) ft compacted soil layer and on top of it, one (1) ft of surface layer which was comparatively less compacted to aid in the growth of vegetations. Disturbed soil samples were collected from all of the six lysimeters at different depths during the construction phase. As the construction of compacted storage layer was done on three (3) lifts, each having 12-inch depth, three buckets (20 liters/bucket) of soil samples were collected from each lift and transported to the UTA facilities for conducting the required tests.

3.3.2 Determination of Geotechnical Properties of Soil

Grain Size Distribution

Grain size distribution analysis was performed according to the ASTM D422-63 standard test method. Initially, the collected soil samples were oven dried for 24 hours at 100°C. The oven dried samples were then grinded through a soil grinder to break the lumps. Approximately 500 gm of grinded sample were considered for sieve analysis. After the proper arrangement of the sieves, they were placed on a mechanical shaker for vibration around 10 minutes (Figure 3.6). After completion of the vibration, the weight of soil samples retained on each sieve was measured. The amount of soil which was passed through #200 sieve, was further analyzed using hydrometer to observe the fraction of silt and clay in the fine contents.

Figure 3.6 Arrangement of the sieves in a mechanical shaker

Moisture Density Relation

The variation of dry density of the collected soil samples with different moisture content was observed through standard proctor compaction test in accordance with ASTM D 698 standard. The soil samples were dried for 24 hours and then grinded in a similar way that was done for grain size distribution analysis. The grinded samples were then mixed with water uniformly to observe different moisture content and placed in a standard proctor mold in three (3) layers. Each layer was compacted by 25 blows with a 10-lb hammer. Once the soil placement and compaction were done, moist unit weight of the sample was determined along with corresponding moisture content. Finally, the maximum dry density at optimum moisture content was determined and the corresponding dry density at 95% compaction on both the dry and wet side of the optimum was determined.

Specific Gravity

Specific gravity of the collected soil samples was determined following ASTM D854-00 standard test method. Approximately 125 gm of dry soil samples (passed through #10 sieve) were considered for the test. Initially, an empty pycnometer was cleaned and weighted, after that it was re-weighted with distilled water filled up to a specified mark on the pycnometer. After that the

pycnometer was emptied, cleaned and filled with soil specimen. Distilled water was added to the pycnometer to fill about half to three-fourth of the pycnometer. Then, partial vacuum was applied to remove the entrapped air for around 10 minutes and afterwards, the remaining space up to the specified mark was filled with distilled water. Finally, the weight of the pycnometer at this condition was measured. From the observed weights, the specific gravity of the soil samples was determined.

Atterberg Limits

Soil samples passed through #40 sieve was considered for Atterberg limits test and the test was done following ASTM D4318 standard method. A Cassagrande liquid limit device was used to perform the liquid limit test. A uniform soil paste was prepared by adding water, chopping, stirring and kneading. After that the paste was placed on the liquid limit device and a groove was cut at the middle of the cup. Afterwards, a vibratory motion was employed until the groove was around 10 mm. The corresponding number of blows was recorded. The test was repeated for several times at different moisture content and the variation of moisture content with number of blows was observed. The moisture content corresponding to 25 blows was recorded as liquid limit.

Again, a uniform soil paste was prepared in a similar way for plastic limit determination. The soil paste was then rolled with hand over a glass plate until a 3 mm diameter rod shape was reached. The water content at which the 3 mm diameter shape was ruptured, was recorded as plastic limit.

Lab Scale SWCC Determination

Among several methods to investigate the soil moisture-suction properties, pressure cell apparatus was used in this current study to determine the SWCC of the collected soil samples. The test was conducted according to ASTM D 6836-02 standard procedure. The apparatus is also named as Fredlund SWCC device and consists of three-inch diameter exchangeable ceramic disks (high air-entry disks) which can measure up to 1500 kPa of applied suction. Collected soil samples were compacted at 95% of its MDD and utilized in this study to develop SWCC.

Figure 3.7 Pressure Cell apparatus

3.4 Geophysical Investigation of ET Cover Soil (ERI Technique)

Continuous monitoring of the soil suction and moisture content along with temperature was performed through the installed tensiometers, moisture and temperature sensors and the data were obtained from the onsite data logger system. Electrical resistivity imaging (ERI) tests were done on monthly basis throughout the study period using a Supersting R8/IP Resistivity Meter. The resistivity meter was manufactured by Advanced Geosciences Institute (AGI) and has a programable eight channel option. ERI test was done across the locations of the installed sensors. A total of 28 electrodes were hammered into the ground up to around 2-inch depth with 6 inches of spacing between the electrodes. The schematic of the arrangement of the electrodes over the ET cover surface with moisture and temperature sensors is illustrated in Figure 3.8(b). Electrical cables were used to connect the electrodes with resistivity meter. Once the arrangement of the electrodes and resistivity meter with the cables was done, the test was run, and the data was stored in the resistivity meter box. 2D dipole-dipole array was employed in analyzing the resistivity values for better resolution and accurate quantitative results. Figure 3.8(a) illustrates the ERI test conduction over ET cover soil.

(a)

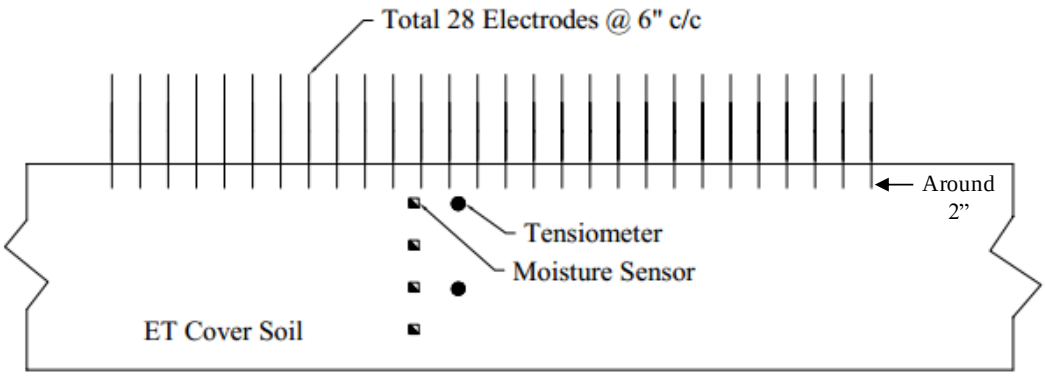

(b)

Figure 3.8 (a) ERI test conduction and (b) schematic of the arrangement of electrodes across the installed sensors over ET cover soil

3.4.1 Data Extraction

Earth Imager 2D software (AGI, 2008) was utilized for processing the raw resistivity data extracted from the equipment after every field investigation. This software uses a forward modeling to calculate the apparent resistivity values. The apparent resistivity was then converted to inverted resistivity value through inversion algorithm.

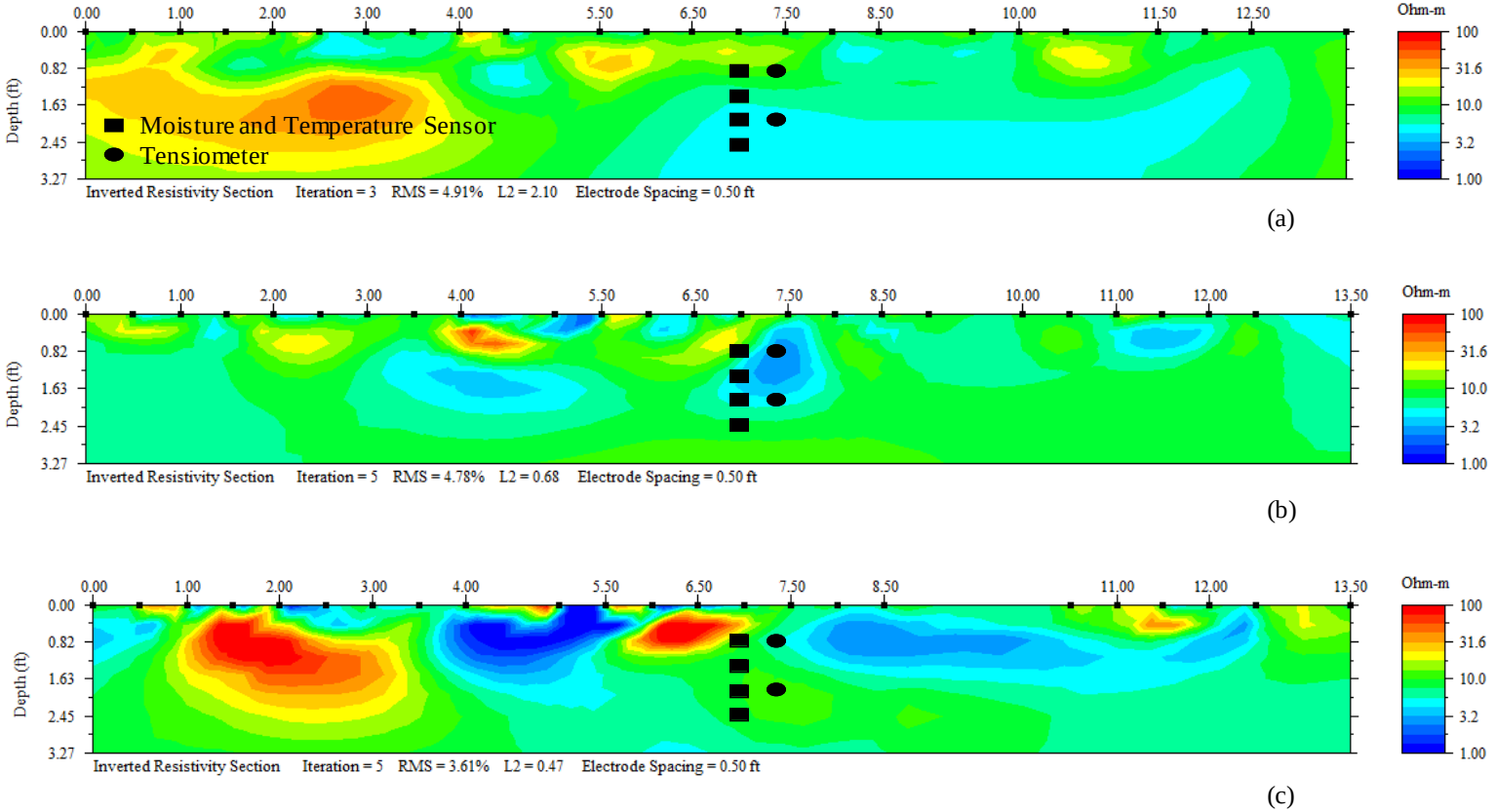

Figure 3.9 Resistivity profile for (a) 12th June, 2017, (b) 11th August, 2017 and (c) 15th October, 2017 across the sensors' location on the west side of Lysimeter 1

The inverted resistivity value was limited within 10% relative data misfit. A horizontal-vertical ratio of 0.2 was used for the analysis and several iterations were performed until the RMS error went below 5%. The finite element method with Cholesky decomposition was considered for forward modeling with a thickness incremental factor of 1.1 and a depth factor of 0.7. The resistivity contour level is set between 1 to 100 for ease of the comparison among different observations. Red contour indicates the maximum resistivity while blue contour designates minimum. For each test run, a resistivity log was obtained from where quantitative values were extracted in the units of Ohm-m. Figure 3.9 represents the resistivity log across the installed sensors obtained from field observations conducted at different times in 2017.

3.4.2 Temperature Correction

The effect of temperature variation was considered for analyzing the resistivity value to enhance the competency of the ERI test in predicting actual field condition. According to Campbell et al., (1948), electrical properties of the soil changes with the variation of temperature. As Texas is located in the semi-arid or semi-humid region, it undergoes with a significant temperature variation throughout the year. In summer, soil temperature varies between 15°C to 40°C while in winter, it decreases to -5°C to 18°C. So, the range of temperature variation is substantial. After obtaining the raw data from the resistivity log, concurrent soil temperature was extracted from the temperature sensors' reading and correction to the raw resistivity data was performed using the following equation provided by Samouëlian et al., (2005).

$$\rho = \rho T \times \{1 + \alpha(T - 25)\}$$

Where, ρ is the corrected resistivity at a reference temperature of 25°C in Ohm-m, ρT is the raw resistivity at field temperature in Ohm-m, T is the field soil temperature in °C and α is a correction factor equals to 0.0202.

3.5 Statistical Modeling

Once the resistivity and the concurrent moisture content and soil suction data were obtained for all of the lysimeters, the dataset were subdivided by the vegetation type and depth. For monitoring the variation of the dataset along depth, observations from two different depths; 12-inch and 30-inch from the ET cover surface, were studied. Field resistivity suction characteristic curve (FRSCC) and field resistivity water characteristic curve (FRWCC) were developed by using a statistical software Minitab. For measuring the competency of the generated curves in predicting the field conditions, statistical parameters, such as, standard deviation, mean squared errors, sum of the squared residuals and error degrees of freedom were determined. Later, field soil water characteristic curve (FSWCC) was also developed from the obtained datapoint extracted from FRSCC and FRWCC using the same program.

3.5.1 Selection of Model Equation

The variation of soil suction and moisture content in terms of resistivity was observed through lab scale measurement by Kong et al., (2017) and the observed sigmoidal relationship between soil suction and resistivity is as follows:

$$R_{\psi}(\psi, Y) = R_r + \frac{R_s - R_r}{[1 + (p\psi)^q]^r}$$

Where, R_{ψ} is the resistivity with respect to the matric suction, ψ and a parameter vector Y (R_s, R_r, p, q, r) where R_s is saturated resistivity, R_r is residual resistivity and p, q, r, are empirical constants.

In this study, the above equation was created in Minitab and non-linear regression analysis was performed. The components of parameter vector Y were determined providing the observed values of resistivity and corresponding soil suction as input parameters in the program. The initial values of the components of Y were assumed in the program and after several iterations, best fitted values of the components were determined. Statistical parameters such as standard deviation (S),

sum of the squared residuals (SSE), error degrees of freedom (DFE) and mean square errors (MSE) associated with each of the generated curve were also observed from the non-linear regression analysis output.

Kong et al., (2017) also observed the variation of moisture content in the soil mass in terms of changes in resistivity in laboratory setup and provided the following relation between them.

$$R_\theta(\theta, X) = R_r + \frac{R_s - R_r}{[1 + (a/\theta)^b]^c}$$

Where, R_θ is the resistivity with respect to the volumetric moisture content, θ and a parameter vector X (R_s, R_r, a, b, c) where R_s and R_r are the saturated and residual resistivity, respectively and a, b, c are fitting parameters. The b parameter is related to the compaction, porosity and particle size distribution of the soil whereas c parameter determines the shape of RWCC curve.

In this study, the variation of field moisture content with resistivity was analyzed using the same relation provided by Kong et al., (2017). The components of parameter vector X with associated statistical variables were determined in a similar way that was considered for FRSCC construction.

Once FRSCC and FRWCC were determined, best fitted coefficients for field soil water characteristic curve (FSWCC) were determined in Minitab for each of the studied case in terms of resistivity. For the determination of FSWCC, Van Genuchten SWCC model was considered for the analysis which is shown below.

$$\theta = \theta_r + (\theta_S - \theta_r) \left\{\frac{1}{1 + (\alpha\psi)^n}\right\}^m$$

Where, θ is the volumetric moisture content (VMC) in terms of matric suction, ψ, α and n are shape parameters and $m = 1 - 1/n$. θ_s is the saturated VMC while θ_r is the VMC at residual condition. Initial values of θ_s, θ_r, α and n were assumed and after several iterations best fitted values were obtained. For the construction of FSWCC, the values of soil suction and related moisture

content were extracted from the developed FRSCC and FRWCC in terms of resistivity and used as input parameters in Minitab.

3.5.2 Boundary Conditions

For the construction of FSWCC, boundary conditions on VMC were applied where saturated VMC, θ_s designates upper limit and residual VMC, θ_r designates lower limit for FSWCC. Lab scale measurements of SWCC were performed in UTA facilities. The values of θ_s and θ_r were assumed from the lab testing for the development of FSWCC in Minitab.

3.6 Soil Water Storage (SWS) and Unit Cross Sectional Area Resistance

Moisture and temperature sensors were installed at two opposite sides of a lysimeter. Each side had four sensors buried under the ground with 9-inch vertical spacings between each other. Though only point measurements were observed through the sensors, it was assumed that the average measurements from the two sides were uniformly distributed throughout the whole cover soil mass within a lysimeter. Average SWS was then determined concurrently during ERI tests. SWS in each side was calculated from the obtained readings provided by the installed moisture sensors using the following equation.

$$S = x_1 v_1 + \left(\frac{v_1 + v_2}{2}\right) x_2 + \cdots\cdots + v_n x_n$$

Where, S is the soil water storage at a particular time and measured in units of length. V_1, V_2 …. Vn is the observed volumetric moisture content up to n^{th} number of sensors and x is the vertical distance between the sensors. Figure 3.10 represents the illustration of the moisture sensors positioning with each other. For the estimation of SWS in each side, it was assumed that average moisture content between two co-located sensors was distributed uniformly throughout the distance between them. Again, for the top 12-inch distance, moisture content from the top sensor was considered throughout the distance. In this study, SWS was determined for three different thicknesses of the ET cover.

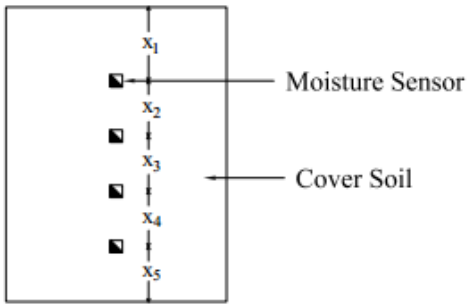

Figure 3.10 Schematic of moisture sensors' position for SWS evaluation

Resistivity values across the sensor's position were also determined through ERI testing. As electrical resistivity changes with depth, a term "unit cross sectional area resistance" was introduced to represent the complete electrical properties up to the entire ET cover thickness. Theoretical background behind "unit cross sectional area resistance" is explained on the following.

If a soil section with a cross sectional area "A" and sample length "L" is considered, its resistivity can be expressed as,

$$\rho = R\left(\frac{A}{L}\right)$$

Where, R = Resistance in ohms, ρ = Electrical Resistivity in ohm-m.

If resistivity varies throughout the entire sample length, unit cross sectional area resistance can be considered for the evaluation of entire soil electrical properties. Thus, unit cross sectional area resistance, ρ_a for a distance, x can be introduced as,

$$\rho_a = \rho x = \frac{RAx}{L}$$

Where, x is an integral distance within L where it is assumed that the electrical resistivity remains constant within that distance. In this study, ρ_a was estimated using the following equation.

$$\rho_a = x_1 R_1 + \left(\frac{R_1 + R_2}{2}\right) x_2 + \cdots\cdots + R_n x_n$$

Where, R1, R_2, …. R_n are the resistivity up to n^{th} observation and x is the distance between two successive observations at vertical direction. The unit of ρ_a is measured in Ohm-m^2.

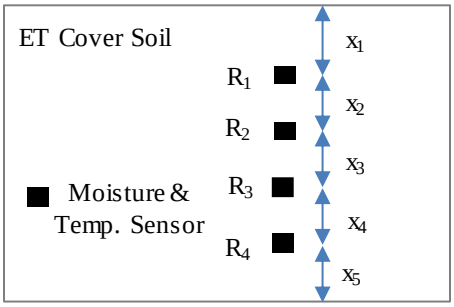

Figure 3.11 Unit cross sectional area resistance determination across sensor's location

Figure 3.11 illustrates the procedure for the determination of ρ_a from an observed resistivity log across the location of the buried sensors. P_a was determined at each side of a lysimeter across the sensor's location and the average of the two sides was considered to correlate it with SWS.

Chapter 4

Results and Discussion

4.1 Introduction

In this study, soil electrical resistivity in six different ET lysimeters at different depths was measured through field soil resistivity test using Supersting R8/IP Resistivity Meter. Concurrent soil suction, moisture content and temperature were also investigated using co-located tensiometers and soil moisture sensors. The data was grouped by soil vegetation type and depth to explore the efficacy of soil resistivity in estimating the unsaturated soil behavior and its water retention capacity with different vegetations. The study was conducted for a period of 3.5 years (from January 2015 to June 2018) on a monthly basis. Geotechnical properties of the soil were also determined through laboratory tests following ASTM International Standards. Soil suction-moisture relationship according to Van Genuchten SWCC model was also determined through laboratory testing for all of the vegetated lysimeters and corresponding SWCC parameters obtained in lab setup were also presented in this chapter. Field resistivity suction characteristic curves (FRSCC) and field resistivity water characteristic curves (FRWCC) were developed for the depth of 12-inch and 30-inch for all lysimeters. As soil suction and moisture content both are related with the change in electrical resistivity, relations between themselves were also established following Van Genuchten SWCC model at each depth of consideration for all vegetated lysimeter soil. Correlation and regression analyses were conducted using Minitab and statistical parameters for each generated curve were also determined. It is worth mentioning that the separation of dataset by depth and vegetation type provided a significant difference in SWCC behavior of the ET cover soil. Soil water storage or the amount of water that soil holds at a time was also measured through electrical resistivity imaging technique for ET cover soil of various depths. Field capacity, permanent wilting point and plant available water were also measured from developed SWCC equation. To monitor the possible

occurrence of moisture percolation through ET cover soil, existing soil moisture retention capacity for different ET cover soil depths was also studied in this chapter.

4.2 Soil Classification and Geotechnical Properties

Grain Size Distribution

Sieve analyses were conducted on the collected soil samples from different lysimeters. It was found that more than 80% of the soil were composed of fine particles passing through the No. 200 sieve. To observe the clay and silt contents in the fine fraction, hydrometer analyses were also performed, and it was noticed that both the clay and silt amounts were very close to each other. From the tests, the silt fraction was found to be ranged between 35% to 56% and the clay fraction was found to be 36% to 43%. The summary of the grain size distribution analysis is presented in Table 4.1. Figure 4.1 illustrates the grain size distribution curve for lysimeter 1 and lysimeter 3 soil.

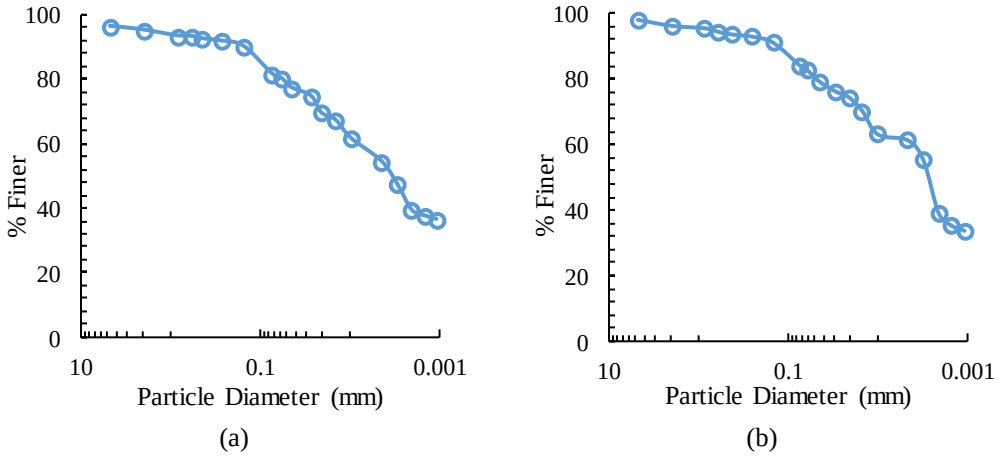

Figure 4.1 Grain size distribution curve for (a) lysimeter 1 and (b) lysimeter 3 soil samples

Atterberg Limits

Liquid limits (LL) and plastic limits (PL) were observed through laboratory testing. Plasticity index (PI) was determined from the difference between LL and PL. LL and PI were found in a range between 51 to 60 and 28 to 32, respectively. The results of Atterberg limit tests are

summarized in Table 4.1. Plasticity indexes for all the soil samples tested were found above A-line in a plasticity chart. Based on grain size analysis and Atterberg limit test results, the soil from all of the lysimeters were classified as "High Plastic Clay (CH)" as per Unified Soil Classification System (USCS). A Casagrande's A-chart (also called Plasticity Chart) showing the Atterberg limit test results is presented in Figure 4.2.

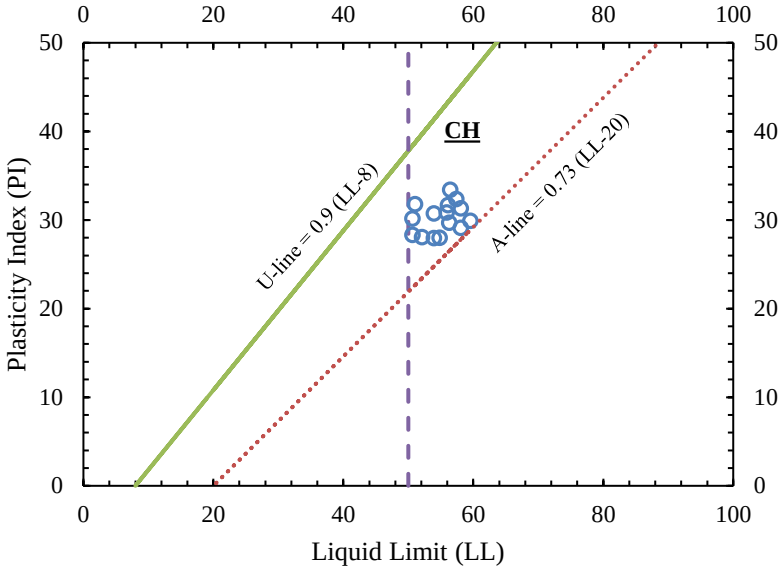

Figure 4.2 Casagrande's A-chart for ET cover soil

Specific Gravity

According to ASTM International standard, specific gravity of the collected soil samples was determined and found to be 2.75 on average which means the soil is 2.75 times heavier than the water. The results of the observed specific gravity for different lysimeters soils are summarized in Table 4.1.

Table 4.1 Summary of index properties of the ET cover soil with classification

Lysimeter	Gravel (%)	Sand (%)	Silt (%)	Clay (%)	Liquid Limit (LL)	Plasticity Index (PI)	USCS Classification	Specific Gravity (G_s)
1	0	16-19	41-43	39-42	54-60	28-30	CH	2.75
2	0	16-19	42-43	38-42	51-58	29-32	CH	2.75
3	0	16-22	35-47	38-43	51-57	28-31	CH	2.77
4	0	7-14	43-56	38-42	53-60	28-32	CH	2.76
5	0	6-11	48-55	36-42	53-56	28-30	CH	2.75
6	0	9-14	46-52	36-40	55-59	30-33	CH	2.75

Maximum Dry Density and Field Compaction

As soil density or field compaction affects the electrical resistivity in the soil (Abu-Hassanein et al., 1996; and Kong et al., 2017), maximum dry density was observed for each lysimeter soil through standard proctor compaction test in the laboratory. The maximum dry density was found to be 16.94 kN/m^3 on average at a range of 17% to 18% optimum moisture content. Table 4.2 summarizes the results of standard proctor compaction tests.

Table 4.2 Moisture density relation for different lysimeter soils

Lysimeter	Optimum moisture content (%)	Maximum dry density (kN/m^3)
1	17.6	16.94
2	17.3	16.98
3	17.1	16.9
4	17.9	16.84
5	18.2	17
6	17.5	16.96

SWCC Determination in Lab

Suction-moisture relationship was determined from the remolded soil samples at UTA facilities using Fredlund SWCC device. Soil samples were compacted to 95% of its maximum dry density at dry of optimum side to represent the actual field condition. Van Genuchten (VG) SWCC model was utilized to fit the curve through the observations. SWCC parameters were determined for all of the lysimeter soil and reported in Table 4.3. Figure 4.3 illustrates the SWCC for lysimeter 1 and lysimeter 3 soil.

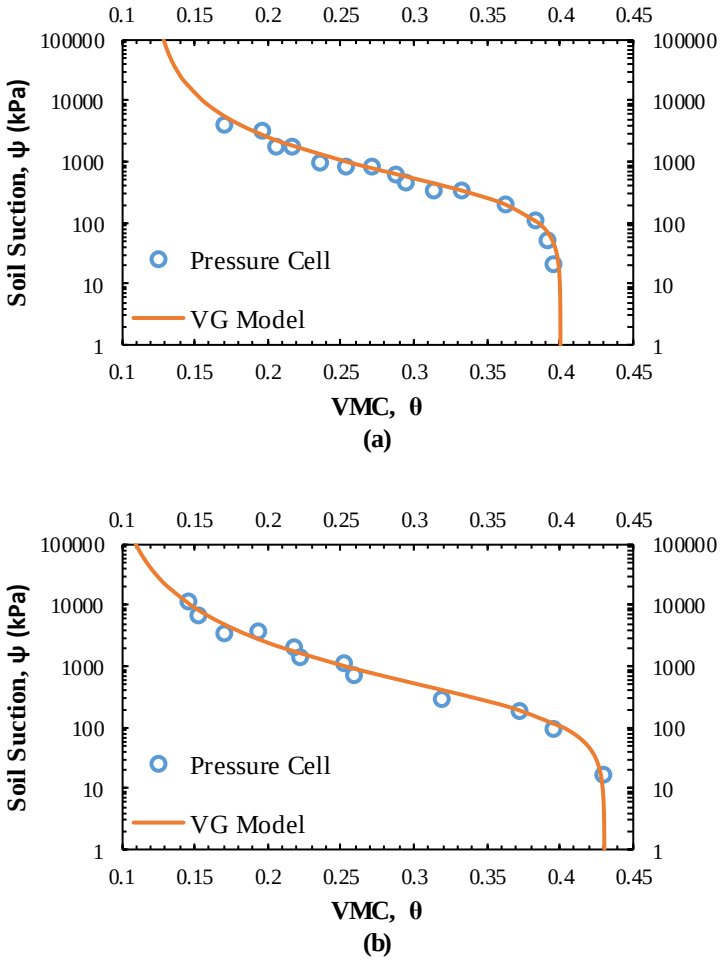

Figure 4.3 SWCC for (a) lysimeter 1 and (b) lysimeter 3 soil

Table 4.3 Van Genuchten's SWCC parameters obtained from Laboratory Testing

Lysimeter	α	n	m	θ_s	θ_r
1	0.0031	1.6	0.375	0.4	0.12
2	0.00514	1.53	0.26	0.41	0.13
3	0.00445	1.47	0.319	0.43	0.09
4	0.0037	1.96	0.5	0.4	0.11
5	0.0031	1.77	0.43	0.4	0.11
6	0.00345	1.74	0.42	0.41	0.1

From the lab constructed SWCC, the value of α was found to vary between 0.0031 to 0.00514 (kPa^{-1}) and air entry suction was found in the range of 80 to 180 kPa.

Field Capacity (FC) determination from lab SWCC

Typically, FC is determined from the water content corresponding to 33 kPa matric suction (Alam, 2017). In this study, typical value of suction was assumed for the determination of the FC. Table 4.4 summarizes the outcomes of FC of 4 ft cover soil thickness which were extracted from the lab experimented SWCC. It was found that the FC obtained from lab constructed SWCC varies between 480 to 505 mm for 4 ft thickness of ET cover soil.

Table 4.4 Average FC obtained from lab SWCC for 4 ft cover soil thickness

Lysimeter	FC (inch)/ 4 ft cover soil	FC (mm)/ 4 ft cover soil
1 & 4	19.07	484.38
2 & 5	19.41	493.07
3 & 6	19.88	505.08

In lab scale determination, FC was obtained for a uniformly compacted soil without any plant roots. However, in the actual field condition, soil density was found to vary with depth and the upper layer of 1 to 1.5 ft was covered with surface vegetation. Again, it was difficult to simulate the

actual field condition in lab, because there are certain environmental factors such as hysteresis effect, surface vegetation, relative humidity etc. in field which influences the field SWCC; thus, FC is also subjected to change.

4.3 Relationship between ERI and Soil Suction

Continuous monitoring of soil suction was made through the data logger system which was connected to the tensiometers and electrical resistivity tests were done on a monthly basis throughout the study period on each lysimeter. Corresponding temperature was recorded using temperature sensors installed at studied depths and resistivity values were corrected at 25°C.

Figure 4.4 represents the actual resistivity profile and the sensor locations for RI test in lysimeter 1. Resistivity profile for three different times in a year are presented only: one on 23rd June when high temperature sustained for long time without rainfall (Figure 4.4a), 2nd one on 19th July which was conducted one day after heavy rainfall (Figure 4.4b) and the other one on 22nd August which was conducted 7 days after a rainfall (Figure 4.4c). A clear contrast can be observed among those resistivity profiles. In Figure 4.4(a), top 1 ft. to 1.5 ft. of the cover soil exhibits high resistivity zone as shown through the red contour. The bottom of the cover soil indicates the existence of moisture, thereby lower suction as the resistivity value is lower relative to the top soil layer. In Figure 4.4(b), a significant reduction in the resistivity value was observed which illustrates the moisture intrusion into the ET cover after precipitation as the resistivity contour turned to almost green to blue from a condensed red contour. At this point soil suction was found to be lower compared to the dry condition due to the moisture intrusion into the soil body. Figure 4.4(c), a moderate resistivity value was observed compared to Figure 4.4(b) as the soil was subjected to dry with time after a rainfall. Soil suction value was found to be increased somewhat at this point compared to the wet condition after heavy rainfall.

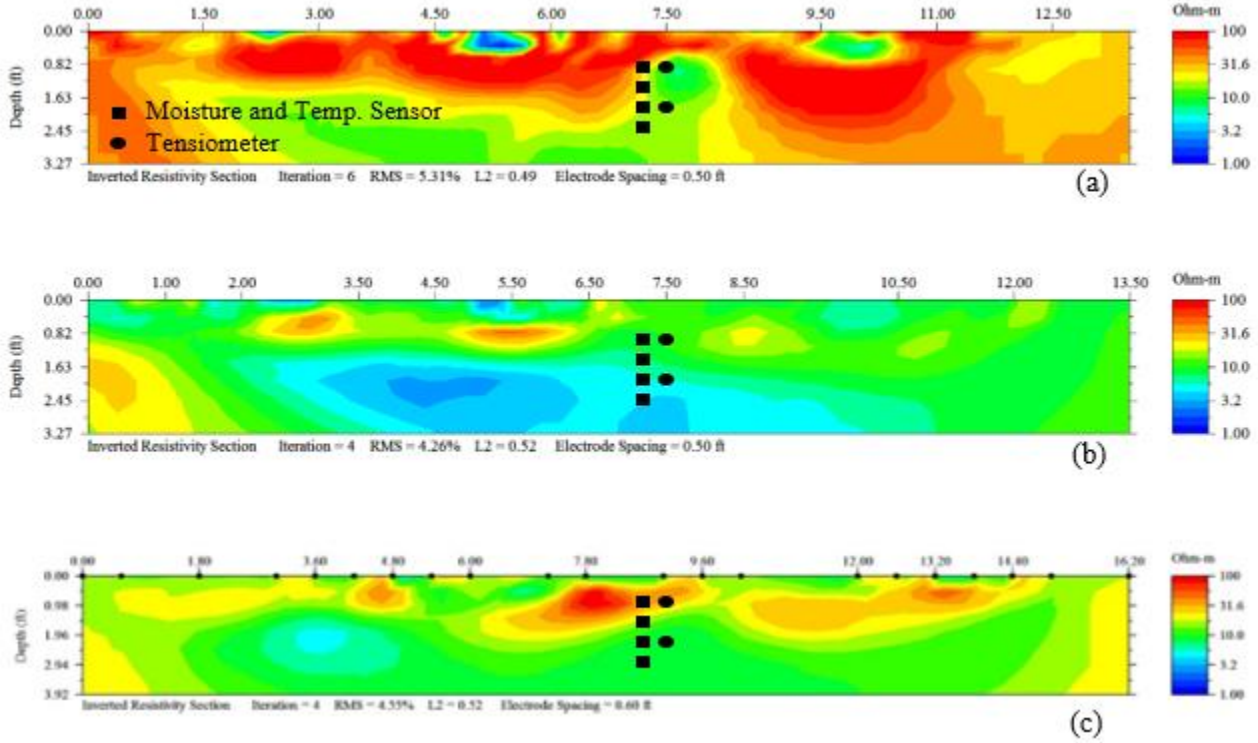

Figure 4.4 Resistivity imaging result for (a) 23rd June, 2016, (b) 19th July, 2016 and (c) 22nd August, 2016 across sensor's location on the west side of Lysimeter 1

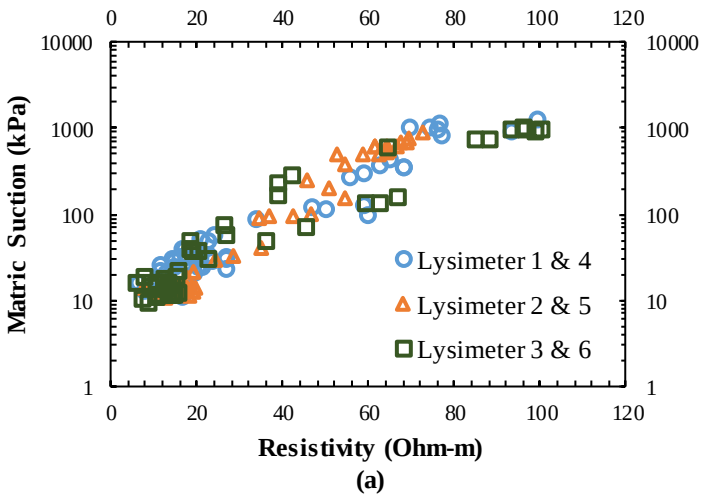

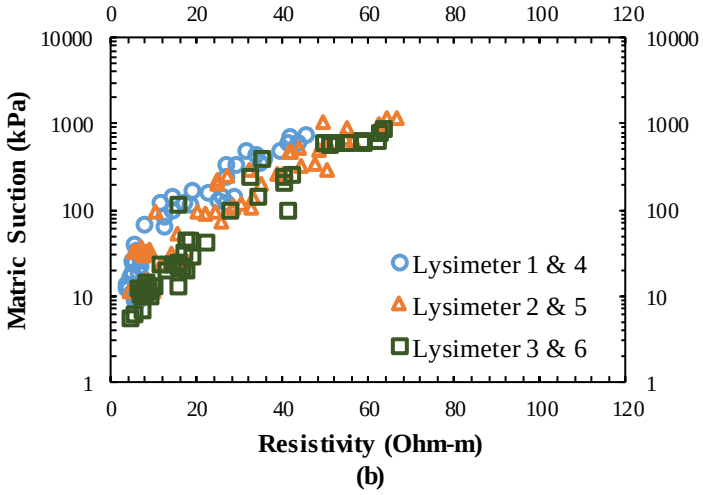

Figure 4.5 Observation of field soil matric suction with concurrent soil resistivity (a) at 12-inch depth and (b) at 30-inch depth for ET cover soil with different vegetations before temperature correction.

According to Alam (2017), the average root depth for the studied vegetations varies between top 15 to 18 inches. So, the study was done at two different depths; top 12-inch with possible root effects and bottom 30-inch without root effects. The dataset was divided according to the vegetation type and depth. Field observations of electrical resistivity for lysimeters covering with native trail grass, switchgrass and Bermuda grass at two different depths (12-inch and 30-inch)

with concurrent soil suction were shown on Figure 4.5(a) and 4.5(b), respectively, before temperature correction. The dataset was found scattered without temperature correction. The temperature variation in the studied soil was observed as low as -4°C to as high as 38°C. A reference temperature of 25°C was considered and the field resistivity values were corrected according to the relation given by Samouëlian et al., (2005).

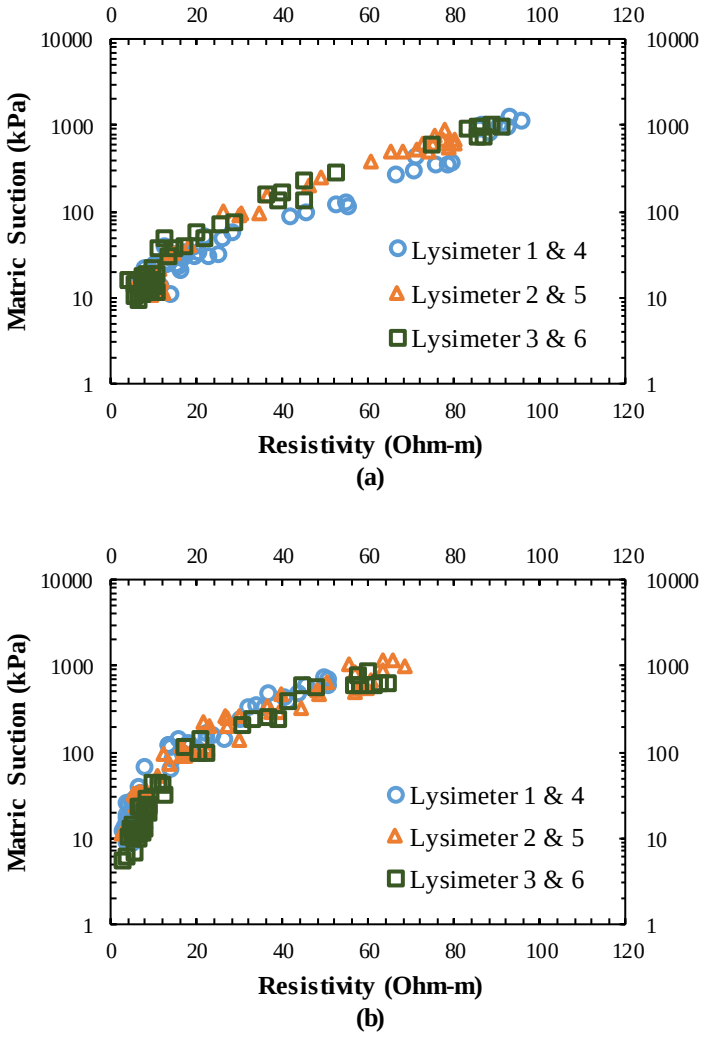

Figure 4.6 Observation of field soil matric suction with concurrent soil resistivity (a) at 12-inch depth and (b) at 30-inch depth for ET cover soil with different vegetations after temperature correction.

Figure 4.6 (a) and Figure 4.6 (b) represent the variation of soil suction with resistivity after temperature correction for all lysimeters at 12-inch and 30-inch depth, respectively. It was found that the dataset was closely packed after temperature correction. An increasing trend of matric suction was found with increasing soil resistivity. The variation of matric suction with resistivity for Native Trail grass, Switchgrass and Bermuda grass vegetated soil displayed almost similar kind of trend for each depth. But a significant difference on the relationship was found between these two depths. It was found that soil resistivity at 30-inch depth is much lower than the soil resistivity at 12-inch depth on average at dry season. The difference in soil condition between these two depths are accountable for the observed discrepancy. The upper surface zone remains exposed to the surrounding environment at all the time and goes through several wet dry cycle with time. Again, the vegetation root zone depth extends up to top 15 to 18 inches (Alam, 2017) creating a more void space in that region compared to the bottom soil zone after that vegetation zone. As a result, bottom soil zone is subjected to less disturbance compared to upper vegetated soil zone and stays more compacted. According to Kong et al. (2017), soil resistivity decreases with increasing dry density at a certain soil suction which explains the low resistivity zone for the bottom 30-inch depth.

4.4 Relationship between ERI and Soil Moisture

Volumetric moisture content (VMC) at 12-inch and 30-inch depth was also monitored continuously through the data logger system which was connected to the moisture sensors. Electrical resistivity values in these depths were extracted from the concurrent ERI profile. Figure 4.7 and Figure 4.8 represents the variation of VMC with resistivity at 12-inch and 30-inch depth for the lysimeters with different vegetations, before and after temperature correction, respectively. A decreasing trend of VMC was found with increasing resistivity values for all lysimeters.

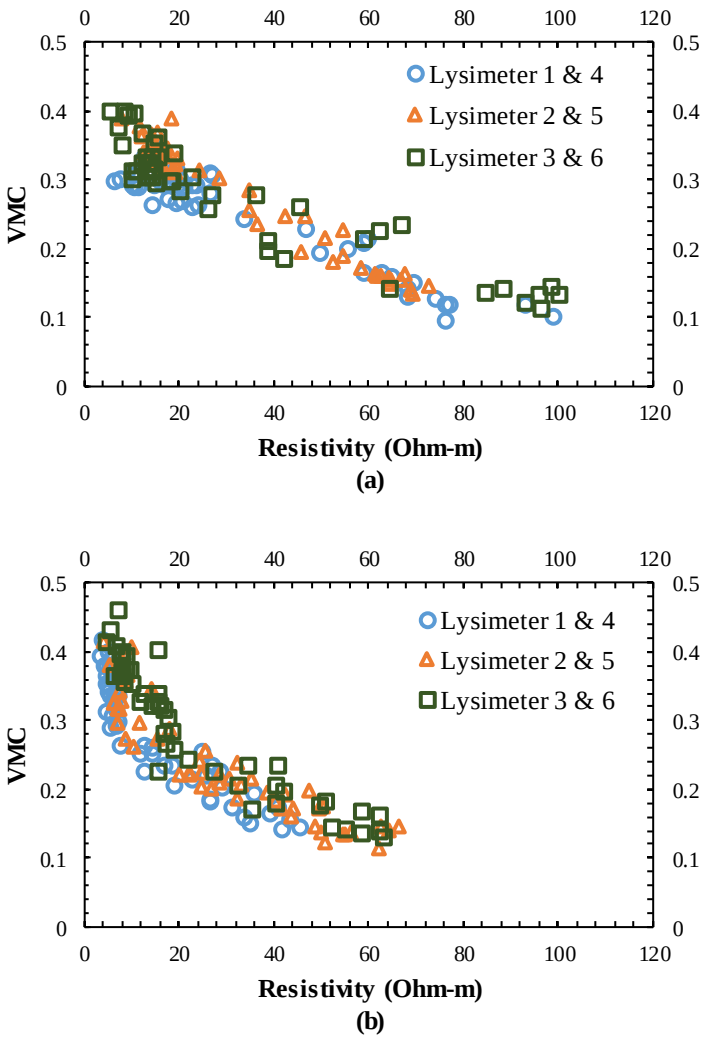

Figure 4.7 Observation of field volumetric moisture content (VMC) with concurrent soil resistivity (a) at 12-inch depth and (b) at 30-inch depth for ET cover soil with different vegetations before temperature correction

A similar kind of trend was observed for Native Trail grass, Switchgrass and Bermuda grass vegetated soil at each depth but a significant difference in resistivity values was observed between these two depths at particular VMC when the observation was made during a period without rainfall. According to Kong et al. (2017), resistivity and dry density show an inverse relationship with each other for a certain VMC. As the top 12-inch soil layer was less compacted compared to

the bottom 30-inch soil zone, a relatively high resistivity value was observed in that zone for a particular VMC.

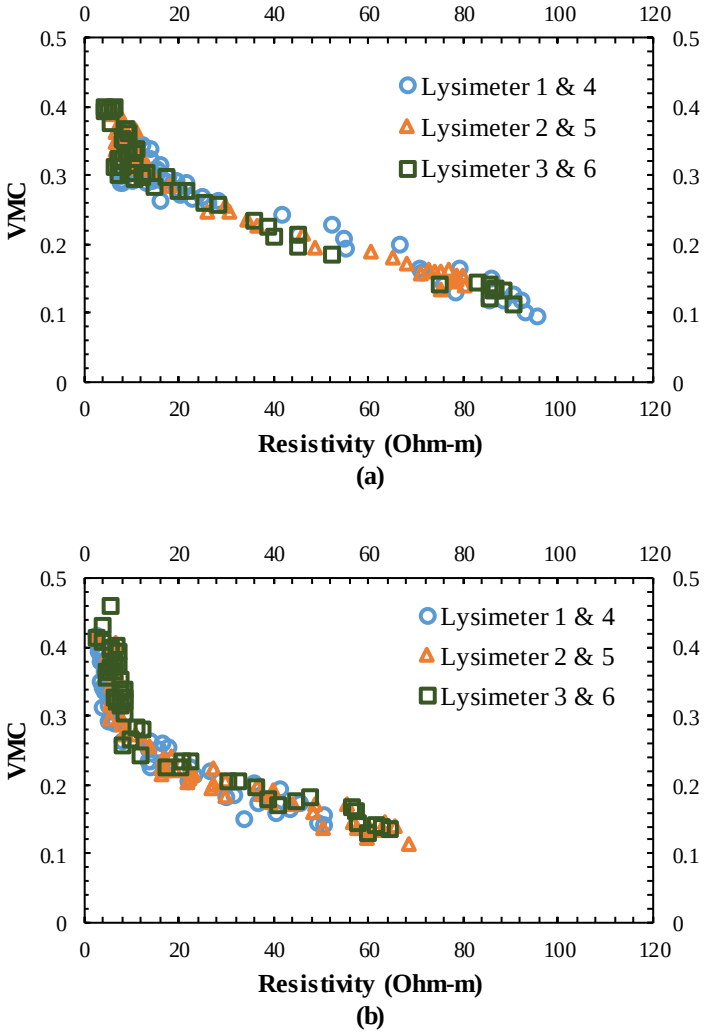

Figure 4.8 Observation of field volumetric moisture content (VMC) with concurrent soil resistivity (a) at 12-inch depth and (b) at 30-inch depth for ET cover soil with different vegetations after temperature correction

4.5 Statistical Analysis and Curve Generation

To observe the best fitted correlation among field resistivity, soil suction and field moisture content, a statistical software Minitab was used. It was found that both the relationship between

field resistivity and soil suction; and field resistivity and moisture content follow a non-linear sigmoidal trend. To measure the competency of a non-linear curve in representing the observed field dataset, several statistical parameters; standard deviation (S), sum of the squared residuals (SSE), error degrees of freedom (DFE) and mean square error (MSE) were determined using Minitab. Standard deviation measures the dispersion of the data from the mean. In case of a non-linear curve, standard deviation represents the inconsistency between the data values and the fitted values. Therefore, S is an important measure of the goodness-of-fit for a nonlinear model rather than coefficient of determination (also called "R-squared") which can be satisfactory in describing a linear model. A low standard deviation indicates that most of the field observations are very close to the fitted values whereas a high standard deviation represents the scattering of the data around the fitted values. Deviations of the predicted data from the actual empirical observations can also be measured through SSE. A small number of SSE indicates a tight fit of the model to the data. Therefore, SSE is used as an optimality criterion in parameter selection and model selection. Again, DFE equals the difference between the sample size and the number of parameters. Minitab uses the value of DFE to estimate the values of the parameters. Moreover, MSE estimates the variance of the field observations around the fitted values. Best fitted curves were generated along with the statistical parameters using Minitab to establish the relationships among electrical resistivity, soil suction and field moisture content.

4.5.1 Field Resistivity Suction Characteristic Curve (FRSCC) Coefficient p, q and r

Tensiometer data and electrical resistivity data were analyzed to determine the response of electrical resistivity at different soil suction. A field resistivity suction characteristic curve (FRSCC) was generated based on the field observations at different times during the monitoring period for each depth of analysis and vegetation type. Based on the regression analysis, Van Genuchten (1980) sigmoidal model was found best suited for the field observation points of resistivity and matric suction. The model equation is as follows;

$$R_\psi(\psi, Y) = R_r + \frac{R_s - R_r}{[1 + (p\psi)^q]^r}$$

Where, R_ψ is the resistivity with respect to the matric suction, ψ and a parameter vector Y (R_s, R_r, p, q, r), where R_s is saturated resistivity, R_r is residual resistivity and p, q, r, are curve fitting constants. The curve fitting parameters define the shape of the FRSCC. The curve fitting constants with associated statistical parameters for each developed curve at 12-inch depth and at 30-inch depth for different vegetation were shown on Table 4.5 and Table 4.6, respectively. Once the fitting constants were determined, best fitted curves were plot against field observations for each of the above described case and depicted on Figure 4.9 and Figure 4.10 for different vegetated soil at 12-inch and 30-inch depth, respectively. In this statistical analysis, R_s and R_r set the boundary conditions for the FRSCCs. The values of R_s were found almost similar for all depth and all types of vegetated soil during construction of FRSCC. But a comparatively low value of R_r was observed in the deeper depth, specifically for Native Trail grass and Switchgrass vegetated soil.

Table 4.5 FRSCC (at 12-inch depth) coefficient p, q and r with non-linear regression parameters for different vegetated ET cover soil

Vegetation Type	p	q	r	R_s	R_r	Standard Deviation (S)	Sum of the Squared Residuals (SSE)	Error Degrees of Freedom (DFE)	Mean Square Error (MSE)
Native Trail grass (Lysimeter 1 & 4)	0.019	1.479	0.386	2	110	0.1118	0.6130	49	0.0125
Switchgrass (Lysimeter 2 & 5)	0.006	1.033	0.864	3	100	0.1389	0.9651	50	0.0193
Bermuda grass (Lysimeter 3 & 6)	0.002	1.081	2.168	3	100	0.1959	1.7649	46	0.0384

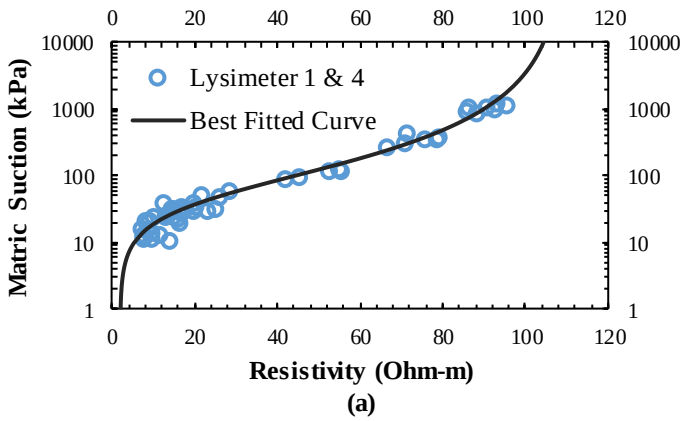

Figure 4.9 FRSCC at 12-inch depth along with the field observations for (a) Native Trail grass, (b) Switchgrass and (c) Bermuda grass vegetated ET cover soil

For 12-inch depth analysis, the standard deviations of FRSCC curves for Native Trail grass, Switchgrass and Bermuda grass vegetated soil were found to be 0.112, 0.139 and 0.196 respectively which indicates a good fit of the data. Mean square errors were also between 1.25% to 3.84% which also represents the efficacy of the field observations towards developed curve after temperature correction.

Table 4.6 FRSCC (at 30-inch depth) coefficient p, q and r with non-linear regression parameters for different vegetated ET cover soil

Vegetation Type	p	q	r	R_s	R_r	Standard Deviation (S)	Sum of the Squared Residuals (SSE)	Error Degrees of Freedom (DFE)	Mean Square Error (MSE)
Native Trail grass (Lysimeter 1 & 4)	0.003	1.213	1.334	2	60	0.1676	1.3763	49	0.0280
Switchgrass (Lysimeter 2 & 5)	0.002	1.145	1.538	3	80	0.1388	0.9443	49	0.0193
Bermuda grass (Lysimeter 3 & 6)	0.006	1.138	0.469	3	100	0.1500	0.9903	44	0.0225

For 30-inch depth analysis, the standard deviations of FRSCC curves for Native Trail grass, Switchgrass and Bermuda grass vegetated soil were found to be 0.168, 0.139 and 0.15 respectively which indicates a good fit of the data. Mean square errors were also between 1.93% to 2.80% which also represents the efficacy of the field observations towards developed curve after temperature correction.

Best fitted FRSCCs for different vegetation at 12-inch depth and 30-inch depth were shown on Figure 4.11(a) and 4.11(b), respectively. The FRSCC trends for Native Trail grass, Switchgrass and Bermuda grass vegetated lysimeters were found quite similar with each other which means the variation of root distribution for different vegetation in ET cover soil was insignificant for the determination of resistivity suction relationship.

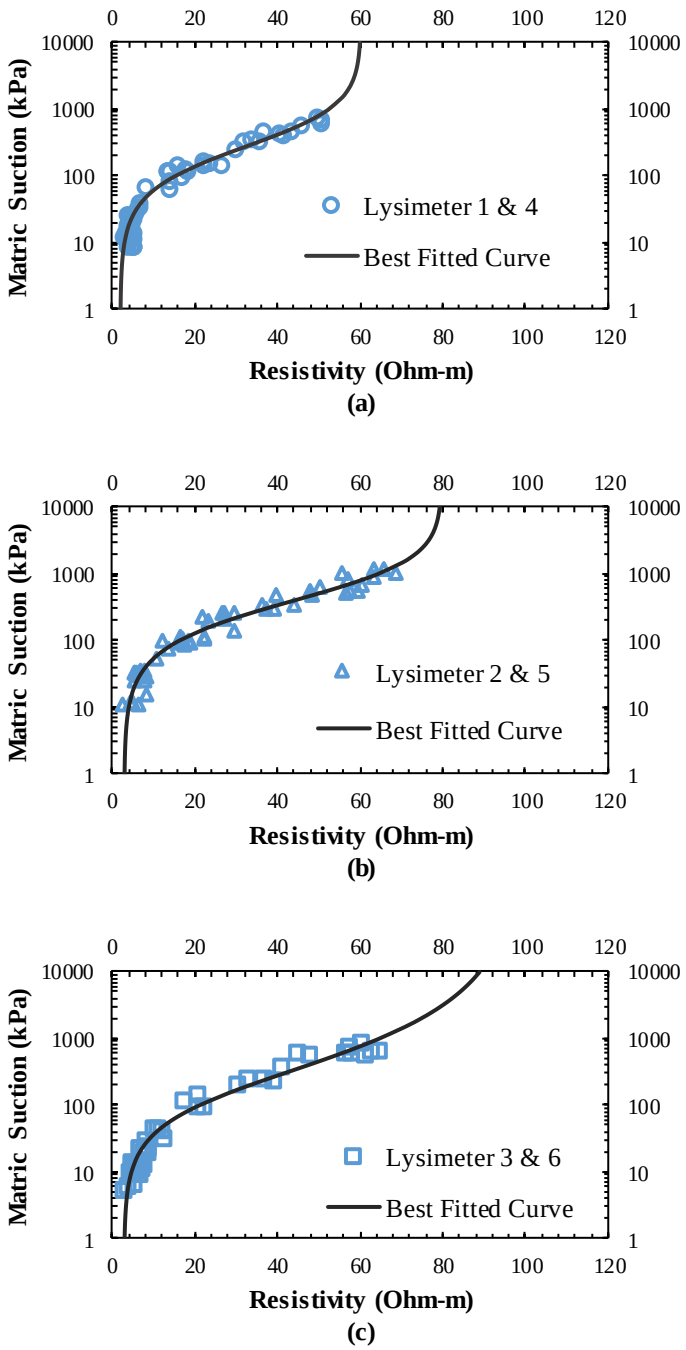

Figure 4.10 FRSCC at 30-inch depth along with the field observations for (a) Native Trail grass, (b) Switchgrass and (c) Bermuda grass vegetated ET cover soil

However, the first break point of the FRSCC for 12-inch depth was found at around 40 kPa for all types of vegetated lysimeters while at 30-inch depth it was found at around 80 kPa. As the soil at 12-inch depth was subjected to high disturbance caused by the surrounding environment and also influenced by root effects, soil integrity was affected at that depth resulting in lower soil density compared to the bottom. Differences in soil density between these two depths may be accountable for that incongruity. However, in field, installed tensiometers at different depths offer only the point measurements of the data at a particular place which may fail to represent the whole scenario.

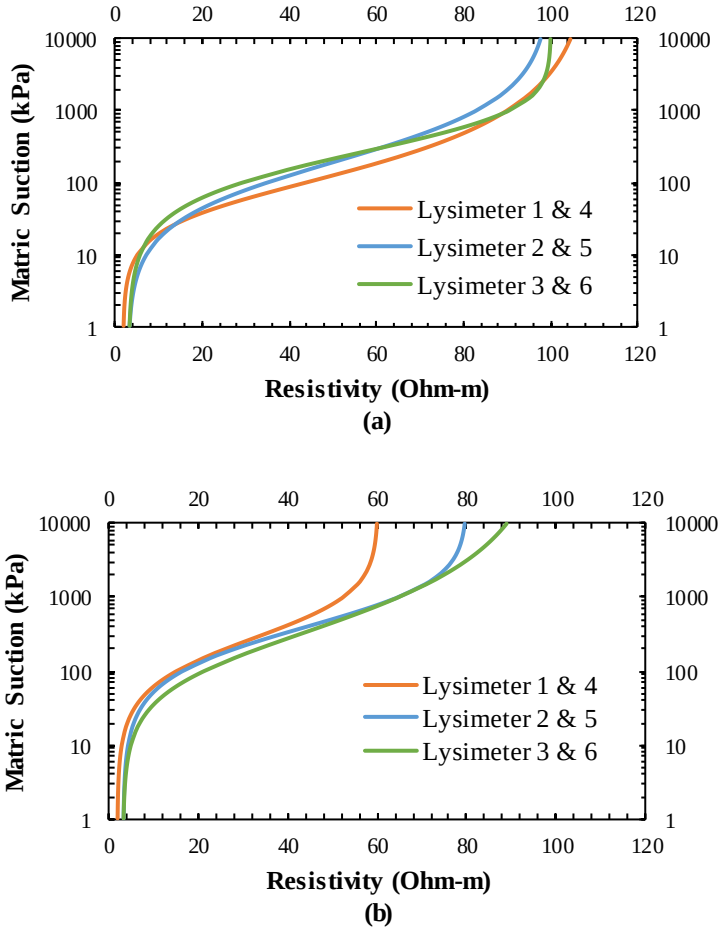

Figure 4.11 Comparison among different FRSCCs (a) at 12-inch depth and (b) at 30-inch depth for ET cover soil with different vegetation

4.5.2 Field Resistivity Water Characteristic Curve (FRWCC) Coefficient a, b and c

Soil moisture sensor data and electrical resistivity data were analyzed to determine the response of electrical resistivity at different moisture content. A field resistivity water characteristic curve (FRWCC) was generated based on the field observations at different times during the monitoring period for each depth of analysis and vegetation. Based on regression analysis, a sigmoidal function was found to best fit the data points. The sigmoidal function is similar to the Van Genuchten (1980) SWCC model which can be presented through the following equation;

$$R_\theta(\theta, X) = R_r + \frac{R_s - R_r}{[1 + (a/\theta)^b]^c}$$

Where, R_θ is the resistivity with respect to the VMC (θ) and a parameter vector X (R_s, R_r, a, b, c), where R_s is the soil resistivity at saturated condition, R_r is the residual soil resistivity at dry condition, and a, b, c are curve fitting parameters. The b parameter is related to the compaction, porosity and particle size distribution of the soil whereas c parameter determines the shape of RWCC curve. The values of R_s and R_r set the boundary condition for FRWCC.

Table 4.7 FRWCC (at 12-inch depth) coefficient a, b and c with non-linear regression parameters for different vegetated ET cover soil

Vegetation Type	a	b	c	R_s	R_r	Standard Deviation (S)	Sum of the Squared Residuals (SSE)	Error Degrees of Freedom (DFE)	Mean Square Error (MSE)
Native Trail grass (Lysimeter 1 & 4)	0.255	6.612	0.362	2	110	0.0183	0.0165	49	0.000337
Switchgrass (Lysimeter 2 & 5)	0.263	6.655	0.387	3	100	0.0142	0.0101	50	0.000202
Bermuda grass (Lysimeter 3 & 6)	0.262	7.728	0.357	3	100	0.0205	0.0190	45	0.000422

The values of R_r were found to vary between 100 to 110 for 12-inch depth analysis of FRWCC, whereas comparatively low values were obtained at 30-inch depth, specifically for Native

Trail grass and Switchgrass vegetated lysimeters. Saturated resistivity, R_s was found almost same for all vegetation and depth. The curve fitting parameters with related statistical variables were determined using Minitab and summarized in Table 4.7 and Table 4.8, for different vegetation at 12-inch depth and 30-inch depth, respectively. Once the fitting constants were determined, best fitted FRWCC curves were plot against field observations for each of the above described case and demonstrated on Figure 4.12 and Figure 4.13 for different vegetated soil at 12-inch and 30-inch depth, respectively. The standard deviation for 12-inch depth analysis varies between 0.014 to 0.02 which indicates a well correlation between the VMC and soil resistivity. Mean square errors were also limited between 0.02% to 0.04% which represents a good fit of the data after temperature correction.

Table 4.8 FRWCC (at 30-inch depth) coefficient a, b and c with non-linear regression parameters for different vegetated ET cover soil

Vegetation Type	a	b	c	R_s	R_r	Standard Deviation (S)	Sum of the Squared Residuals (SSE)	Error Degrees of Freedom (DFE)	Mean Square Error (MSE)
Native Trail grass (Lysimeter 1 & 4)	0.227	6.410	0.584	2	60	0.0235	0.0271	49	0.0006
Switchgrass (Lysimeter 2 & 5)	0.173	4.835	1.013	3	80	0.0216	0.0228	49	0.0005
Bermuda grass (Lysimeter 3 & 6)	0.257	6.209	0.239	3	100	0.0296	0.0386	44	0.0009

The standard deviation for 30-inch depth analysis varies between 0.021 to 0.03 which indicates a well correlation between the VMC and soil resistivity. Mean square errors were also limited between 0.05% to 0.09% which represents a good fit of the data after temperature correction. Sum of the squared residuals were also found to be in the range of 2% to 4% which indicates the field observations were in close range around the generated curve.

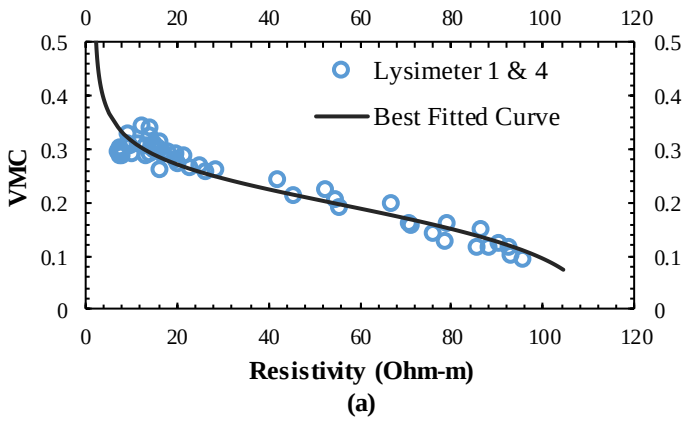

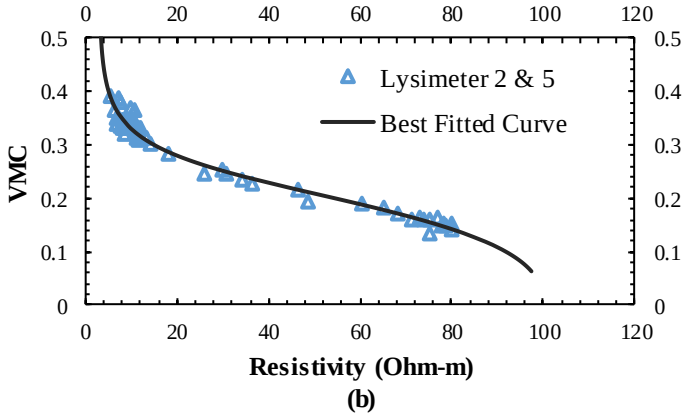

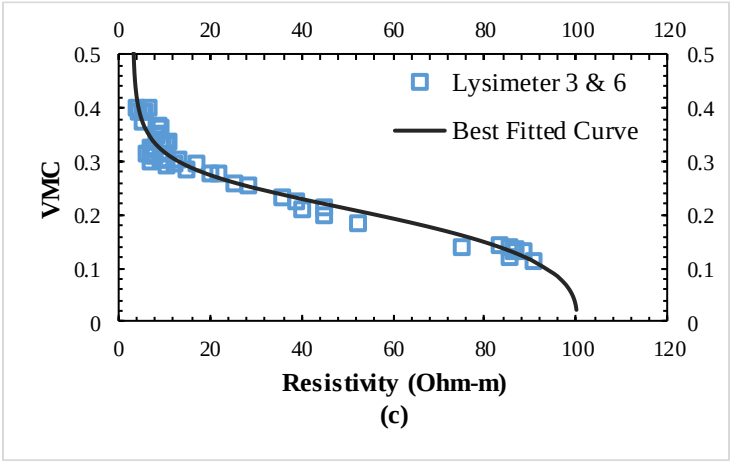

Figure 4.12 FRWCC at 12-inch depth along with the field observations for (a) Native Trail grass, (b) Switchgrass and (c) Bermuda grass vegetated ET cover soil

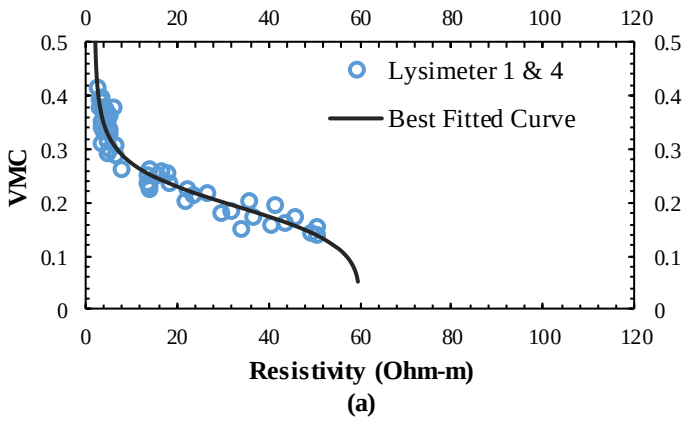

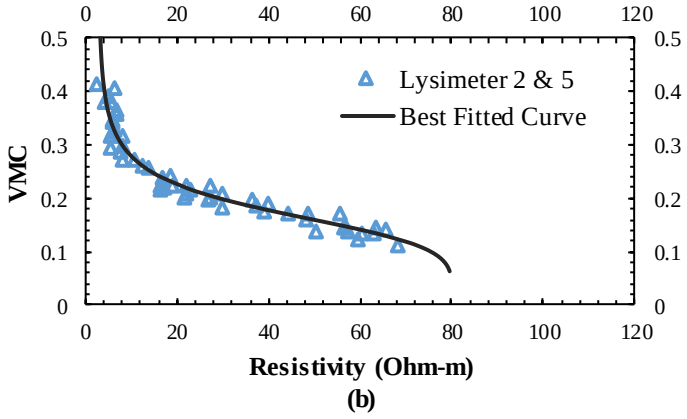

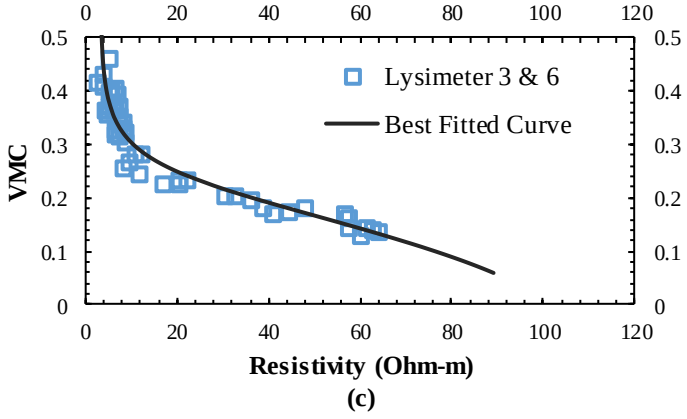

Figure 4.13 FRWCC at 30-inch depth along with the field observations for (a) Native Trail grass, (b) Switchgrass and (c) Bermuda grass vegetated ET cover soil

Best fitted FRWCCs for different vegetation at 12-inch depth and 30-inch depth were shown on Figure 4.14(a) and 4.14(b), respectively. The trend of FRWCC for Native trail grass, Switchgrass and Bermuda grass vegetated soil was found quite similar at 12-inch depth. But at 30-inch depth, the upper limit of resistivity was found quite low compared to what was found for 12-inch depth. Because of the root distribution and continuous wet dry cycle at the top 12-inch depth, more void spaces were created on that zone causing a significant moisture deficiency during the dry season where moisture was released to the surrounding environment. This phenomenon resulted a high resistivity zone at the top 12-inch depth than compared to the below 30-inch depth where moisture was sustained between soil particles due to less disturbance and lack of exposure to the environment.

The first break point of the FRWCC curve for 12-inch depth was found around at a VMC of 0.32 whereas for 30-inch depth it was found around at a VMC of 0.25. Differences in void spaces between the two depths is accountable for that discrepancy. Due to frequent water store release occurrence and environmental exposure on the top soil layer, more void spaces were created on that zone increasing its ability to sustain more water at the wet condition. For that reason, resistivity approaches to its saturated limit at a higher VMC for the upper depth of analysis compared to the depth below. The second break point represents the dry situation of the FRWCC curve and it was found around at a VMC of 0.09 for both the depths. After that point, resistivity value approaches towards its residual limit. Again, there are other factors such as; presence of salts, contaminants, metallic components, ionized compounds etc. in soil mass which influences the electrical resistivity and causes to obtain a higher value which may not entirely represent the actual degree of saturation.

In this study, moisture sensors were installed only at two opposite sides in a lysimeter. The distribution of precipitation may not be uniform throughout the entire soil mass and sometimes the flow path of moisture may miss the sensors. As moisture sensors installed at different depths only

offer the point measurement of the moisture content at a particular place, it may fail to represent the overall condition.

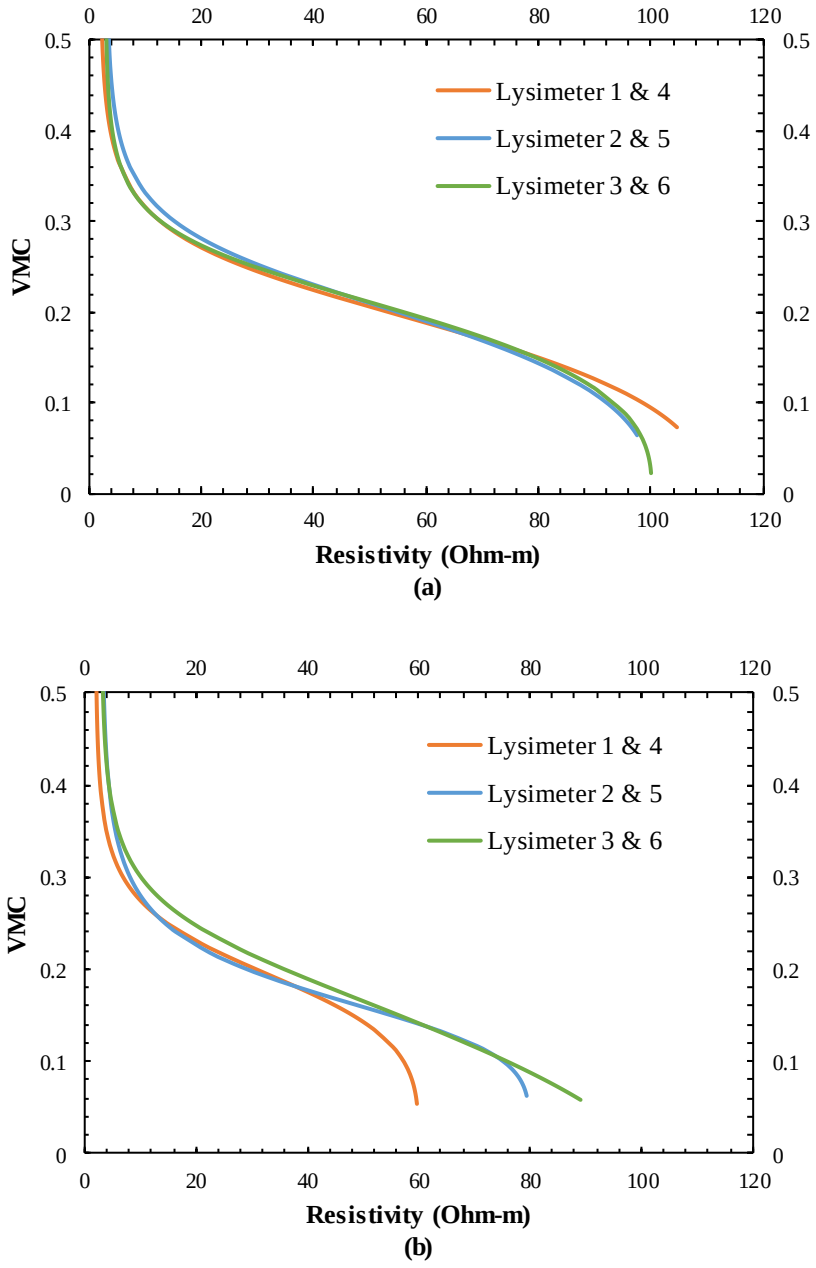

Figure 4.14 Comparison among different FRWCCs (a) at 12-inch depth and (b) at 30-inch depth for different vegetated lysimeters

4.5.3 Development of Field Soil Water Characteristics Curve (FSWCC)

Suction-moisture relationship in the field was found slightly different from the observed relationship in the lab. In lab, SWCC was performed only on remolded soil specimens without any roots. But in an actual field condition, there were root effects along with other environmental factors which influences the SWCC. Again, it was difficult to simulate the field condition with root distribution in laboratory setup. As electrical resistivity can represent both the moisture and suction phenomenon simultaneously in the field, it is proved to be an effective non-destructive alternative way to bridge between field soil suction and moisture. The correlation between VMC and matric suction has been investigated based on the curve matching in terms of soil resistivity as shown in Figure 4.15. The shapes of the curves are similar, and both the curves exhibits non-linear relationship which have been described through Van Genuchten sigmoidal function (1980). A sigmoidal curve contains two break points. The first break point signifies the desaturation and resistivity value starts increasing. The second break point is near the high resistivity value or lower VMC, and after the break point, the rate of increment of resistivity slows down. Therefore, the second break point is termed as residual condition at which water removal from the soil is quite difficult.

Analyzing both the curves, FRWCC and FRSCC, Van Genuchten SWCC model is proposed to establish the field relationship between VMC and matric suction for each of the studied case. The equation for the SWCC model is as follows;

$$\theta = \theta_r + (\theta_s - \theta_r) \left\{ \frac{1}{1 + (\alpha\psi)^n} \right\}^m$$

Where, θ is the volumetric water content in terms of matric suction, ψ, α and n are shape parameters and $m = 1 - 1/n$. From FRSCC and FRWCC, data points of matric suction with corresponding VMC were extracted in terms of resistivity. Later in Minitab, those equivalent data points were used as input parameters for non-linear regression in order to construct SWCC model.

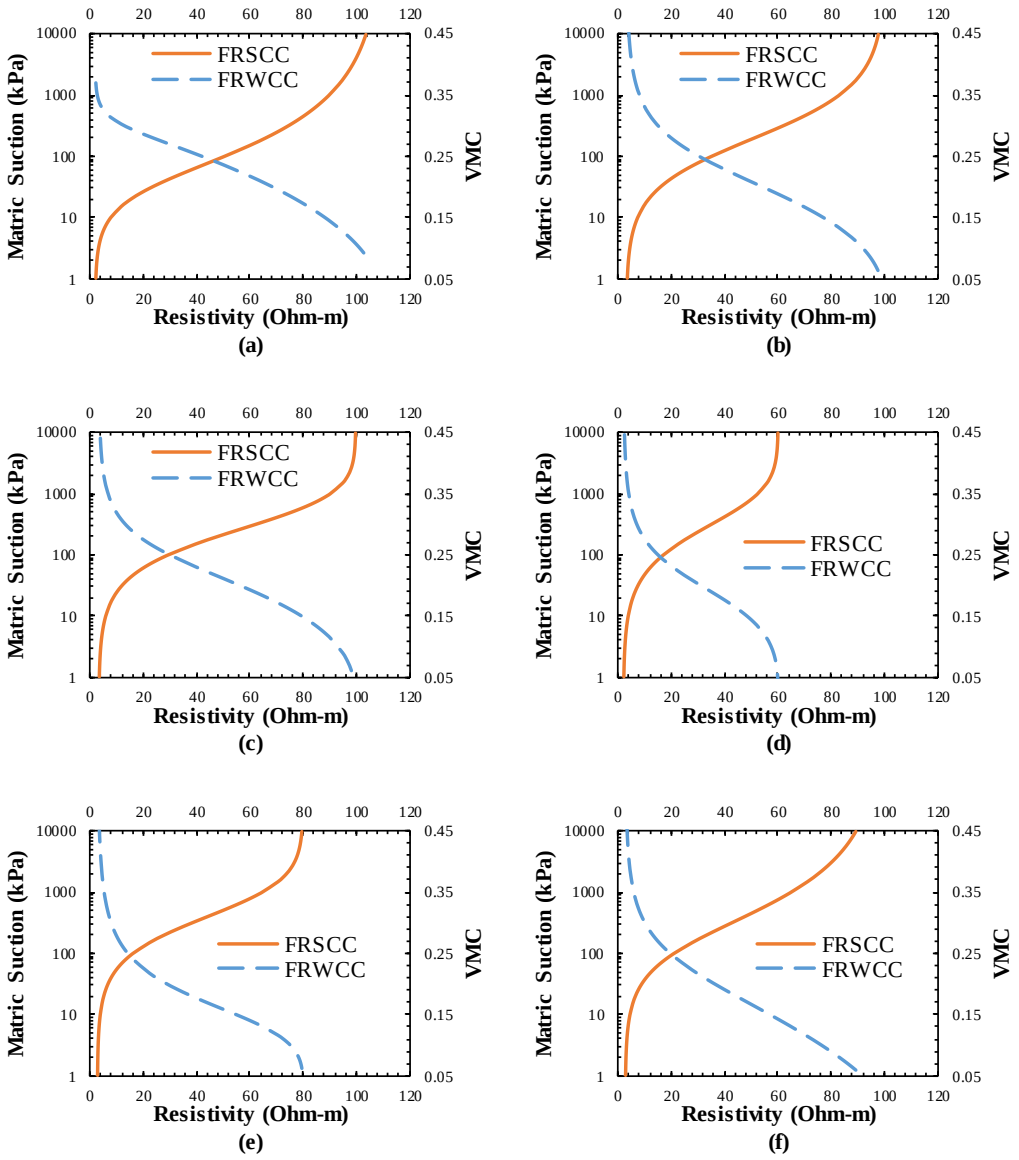

Figure 4.15 Relationship between VMC and matric suction with respect to resistivity for (a) Native Trail grass; (b) Switchgrass; (c) Bermuda grass vegetated soil at 12-inch depth and for (d) Native Trail grass; (e) Switchgrass and (f) Bermuda grass vegetated soil at 30-inch depth

4.5.3.1 FSWCC Coefficient α, n and m

For the development of FSWCC in the form of sigmoidal equation similar to Van Genuchten's (VG) SWCC model, concurrent observations were extracted from two different

sigmoidal equation, FRSCC and FRWCC. As resistivity varies with other factors in addition with suction and moisture, an accurate sigmoidal trend was not followed by the observed datapoints from FRSCC and FRWCC. However, VG SWCC model was found to be a good fit for the observed datapoints.

Table 4.9 FSWCC (at 12-inch depth) coefficient α, n and m with non-linear regression parameters for different vegetated ET cover soil

Vegetation Type	α	n	m	θ_s	θ_r	Standard Deviation (S)	Sum of the Squared Residuals (SSE)	Error Degrees of Freedom (DFE)	Mean Square Error (MSE)
Native Trail grass (Lysimeter 1 & 4)	0.046	1.839	0.456	0.42	0.12	0.1543	1.0476	44	0.0238
Switchgrass (Lysimeter 2 & 5)	0.051	1.638	0.39	0.41	0.12	0.1484	1.0127	46	0.0220
Bermuda grass (Lysimeter 3 & 6)	0.053	1.538	0.35	0.42	0.09	0.1734	1.4134	47	0.0301

Table 4.10 FSWCC (at 30-inch depth) coefficient α, n and m with non-linear regression parameters for different vegetated ET cover soil

Vegetation Type	α	n	m	θ_s	θ_r	Standard Deviation (S)	Sum of the Squared Residuals (SSE)	Error Degrees of Freedom (DFE)	Mean Square Error (MSE)
Native Trail grass (Lysimeter 1 & 4)	0.031	1.774	0.436	0.42	0.12	0.1545	0.9790	41	0.0239
Switchgrass (Lysimeter 2 & 5)	0.029	1.826	0.452	0.41	0.12	0.1014	0.3496	34	0.0103
Bermuda grass (Lysimeter 3 & 6)	0.031	1.667	0.400	0.42	0.09	0.1930	1.6761	45	0.0372

Limiting conditions on volumetric moisture content (VMC) have been applied where saturated VMC, θ_s designates upper limit and residual VMC, θ_r designates lower limit for SWCC. The values of θ_s and θ_r were determined through laboratory testing and described in Table 4.9.

Corresponding Van Genuchten SWCC parameters α, n and m were investigated for each of the studied case and reported in Table 4.9 and Table 4.10 for 12-inch and 30-inch depth, respectively.

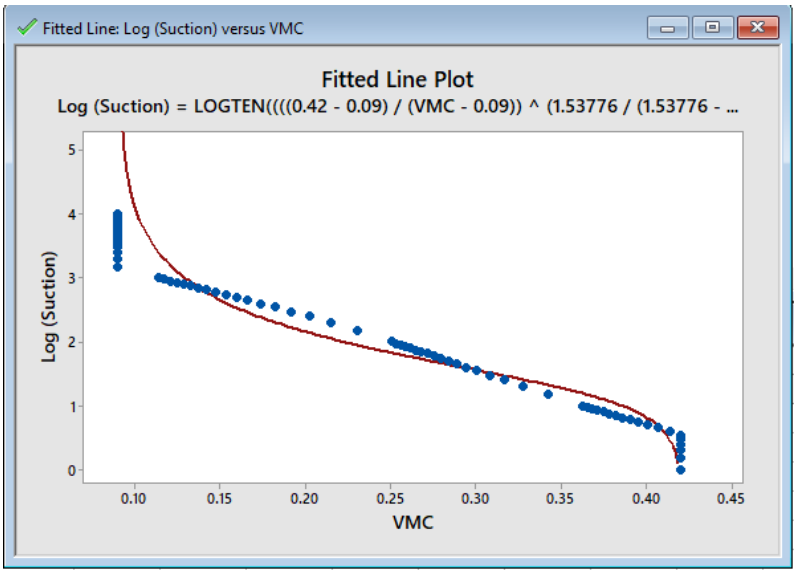

(a)

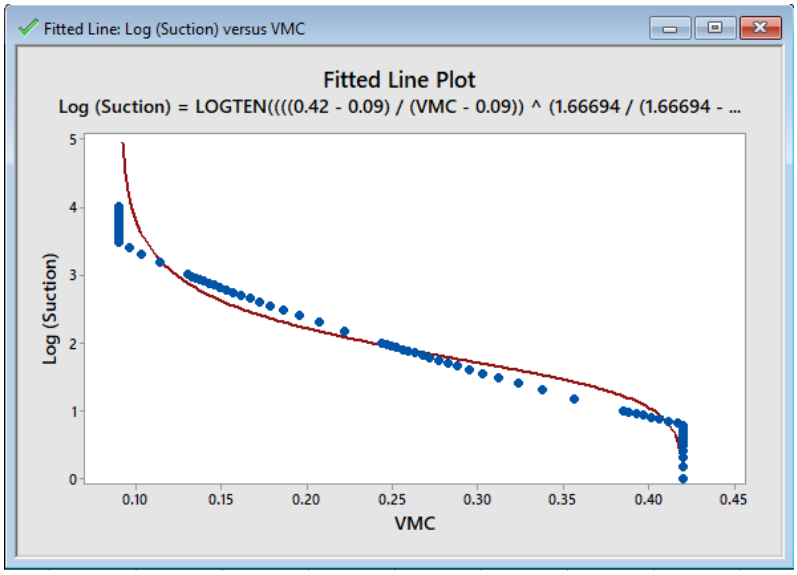

(b)

Figure 4.16 Predicted FSWCC using Minitab for Bermuda grass vegetated ET cover soil (a) at 12-inch depth and (b) at 30-inch depth

Figure 4.16(a) and 4.16(b) illustrates the established SWCC for Bermuda grass vegetated ET cover soil at 12-inch and 30-inch depth, respectively, using Minitab from equivalent VMC and soil suction data points after applying boundary conditions over VMC. FSWCCs for other vegetations were constructed in the similar manner. However, the standard deviation of FSWCC from the equivalent data points for all the three types of vegetation at 12-inch depth was found to vary between 0.148 to 0.173 which shows a good fit of the established model. Mean square errors were found between 2.2% to 3% for all types of vegetated lysimeters. Again, for 30-inch depth analysis, the standard deviation was found to vary between 0.101 to 0.193 which represents a well competency of the established FSWCC model. Mean square errors were also limited between 1.03% to 3.72% for all types of vegetation.

The value of α approximates the inverse of air entry suction (Ψ_b) value of the corresponding soil and is measured in the inverse units of pressure. Ψ_b is defined by the matric suction at which air starts to penetrate into the soil. It is also named as bubbling pressure (Corey, 1977). A lower value of α causes upward shifting of the FSWCC curve. At 30-inch depth, α value was found to be 0.031 (kPa^{-1}), 0.029 (kPa^{-1}) and 0.031 (kPa^{-1}) for Native Trail grass, Switchgrass and Bermuda grass vegetated soil, respectively. Again, at 12-inch depth, α value was found to be 0.046 (kPa^{-1}), 0.051 (kPa^{-1}) and 0.053 (kPa^{-1}) for above mentioned vegetated soil, respectively, which was found to be higher compared to the α values observed in 30-inch depth. Thus, the approximate Ψ_b for Native Trail grass, Switchgrass and Bermuda grass vegetated soil at 12-inch depth was found to be 21.74, 19.61 and 18.87 kPa, respectively, whereas for 30-inch depth it was found to be 32.26, 34.48 and 32.26 kPa respectively. Again, due to the environmental exposure, continuous wet dry cycle and vegetation root effect, larger voids were created in the upper 12-inch zone compared to the bottom 30-inch depth. As a result, bottom zone was more compacted and experienced relatively less disturbance. So, the higher soil density at the bottom depth is accountable for that higher Ψ_b

compared to the top layer. Table 4.11 represents the Ψ_b value for different vegetated lysimeters at two different depths of study.

Table 4.11 Ψ_b for different lysimeters at 12-inch and 30-inch depth

Lysimeter	Ψ_b (at 12-inch depth)	Ψ_b (at 30-inch depth)
	(kPa)	(kPa)
1 & 4	21.74	32.26
2 & 5	19.61	34.48
3 & 6	18.87	32.26

The n parameter is associated with the pore size distribution of the soil. At a certain moisture content, a lower value of n refers to a higher suction value when air entry suction remains unchanged. At 12-inch depth, n value was found to be 1.839 for lysimeters covering Native trail grass, whereas at 30-inch depth, the value was 1.774. However, a higher suction was observed at the bottom depth at a range of VMC between 0.16 to 0.42 (Figure 4.17a). A higher Ψ_b for the bottom depth soil was accountable for that increase in suction within that range of VMC. Again, the value of parameter n was found to be lower at that depth. At VMC below 0.17, suction was found almost similar for Native Trail grass vegetated soil. This phenomenon was found to be quite similar for other vegetated lysimeters also. On the other hand, parameter m is associated with the overall symmetry of the characteristic curve and when it is constrained by parameter n, it reduces the flexibility of the VG model and compromises with the accuracy of the best fit but results in greater stability during parameter optimization and permits closed form solution of the hydraulic conductivity function (Van Genuchten et al., 1991). However, in this study, parameter m was considered dependent on the value of n.

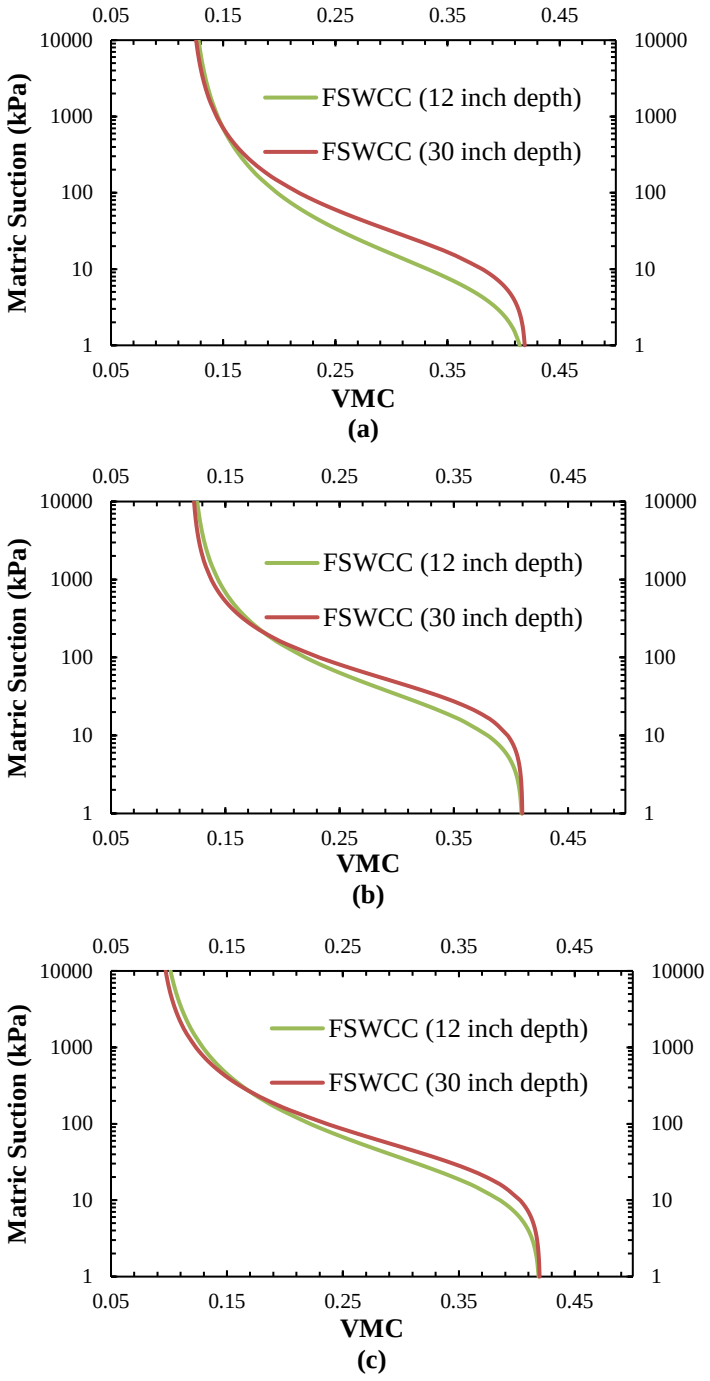

Figure 4.17 Predicted FSWCC for (a) Native Trail grass, (b) Switchgrass and (c) Bermuda grass vegetated ET cover soil at 12-inch and 30-inch depth

Figure 4.17(a), 4.17(b) and 4.17(c) represent the predicted FSWCC for Native Trail grass, Switchgrass and Bermuda grass vegetated lysimeters respectively with a comparison in between for two different depths of study. In lab, Ψ_b was observed between 80 to 180 kPa, while from FSWCC for all the vegetations at 12-inch and 30-inch depth, Ψ_b was found to vary between 18 to 35 kPa which is significantly lower compared to the observations in lab.

Data Validation

A new set of moisture and suction data for lysimeter 1 and lysimeter 4 at 12-inch and 30-inch depth were selected and plotted against the corresponding FSWCC. Figure 4.18 (a) and Figure 4.18 (b) illustrates field observation of VMC and related matric suction with FSWCC for native trail grass vegetated soil at 12-inch depth and 30-inch depth, respectively. An upper bound (UB) and lower bound (LB) of SWCC were also selected to describe the variation of the field data with the developed FSWCC. Table 4.12 and Table 4.13 describes the FSWCC fitting parameters along with UB and LB values for Native Trail grass vegetated soil at 12-inch and 30-inch depth, respectively.

Table 4.12 Fitting parameters of the proposed FSWCC for lysimeter 1 and 4 at 12-inch depth

Predicted SWCC	α	n	m	θ_s	θ_r
Upper Bound	0.026	1.750	0.429	0.42	0.12
FSWCC	0.046	1.839	0.456	0.42	0.12
Lower Bound	0.084	1.880	0.468	0.42	0.11

For 12-inch depth, the value of α parameter was found in the range of 0.026 to 0.084 (kPa^{-1}) to accommodate the field data within the range. From the developed FSWCC, the value of α parameter was found to be 0.046 (kPa^{-1}) which corresponds to a Ψ_b value of 21.74 kPa. From the UB and LB values, the range of Ψ_b was found between 11.90 to 38.46 kPa. So, the Ψ_b value for Native Trail grass vegetated soil was found to vary between 0.55 to 1.77 times of the observed value from FSWCC at 12-inch depth based on the selected field dataset.

Table 4.13 Fitting parameters of the proposed FSWCC for lysimeter 1 and 4 at 30-inch depth

Predicted SWCC	α	n	m	θ_s	θ_r
Upper Bound	0.022	1.680	0.405	0.43	0.12
FSWCC	0.031	1.774	0.436	0.42	0.12
Lower Bound	0.055	1.820	0.451	0.42	0.11

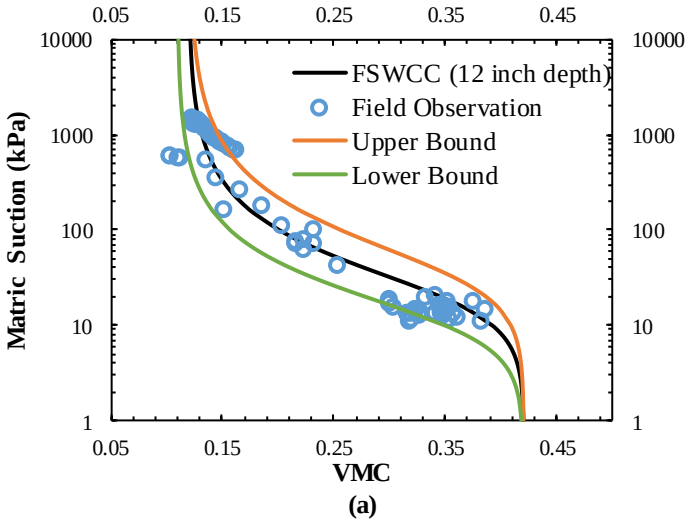

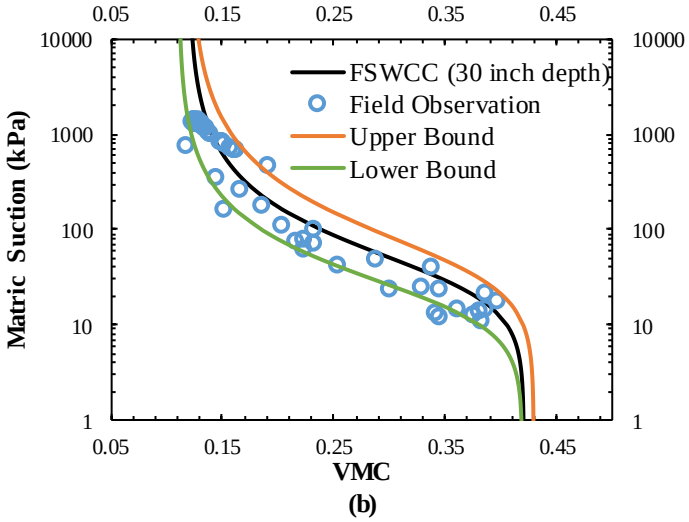

Figure 4.18 Predicted FSWCC for Native Trail grass vegetated soil lysimeters at (a) 12-inch and at (b) 30-inch depth with field observation

Again at 30-inch depth, Ψ_b was found to be 32.26 kPa from the developed FSWCC for Native Trail grass vegetated soil. From the UB and LB values at 30-inch depth, the range of Ψ_b was found between 18.18 to 45.45 kPa. So, at 30-inch depth for lysimeter 1 & 4, Ψ_b was found to vary between 0.56 to 1.41 times of the observed value from developed FSWCC, based on the selected field dataset. The range of variation of Ψ_b was found higher at top soil layer due to the disturbance caused by surrounding environment and variation in soil density.

4.5.3.2 Field Capacity (FC)

Field Capacity is defined by the amount of soil moisture or water content held in the soil after excess water has drained away and the rate of downward movement has decreased. FC is measured by the equivalent water depth in the soil mass. Typically, FC water content is estimated from the VMC at 33 kPa soil suction. However, soil suction corresponding to field capacity is subjected to changes at different climatological condition and different soil texture. In this study, typical condition is assumed for the analysis. FC of the ET cover soil depends on its thickness as it is estimated by multiplying the obtained VMC at 33 kPa soil suction by its cover depth. Average Field capacity was determined from the developed FSWCC for different vegetation and for three different cover soil thickness (4 ft, 3.5 ft and 3 ft) and presented in Table 4.14. For example, VMC at 12-inch depth for Bermuda grass on ET cover soil was found to be 0.31 and at 30-inch depth was found to be 0.34 from FSWCC at 33 kPa soil suction. Average FC water content was assumed in a way that VMC of 0.31 exists uniformly throughout the top 12-inch depth and average VMC of 0.31 and 0.34 exists uniformly throughout the latter depth of concern. Average field capacity is then obtained by the summation of multiplication of the average VMC with the concerned depth up to the total depth of concerned. It was found that FC decreases with decreasing ET cover thickness. It was obvious because with decreasing soil thickness, soil mass was also reduced, thus caused reduction in water holding capacity. Average FC was found almost similar for different vegetated soil.

Table 4.14 Average FC for ET cover soil of different thickness with different vegetation

Vegetation Type	Average FC (inch)/ 4 ft cover soil	Average FC (mm)/ 4 ft cover soil	Average FC (inch)/ 3.5 ft cover soil	Average FC (mm)/ 3.5 ft cover soil	Average FC (inch)/ 3 ft cover soil	Average FC (mm)/ 3 ft cover soil
Native Trail grass (Lysimeter 1 & 4)	15.05	382.27	13.14	333.76	11.23	285.24
Switchgrass (Lysimeter 2 & 5)	15.07	382.778	13.16	334.26	11.25	285.79
Bermuda grass (Lysimeter 3 & 6)	15.27	387.858	13.34	338.82	11.41	289.74

Comparison of field obtained FC with laboratory determined FC

FC capacity observed from FSWCC developed through ERI technique was found to be lower than what was observed in the lab using pressure cell apparatus. In laboratory setup, the soil samples were uniformly compacted, and the test was conducted on remolded soil with no plant roots. But in the actual field condition, at the top 12 to 15-inches soil density was reduced due to environmental exposure, frequent wet dry cycle and presence of plant roots compared to the bottom depth, where it was more compacted and subjected to less disturbance. This reason is accountable for the lower value of FC in actual field condition than the laboratory observation which was overestimated to around 21 to 23% (Table 4.15).

Table 4.15 Comparison between field obtained FC and laboratory determined FC

Average Field Capacity (inch)/ 4 ft of cover soil			
Lysimeter	From Lab based SWCC	From FSWCC	Variation (%)
1 & 4	19.07	15.05	21.08
2 & 5	19.41	15.07	22.36
3 & 6	19.88	15.27	23.19

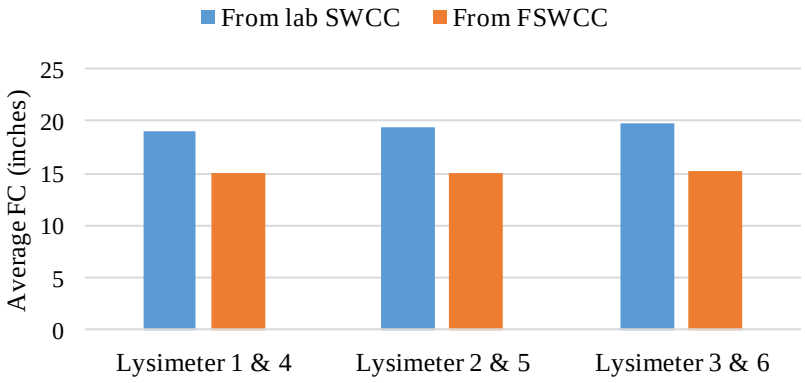

Figure 4.19 Variation of FC between lab testing outcomes and field observation through ERI technique

4.5.3.3 Permanent Wilting Point (PWP)

Permanent wilting point refers to the minimal amount of water that soil needs to hold for the plants not to wilt. Typically, PWP water content is estimated from the VMC at 1500 kPa soil suction. However, it depends on the vegetation type and soil texture. In this study, conventional assumptions are applied to estimate PWP. Soil water storage at PWP for 4 ft, 3.5 ft and 3 ft cover soil thickness was estimated in a similar way as average field capacity determination and summarized in Table 4.16 for different vegetation of study.

Table 4.16 SWS at PWP for different vegetation on ET cover soil

Vegetation Type	SWS at PWP (inch)/ 4 ft cover soil	SWS at PWP (mm)/ 4 ft cover soil	SWS at PWP (inch)/ 3.5 ft cover soil	SWS at PWP (mm)/ 3.5 ft cover soil	SWS at PWP (inch)/ 3 ft cover soil	SWS at PWP (mm)/ 3 ft cover soil
Native Trail grass (Lysimeter 1 & 4)	6.30	160.02	5.50	139.70	4.71	119.63
Switchgrass (Lysimeter 2 & 5)	6.68	169.61	5.84	148.29	5.00	126.97
Bermuda grass (Lysimeter 3 & 6)	5.41	137.41	4.72	119.85	4.03	102.30

4.5.3.4 Plant Available Water (PAW)

Plant available water is defined by the amount of water held in the soil between FC and PWP. Table 4.17 summarizes the PAW storage for different vegetation and different cover thickness of ET cover soil.

Table 4.17 PAW storage for different vegetation on ET cover soil

Vegetation Type	PAW storage (inch)/ 4 ft cover soil	PAW storage (mm)/ 4 ft cover soil	PAW storage (inch)/ 3.5 ft cover soil	PAW storage (mm)/ 3.5 ft cover soil	PAW storage (inch)/ 3 ft cover soil	PAW storage (mm)/ 3 ft cover soil
Native Trail grass (Lysimeter 1 & 4)	8.75	222.25	7.64	194.06	6.52	165.61
Switchgrass (Lysimeter 2 & 5)	8.39	213.17	7.32	185.97	6.25	158.81
Bermuda grass (Lysimeter 3 & 6)	9.86	250.45	8.62	218.96	7.38	187.44

4.6 Soil Water Storage (SWS) Evaluation

Soil water storage is defined by the storage of precipitation in the soil profile. Thus, a larger value of SWS indicates to the minimization of the percolation, which is a vital performance indicator for any ET cover soil. SWS is a function of the surface area of the soil particles and the amount of porosity occurring between these particles. SWS is measured by the average amount of water per unit cross sectional area that the soil is holding at a particular time. Again, soil water storage capacity refers to the maximum amount of water that the soil can hold. ET cover follows water store release principal to restrict the precipitation from becoming percolation through the bottom of the soil layer. From the water balance concept, if precipitation occurs, a certain amount of precipitation infiltrates into the soil body after runoff and was added to the existing SWS in the soil body after the precipitation. Evapotranspiration causes continuous release of a certain portion of that SWS into the environment. If at a certain point of time, SWS of a cover soil exceeds its FC, the additional amount

infiltrates from the bottom of the soil body in the form of percolation which needs to be controlled for proper management of the ET cover soil. Thus, SWS needs to be monitored on a regular basis for continuous evaluation of ET cover system performance. In this study, average SWS were calculated from the installed moisture sensors at different depths of the ET cover soil. Field ERI test was performed concurrently and unit cross sectional area resistance, ρ_a, was determined. Temperature correction on resistivity was done before estimating ρ_a. An inverse relationship between average SWS and ρ_a was observed for different ET cover soil thickness. All the dataset for different vegetation were grouped together in this case for average SWS determination.

4.6.1 Measurement of SWS from Sensors

Average SWS was determined at different times throughout the study period using moisture sensors installed at different depths. For the design of any advanced ET cover system, it is necessary to identify the variation of SWS with depth as the design thickness depends on the water storage capacity of the soil. In this study, average SWS was determined for 4 ft, 3.5 ft and 3 ft cover soil. It was observed that with decreasing depth of the cover soil, average SWS was also decreased (Figure 4.20). In this case, uniform distribution of average VMC is assumed throughout the distance between the two successive moisture sensors in vertical direction. Deviations in the measured average SWS from the actual condition may happen due to the non-uniform dispersion of the moisture throughout the entire cover soil area.

4.6.2 Measurement of SWS from Soil Resistivity

Typically, SWS was measured using sensors buried at different depths in a cover soil. But the main drawbacks associated with sensor technique are, they damage with time and only offers measurements at the installation points. Replacement of the sensors is also costly and time consuming, and again, soil structure is subjected to disturbance during the installation and replacement of those sensors. As soil resistivity changes with the variation of soil moisture, ERI test was proved to be an effective alternative way to measure that variation in terms of SWS; thus,

removing the problems related with the sensor technique. ERI test was performed on a monthly basis to observe the variation of SWS. It was found that electrical resistivity changes with depth. To represent the entire moisture variation up to the total cover thickness, entire soil length in vertical direction was divided into some integral distance where it was assumed that resistivity was uniform throughout that distance. To quantity the entire soil resistivity up to the total depth of the cover soil, unit cross sectional area resistance, ρ_a, was determined. In this study, resistivity value was extracted from the resistivity log at the location of the sensors and it was assumed that average resistivity was uniformly distributed between the distance of the two co-located sensors. Figure 4.20(a), 4.20(b) and 4.21 represent the variation of SWS with ρ_a assuming 4 ft, 3.5 ft and 3 ft cover soil thickness, respectively. It was found that with increasing ρ_a, SWS decreases following a logarithmic trend. Based on non-linear regression analysis, best fitted relationship between SWS and ρ_a was established in both millimeter and inch scale with statistical coefficient of determination (R^2) and displayed in the corresponding figures. The value of R^2 was found in the range of 0.84 to 0.86 for all of the studied cases, which exhibits a good correlation between the concerned parameters. The higher value of ρ_a indicates the residual condition where SWS tends to be almost constant and the lower value of ρ_a indicates the saturated condition where SWS reaches beyond the FC; thus, percolation initiates from the bottom. From the lab scale measurement of SWCC, average FC for all of the lysimeters was found to be 19.45 inches (494 mm) and from field scale measurement through ERI technique, it was found to be 14.41 inches (366 mm) for 4 ft of cover thickness. Thus, from the established relationship between SWS and ρ_a for 4 ft of cover thickness (Figure 4.20a), a range of critical ρ_a was found between 5.92 to 16.18 ohm-m^2 which indicates the soil is closed to its FC and highly susceptible to initiation of percolation.

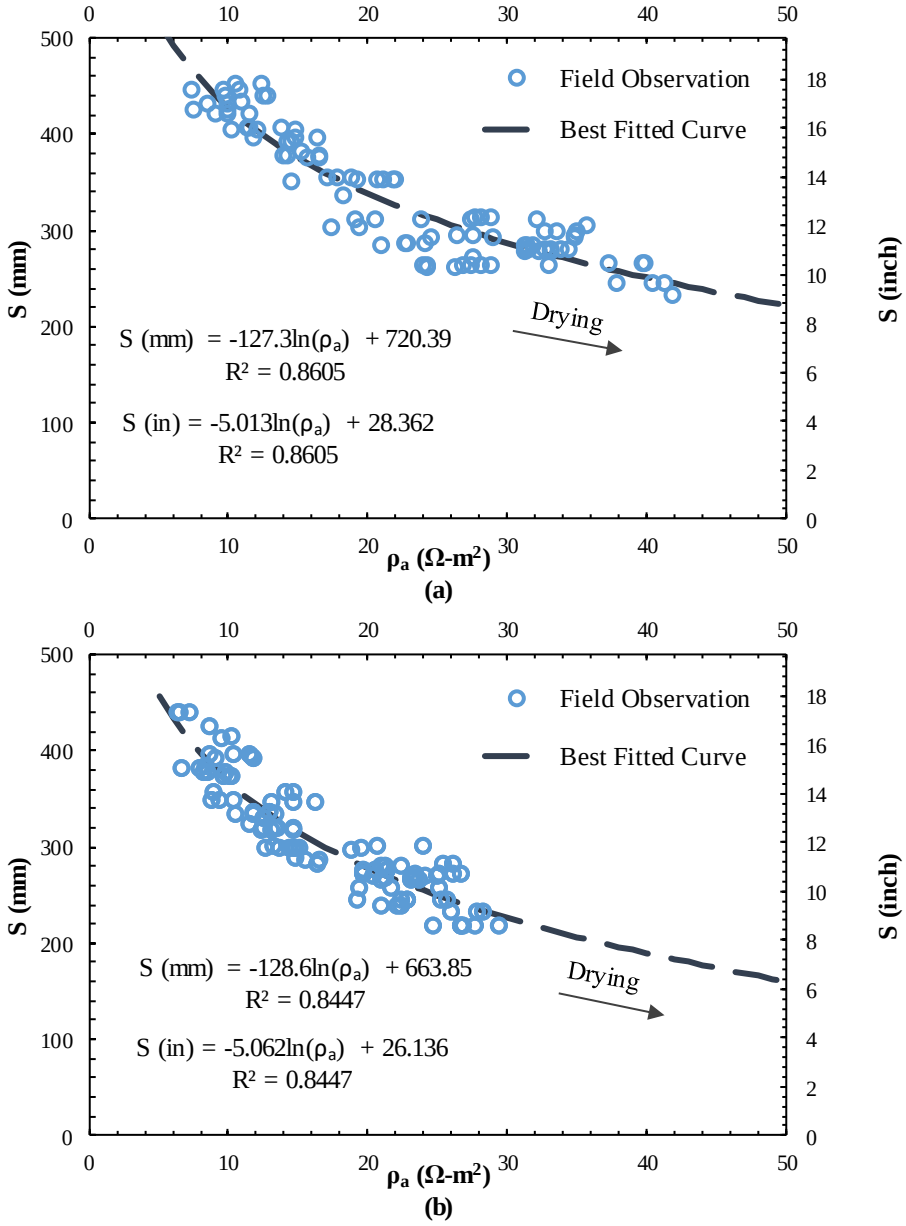

Figure 4.20 Relationship between soil water storage and unit cross sectional area resistance with field observation for (a) 4 ft and (b) 3.5 ft cover soil thickness

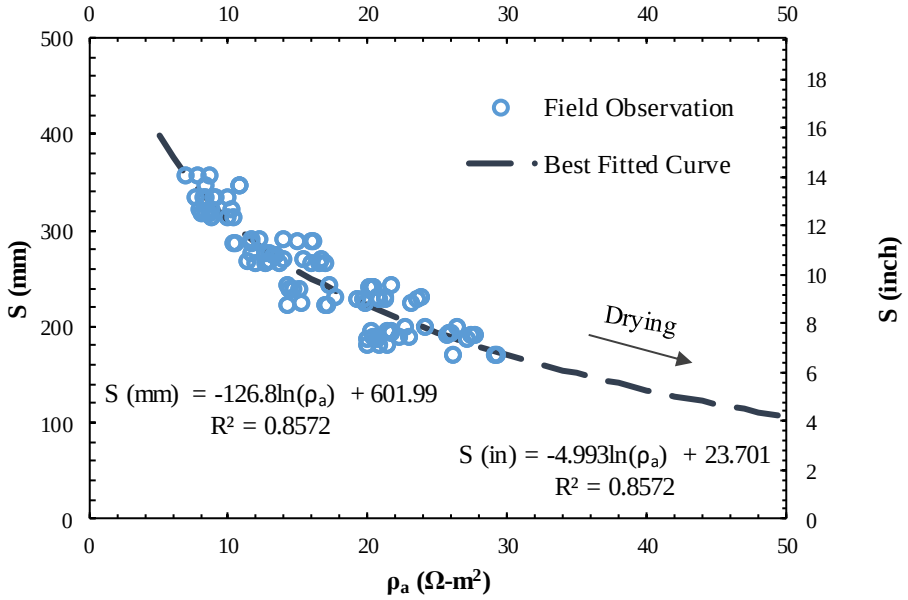

Figure 4.21 Relationship between soil water storage and unit cross sectional area resistance with field observation for 3 ft cover soil thickness

The value of saturated ρ_a was observed to be around 5 to 8 Ohm-m^2 whereas residual ρ_a was found to be around 50. FC of the cover soil for 4 ft thickness was observed to be around 380 mm on average from FSWCC for different vegetations. But the saturated SWS was found to be around 500 to 550 mm from the extension of the SWS curve with ρ_a, for 4 ft cover soil. So, the range between 380 to 550 mm of SWS indicates the initiation of percolation through the bottom of the soil. Figure 4.22 represents the variation of SWS with the changes in ET cover soil thickness in terms of ρ_a. It was observed that SWS decreases with decreasing cover soil thickness at a particular ρ_a. It was obvious because soil mass retains moisture through soil suction in unsaturated condition, but with decreasing thickness, the amount of soil was also reduced resulting decrease in moisture holding capacity. But the variation of SWS with cover soil thickness is proved to be an important design criterion as ET cover thickness selection depends on the required soil water storage capacity which is site specific and varies with the onsite precipitation history.

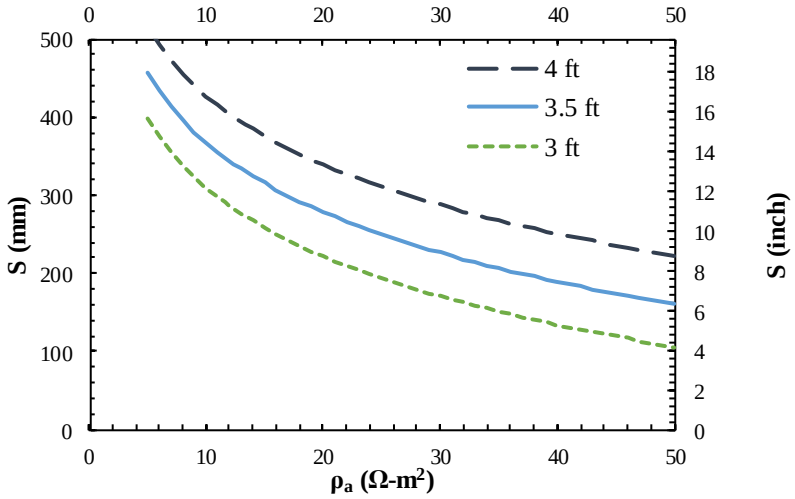

Figure 4.22 Variation of SWS with ρ_a for different ET cover soil thickness

4.6.3 Evaluation of Soil Moisture Retention Capacity

Soil moisture retention capacity (SMRC) refers to the FC which represents the maximum amount of water that soil can hold without having percolation. A greater value of SMRC refers to an improved performance for any ET cover system. SMRC depends on the soil texture, field density and field soil suction-moisture relationship which are subjected to change with time. For the performance analysis of an ET cover system, SMRC needs to be assessed in a regular manner. Again, existing soil moisture retention capacity (ESMRC) is another term which is defined by the difference between FC and existing SWS at a particular time. If SWS at a certain time reaches the FC of the soil, percolation will initiate from the bottom at that point of time. Thus, ESMRC refers to the additional amount of water after existing SWS that soil can hold at a certain time before percolation. ESMRC was determined for three different ET cover soil thickness through ERI technique. As FC was found almost similar for different vegetated lysimeters, the dataset from different lysimeters were grouped together for the evaluation of ESMRC. Average FC obtained from ERI technique was considered for the analysis of ESMRC.

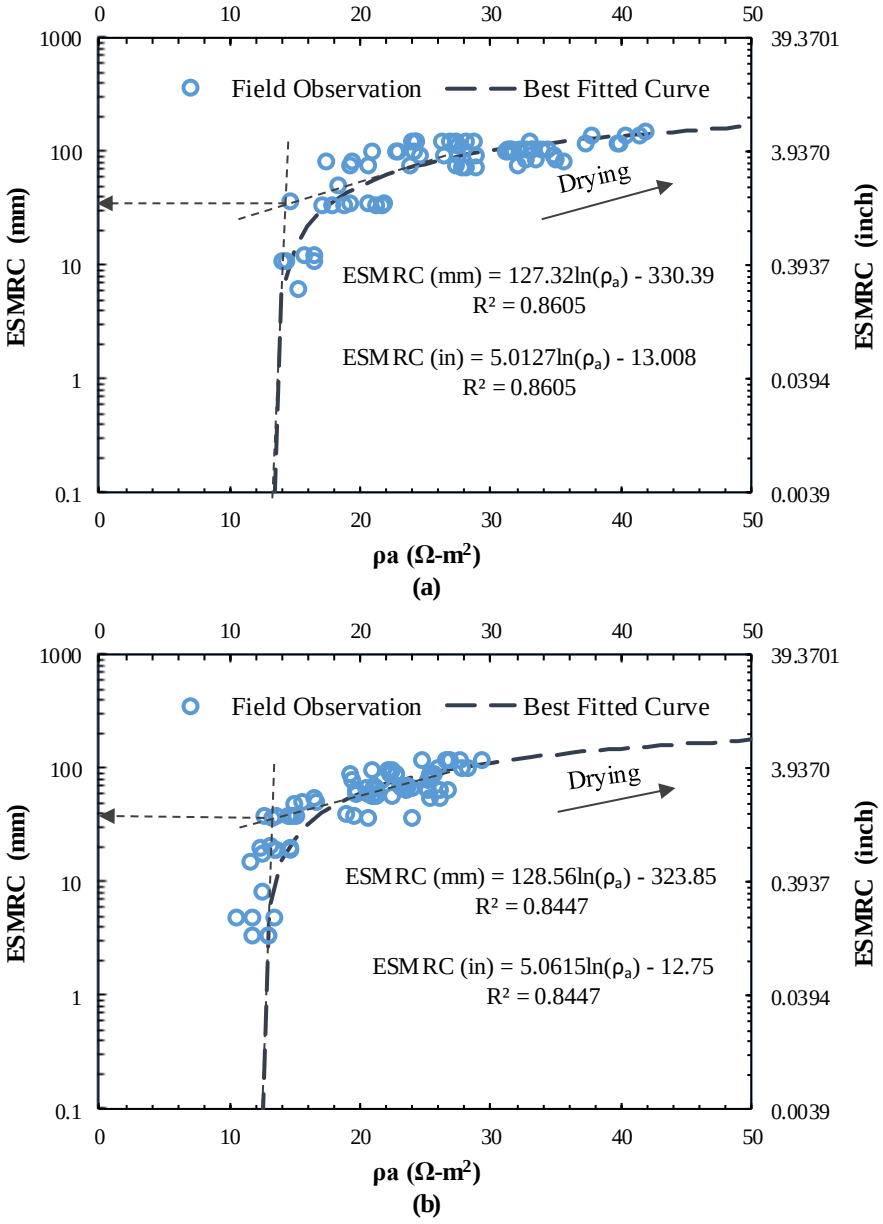

Figure 4.23 Relationship between ESMRC and ρ_a for (a) 4 ft and (b) 3.5 ft thickness of ET cover soil

From the water balance concept, if runoff and evapotranspiration remain constant, a higher value of ESMRC denotes a higher amount of precipitation the soil can store without percolation and a lower value of ESMRC denotes a higher chance of percolation after precipitation. Existing SWS

at a particular time was determined through the readings obtained from the moisture sensors at that time. Average FC was determined from the developed FSWCC for different vegetation through ERI test. The variation of ESMRC with ρ_a is presented in Figure 4.23(a), 4.23(b) and Figure 4.24 for 4 ft, 3.5 ft and 3 ft thickness of ET cover soil, respectively. The best fitted correlations between ESMRC and ρ_a for different cover thicknesses were also established and displayed in the related figures with corresponding coefficient of determination (R^2). The value of R^2 was found in the range of 0.84 to 0.86 which exhibits a good correlation between them.

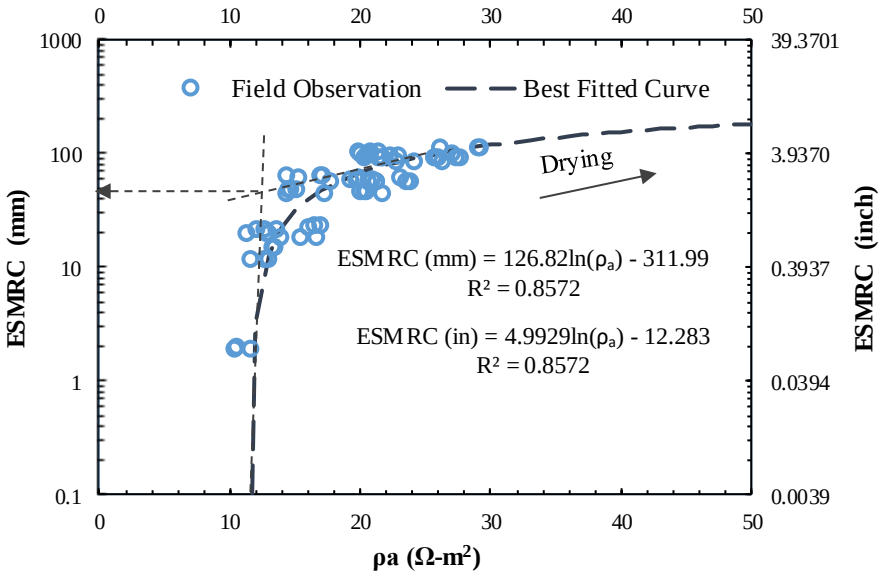

Figure 4.24 Relationship between ESMRC and ρ_a for 3 ft thickness of ET cover soil

The relationship between ESMRC and ρ_a was established considering the data extracted from all of the lysimeters, thus denoting the average measurements for all types of vegetated soil. A threshold point of ρ_a was found at around 16 ohm-m^2 for all of the cover thicknesses of concern which corresponds to an ESMRC of around 40 mm. Below that point, ρ_a decreases drastically towards saturation. A critical point of ρ_a was found at around 12 ohm-m^2 at which the SWS was found to reach its FC. At that point, ESMRC was found to be close to zero which means the soil can

no longer hold any additional precipitation, thus, a drop of additional precipitation will be drained away from the bottom of the soil layer at that point. ESMRC can be explained by the amount of precipitation at a particular time. The annual average precipitation of 2015 and 2016 were recorded to be 1511.3 mm (59.5 inches) and 1333.5 mm (52.5 inches) from onsite weather station. In the month of May 2015, an average precipitation was found to be 60 mm. A certain portion of it was infiltrated into the soil body after runoff and added with the existing SWS at that particular time. The existing average SWS on 13th May 2015 was found to be around 330 mm (13 inches) with corresponding ρ_a of 21.47 Ohm-m^2. At that point ESMRC for 4 ft cover soil was found to be around 57 mm from the developed curve (Figure 4.23a) which indicates that the soil can absorb around 57 mm of additional moisture before percolation at that particular point of time. At that time no percolation was recorded which means more than 3 mm of the precipitation was released to the environment in the form of runoff and evapotranspiration.

Chapter 5

Conclusions and Recommendations

5.1 Summary and Conclusions

The unsaturated behavior of the ET cover soil located at the City of Denton MSW landfill was monitored for a period of 3.5 years starting from January 2015 to June 2018. ERI test was performed on a monthly basis throughout the study period across the installed sensors' location in all of the lysimeters. Concurrent readings from the sensors were observed simultaneously. All of the observations were subdivided by the vegetation type and depth (12-inch and 30-inch). Temperature correction was employed to the raw resistivity values which were extracted from the obtained resistivity log profile. From the field observations of soil suction and moisture content with concurrent resistivity, field resistivity suction characteristic curve (FRSCC) and field resistivity water characteristic curve (FRWCC) were developed for different types of vegetation at 12-inch and 30-inch depth. From the obtained FRSCC and FRWCC, field soil water characteristic curve (FSWCC) was established in terms of resistivity. All of the associated curve fitting parameters along with statistical variables were determined using Minitab. Average field capacity (FC), permanent wilting point (PWP) and plant available water (PAW) were determined from the developed FSWCC for the studied ET cover soil under different vegetations. Soil water storage (SWS) was estimated from the observations through installed moisture sensors at various depths indifferent to the types of vegetation. Variation of SWS with unit cross sectional area resistance (ρ_a) for three assumed thicknesses of ET cover soil; 4 ft, 3.5 ft and 3 ft, was estimated and best fitted correlations were developed. General conclusions that are obtained from the observations are provided below.

- Top 12-inch zone of the cover soil was subjected to high electrical resistivity at dry season compared to the bottom 30-inch depth. Environmental exposure of the top soil layer and evapotranspiration from the top root zone were accountable for the top soil layer to be drier resulting high resistivity compared to the bottom zone without root effects.

- Resistivity increases with increasing soil suction and decreases with increasing moisture content. Both of the relations follow a sigmoidal trend similar to Van Genuchten's SWCC model.
- The first break point of the FRSCC for 12-inch depth was found at suction of around 40 kPa for all types of vegetated lysimeters while for 30-inch depth it was found at around 80 kPa. As the soil at bottom depth was more compacted relative to the top soil layer, the difference in soil density between these two depths may be accountable for that discrepancy. A sharp decrease in matric suction was observed below that break point.
- The first break point of the FRWCC for 12-inch depth was found around at a VMC of 0.32 whereas for 30-inch depth it was found around at a VMC of 0.25. Differences in compaction level between these two depths may be accountable for that discrepancy.
- The second break point of the FRWCC represents the dry situation and it was found around at a VMC of 0.09 for both the depths. After that point, resistivity value approaches towards its residual limit.
- Average field capacity of the ET cover soil of 4 ft thickness was found around 15 inches for all types of vegetated soil from ERI technique whereas from lab constructed SWCC, it was found around 19 inches for all lysimeters. In lab, the SWCC test was conducted on uniformly compacted soil whereas in field, soil compaction varied throughout the depth. Again, in field, the soil integrity was affected at the top soil layer due to the root distribution and continuous environmental exposure which may be accountable for that discrepancy.
- Soil suction and corresponding moisture content data were generated from two other sigmoidal equations in terms of resistivity and the observed dataset was not followed by an exact sigmoidal trend. However, FSWCC similar to Van Genuchten's SWCC model was statistically generated to describe the observation and a good correlation was found with a low standard deviation.

- As the study area was located in a semi-humid region, temperature variation was significant and field resistivity was substantially influenced by that temperature variation before temperature correction.
- SWS showed an inverse relationship with unit cross sectional area resistance (ρ_a) as with increasing soil resistivity, moisture content of the soil mass decreases.
- At ρ_a of around 12 ohm-m^2, SWS was found to be close to the soil field capacity. If corresponding ρ_a goes below the field capacity, it indicates the initiation of percolation which means one drop of additional precipitation will be drained away from the bottom of the ET cover soil. Hence, ERI technique is proved to be an effective tool to monitor the ET cover performance by measuring the probable percolation occurrence.
- It was found that increased cover thickness increases average SWS which proved to be a significant designing parameter for any ET cover thickness selection depending on the onsite precipitation history.
- At high resistivity, SWS tends to be almost constant and the curve of SWS vs. ρ_a becomes almost flat in high resistivity zone designating the residual condition.
- ESMRC showed an inverse logarithmic trend with changes in ρ_a. Thus, decrease in resistivity indicates towards lower amount of precipitation that an existing soil can store at a particular point of time without having any percolation; thus, increasing the chances of percolation.
- The curve of ESMRC becomes flat in the high resistivity zone referring the maximum point has been reached. The soil can store precipitation as much as its field capacity at this point.

5.2 Future Aspects of Current Research

During the investigations of the current research, several topics were identified for the future analysis. Some of them were:

- Field resistivity value not only depends on the onsite moisture-suction relationship but also depends on the presence of onsite chemical and biological components. As the study was done

on top of a landfill intermediate cover, ionic effects due to the presence of chemical and biological compounds may mislead some of the observations. Thus, a future study should be done on the effects of those compounds on the field soil resistivity.

- FSWCC was predicted using Van Genuchten's SWCC model (1980) which was found to be a good fit. But there are other proposed models; such as Brook and Corey model (1964), Fredlund and Xing model (1994) etc. which need to be assessed in measuring the competency of the developed curve.
- Installed sensors below the ground only provide point measurements of the data which sometimes may mislead the actual condition. Therefore, a comprehensive study of the whole scenario should be done to predict the actual field condition.
- SWS for bare soil without vegetation should be studied for drawing the comparison between vegetated and non-vegetated soil in terms of SWS evaluation.
- Relative humidity in the surrounding environment also affects the soil suction. Hence, a future study should be done on the effects of relative humidity on FSWCC and ESMRC.
- As increasing soil density hinders the root growth into the soil, there was no significant effect of roots beyond 12-inch depth. Hence, comparison should be made in terms of SWS evaluation if the soil density is kept under allowable limit for encouraging root growth beyond the studied depth.
- There are several computer programs such as HYDRUS, HELP, UNSAT-H, VADOSE/W etc. which can estimate the water balance components of the ET cover system. Therefore, a comparison may be done to the observed SWS from the current study with the computer simulated outcomes considering the similar site conditions existed in the current study.

APPENDIX A

RESISTIVITY IMAGING RESULTS

RI Test Results on Native Trail grass (Lysimeter 1)

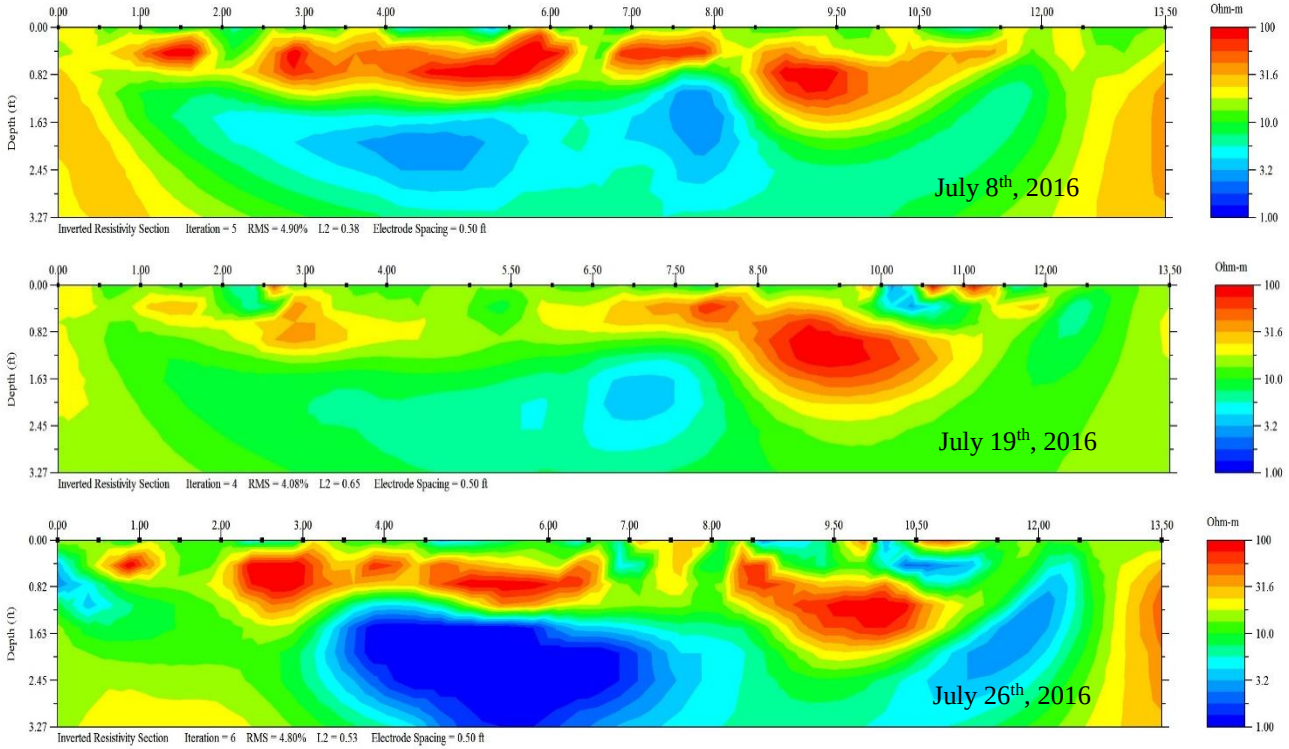

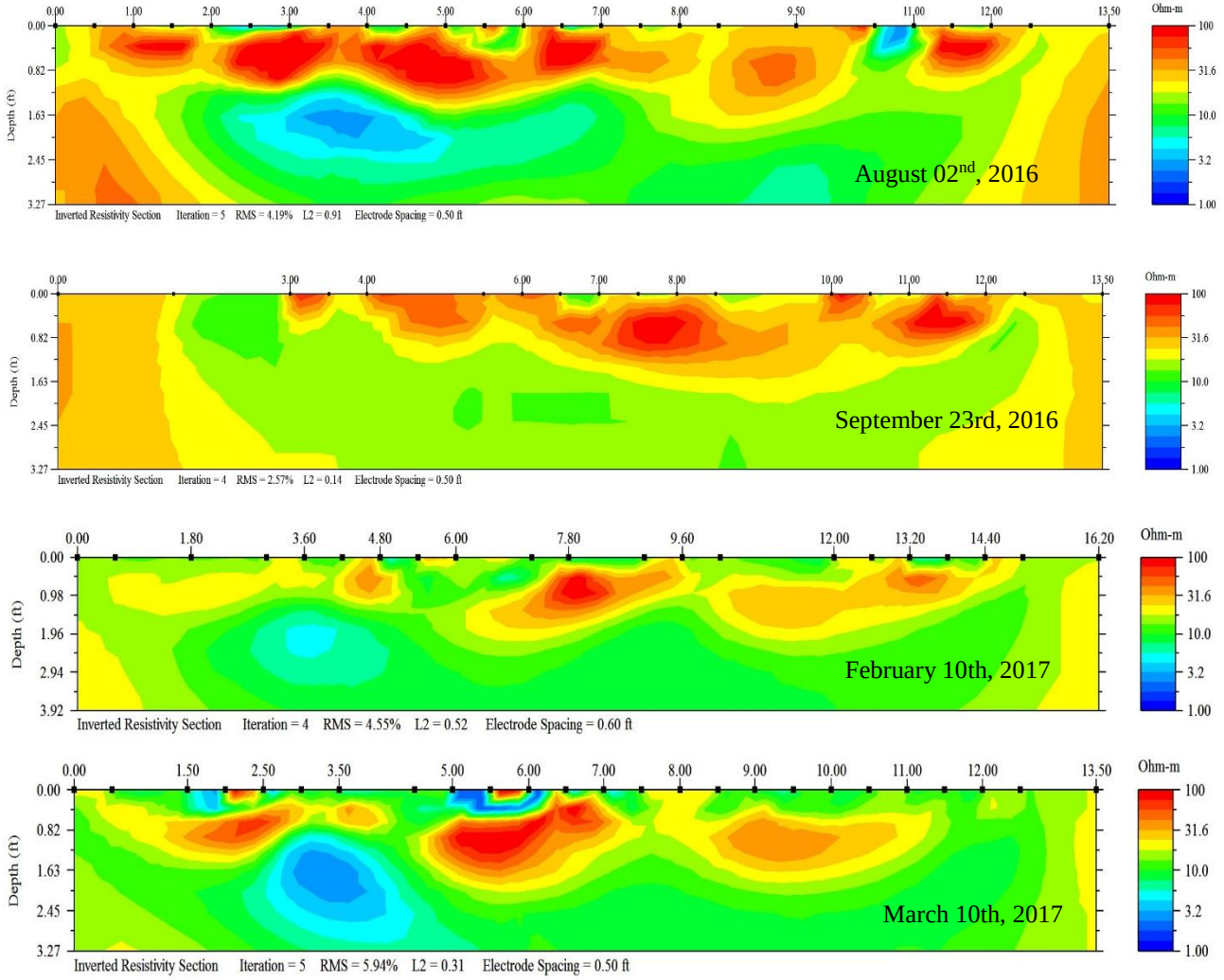
August 02nd, 2016
Inverted Resistivity Section Iteration = 5 RMS = 4.19% L2 = 0.91 Electrode Spacing = 0.50 ft
September 23rd, 2016
Inverted Resistivity Section Iteration = 4 RMS = 2.57% L2 = 0.14 Electrode Spacing = 0.50 ft
February 10th, 2017
Inverted Resistivity Section Iteration = 4 RMS = 4.55% L2 = 0.52 Electrode Spacing = 0.60 ft
March 10th, 2017
Inverted Resistivity Section Iteration = 5 RMS = 5.94% L2 = 0.31 Electrode Spacing = 0.50 ft
Depth (ft)
Ohm-m

RI Test Results on Switch grass (Lysimeter 2)

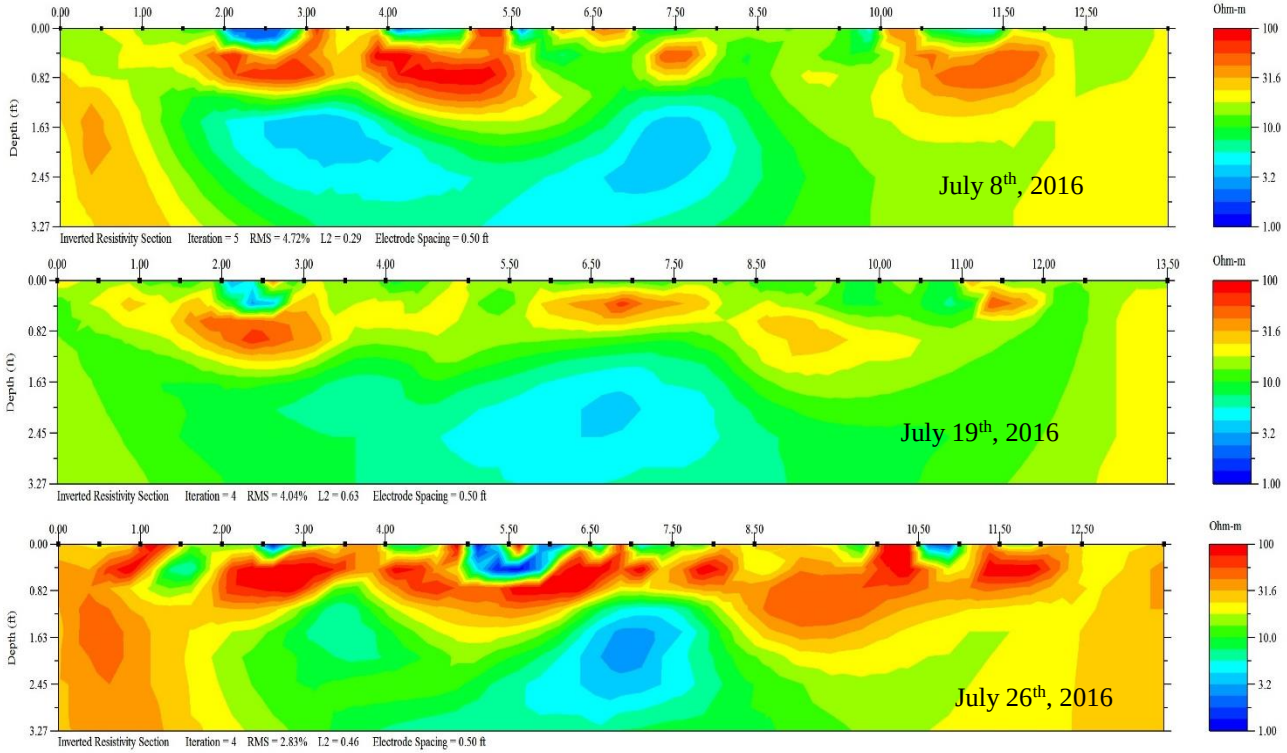

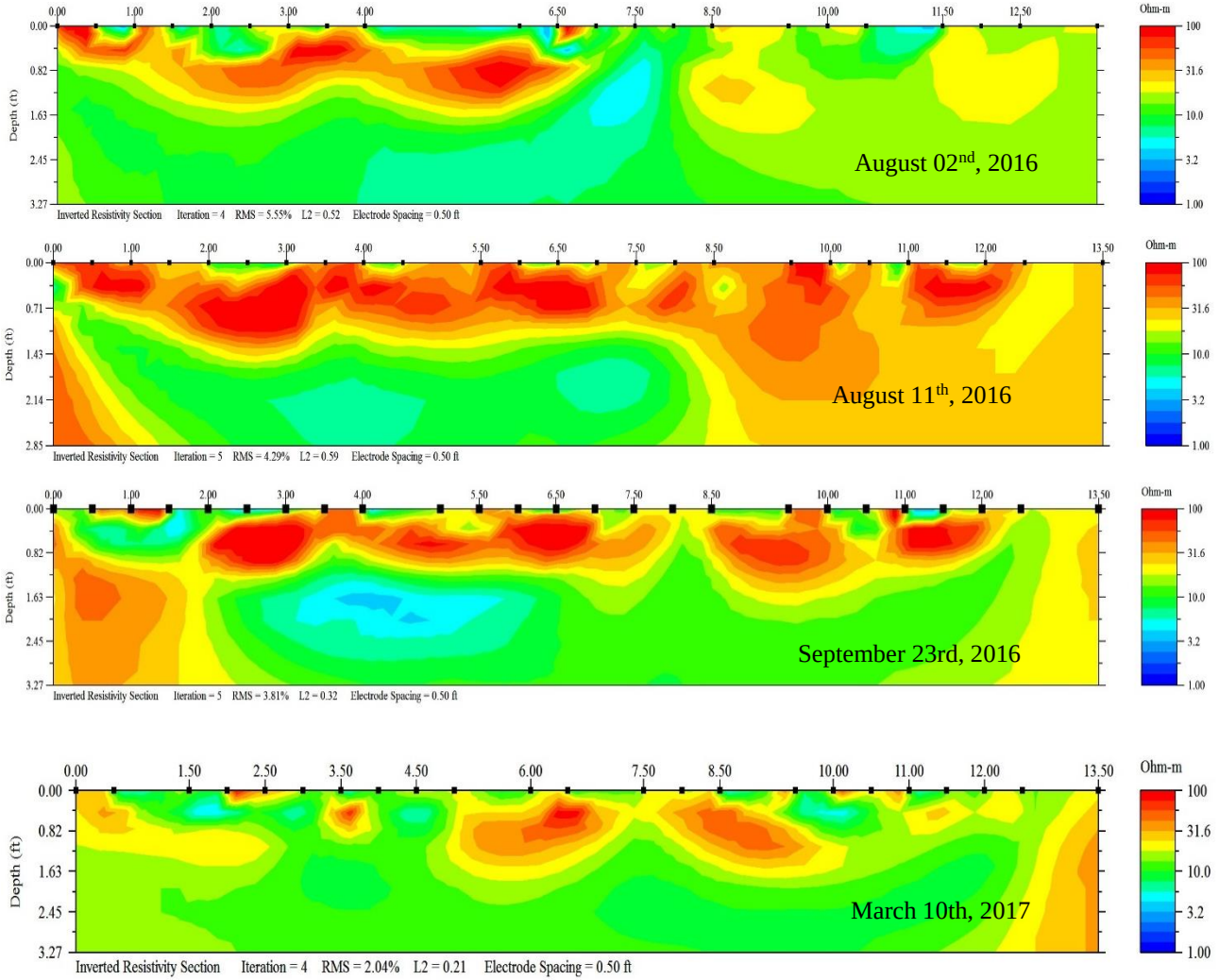
August 02nd, 2016
Inverted Resistivity Section Iteration = 4 RMS = 5.55% L2 = 0.52 Electrode Spacing = 0.50 ft
August 11th, 2016
Inverted Resistivity Section Iteration = 5 RMS = 4.29% L2 = 0.59 Electrode Spacing = 0.50 ft
September 23rd, 2016
Inverted Resistivity Section Iteration = 5 RMS = 3.81% L2 = 0.32 Electrode Spacing = 0.50 ft
March 10th, 2017
Inverted Resistivity Section Iteration = 4 RMS = 2.04% L2 = 0.21 Electrode Spacing = 0.50 ft
Depth (ft)
Ohm-m
100
31.6
10.0
3.2
1.00

RI Test Results on Bermuda Grass (Lysimeter 3)

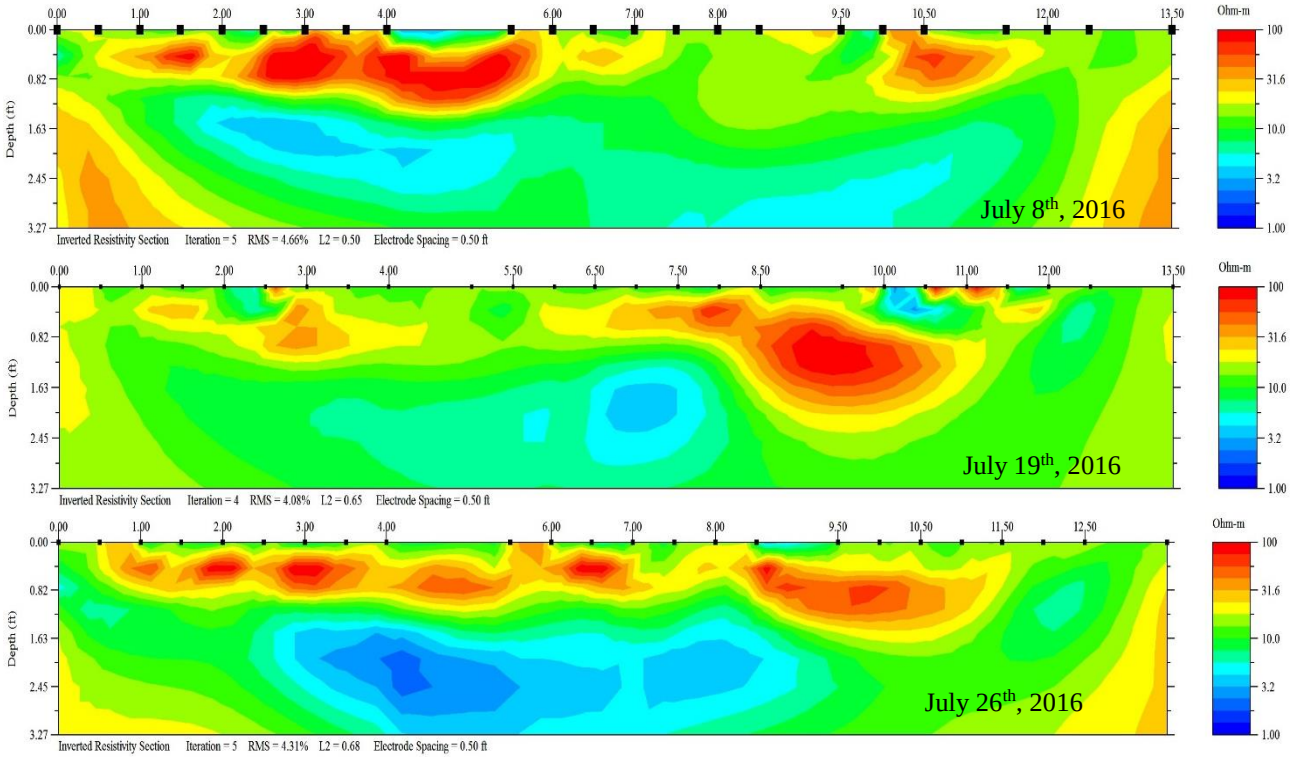

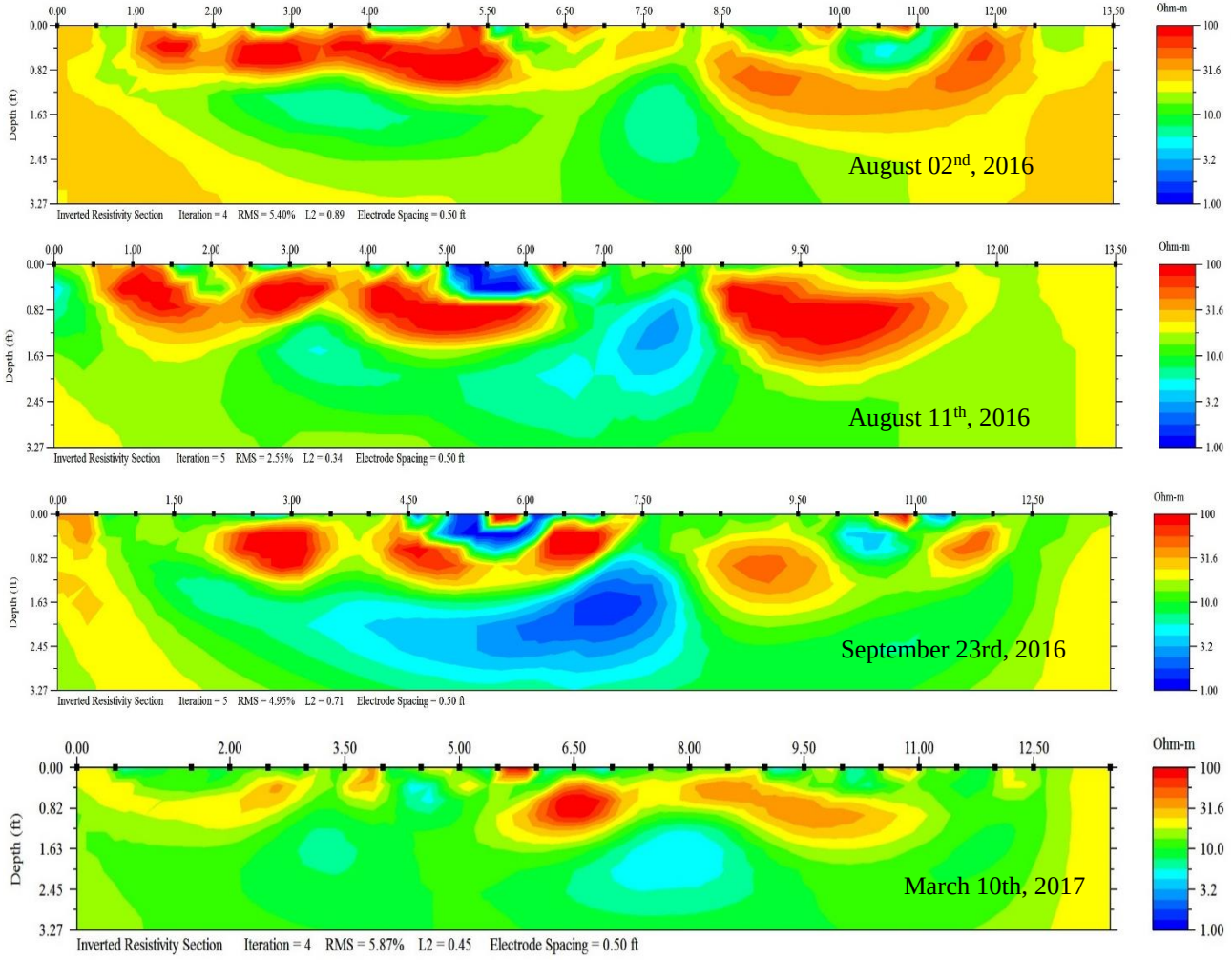
August 02nd, 2016
Inverted Resistivity Section Iteration = 4 RMS = 5.40% L2 = 0.89 Electrode Spacing = 0.50 ft
August 11th, 2016
Inverted Resistivity Section Iteration = 5 RMS = 2.55% L2 = 0.34 Electrode Spacing = 0.50 ft
September 23rd, 2016
Inverted Resistivity Section Iteration = 5 RMS = 4.95% L2 = 0.71 Electrode Spacing = 0.50 ft
March 10th, 2017
Inverted Resistivity Section Iteration = 4 RMS = 5.87% L2 = 0.45 Electrode Spacing = 0.50 ft
Depth (ft)
Ohm-m
100
31.6
10.0
3.2
1.00

APPENDIX B

OUTPUTS OF MINITAB ANALYSIS

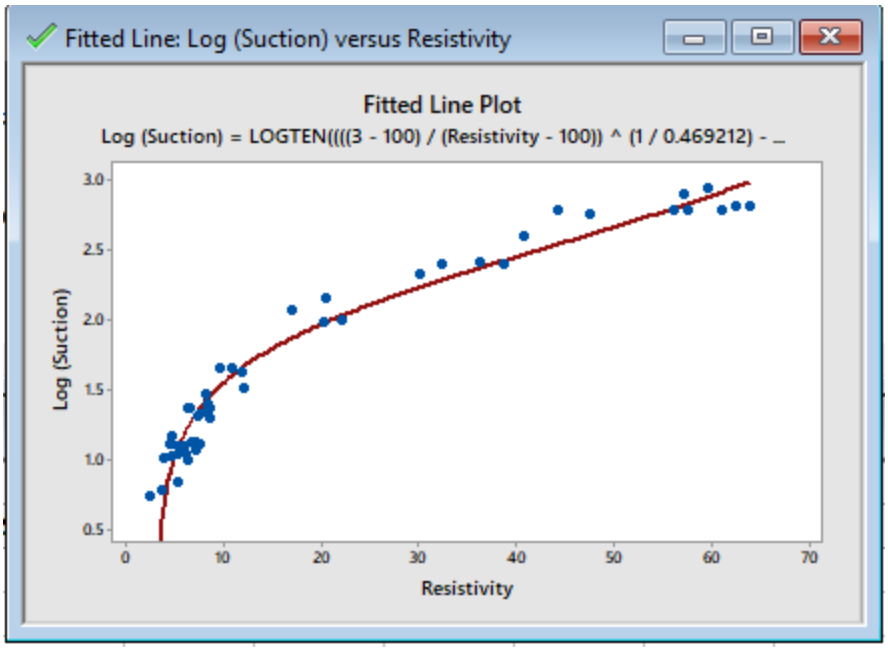

FRSCC for Bermuda grass at 30-inch depth

```
Starting Values for Parameters

Parameter   Value
Theta2          3*
Theta1        100*
Theta5        1.6
Theta4        0.8
Theta3     0.0018

* Locked.


Equation

Log (Suction) = LOGTEN((((3 - 100) / (Resistivity - 100)) ^ (1 / 0.469212) - 1) ^ (1 /
     1.13817) / 0.00589446)


Parameter Estimates

Parameter  Estimate  SE Estimate
Theta2        3.000            *
Theta1      100.000            *
Theta5        0.469     0.162804
Theta4        1.138     0.095254
Theta3        0.006     0.002908

Log (Suction) = LOGTEN((((Theta2 - Theta1) / (Resistivity - Theta1)) ^ (1 / Theta5) - 1) ^ (1
     / Theta4) / Theta3)
```

FRSCC parameters for Bermuda grass at 30-inch depth

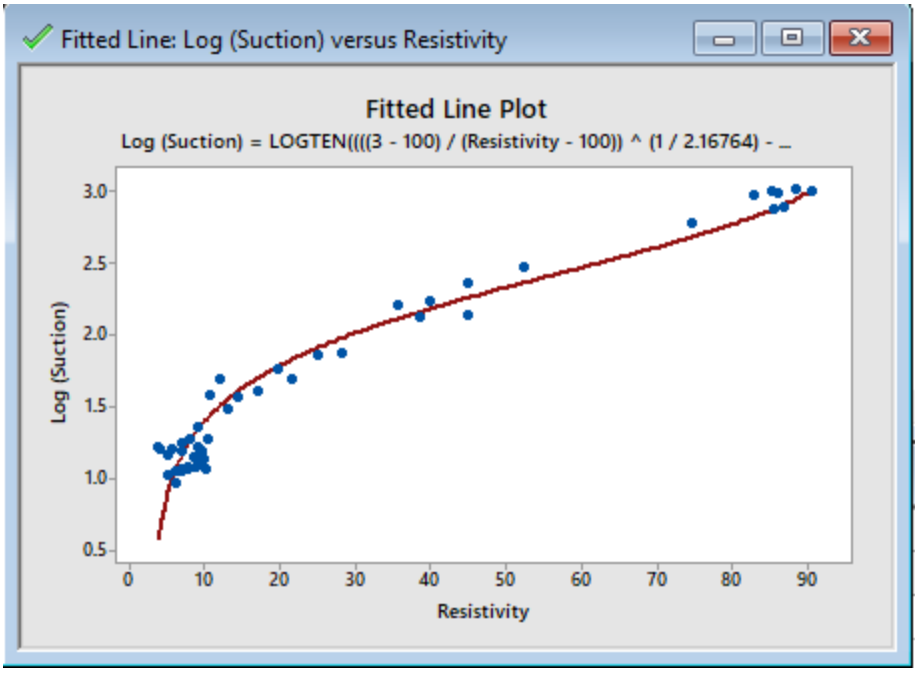

FRSCC for Bermuda grass at 12-inch depth

```
Starting Values for Parameters

Parameter   Value
Theta2          3*
Theta1        100*
Theta5        1.6
Theta4        0.8
Theta3     0.0018*

* Locked.


Equation

Log (Suction) = LOGTEN((((3 - 100) / (Resistivity - 100)) ^ (1 / 2.16764) - 1) ^ (1 / 1.0811)
     / 0.0018)


Parameter Estimates

Parameter  Estimate  SE Estimate
Theta2        3.000            *
Theta1      100.000            *
Theta5        2.168     0.207511
Theta4        1.081     0.037610
Theta3        0.002            *

Log (Suction) = LOGTEN((((Theta2 - Theta1) / (Resistivity - Theta1)) ^ (1 / Theta5) - 1) ^ (1
     / Theta4) / Theta3)
```

FRSCC parameters for Bermuda grass at 12-inch depth

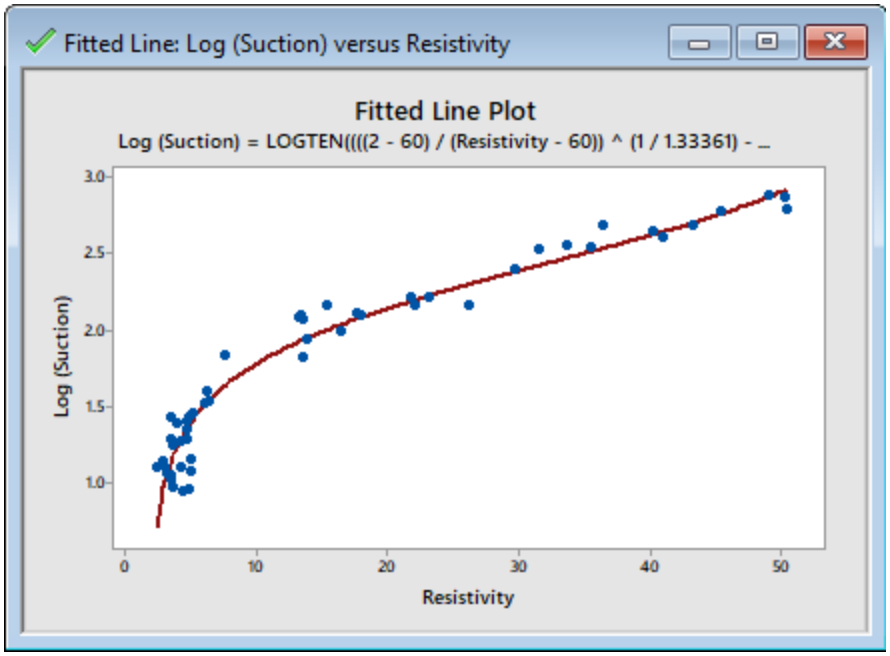

FRSCC for Native Trail grass at 30-inch depth

```
Starting Values for Parameters

Parameter  Value
Theta2         2*
Theta1        60*
Theta5       0.4
Theta4     1.033
Theta3     0.006

* Locked.


Equation

Log (Suction) = LOGTEN((((2 - 60) / (Resistivity - 60)) ^ (1 / 1.33361) - 1) ^ (1 / 1.21267)
     / 0.00283319)


Parameter Estimates

Parameter  Estimate  SE Estimate
Theta2       2.0000            *
Theta1      60.0000            *
Theta5       1.3336     0.817783
Theta4       1.2127     0.097246
Theta3       0.0028     0.002021

Log (Suction) = LOGTEN((((Theta2 - Theta1) / (Resistivity - Theta1)) ^ (1 / Theta5) - 1) ^ (1
     / Theta4) / Theta3)
```

FRSCC parameters for Native Trail grass at 30-inch depth

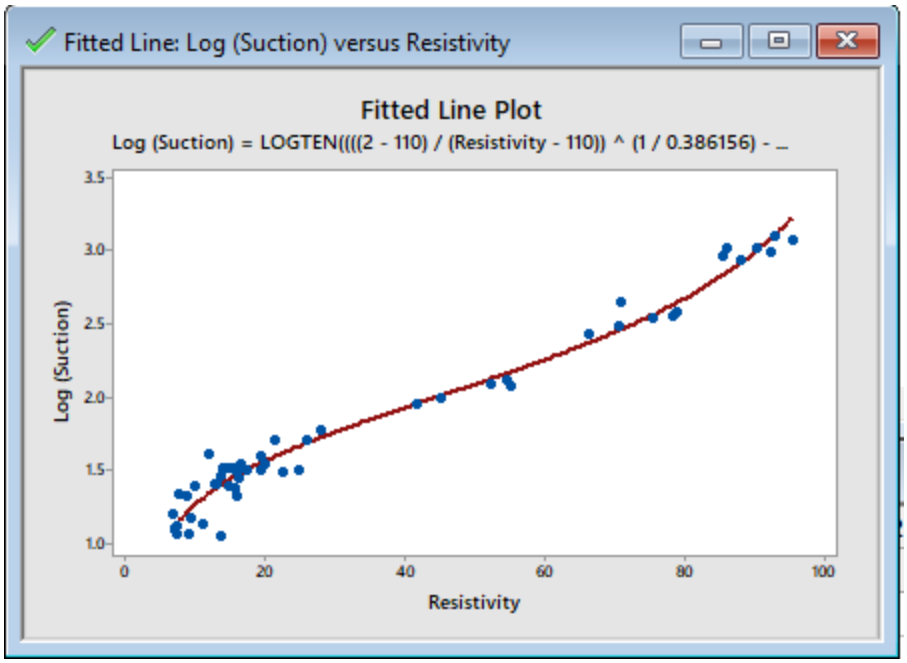

FRSCC for Native Trail grass at 12-inch depth

```
Starting Values for Parameters

Parameter  Value
Theta2         2*
Theta1       110*
Theta5       0.4
Theta4     1.033
Theta3     0.006

* Locked.


Equation

Log (Suction) = LOGTEN((((2 - 110) / (Resistivity - 110)) ^ (1 / 0.386156) - 1) ^ (1 /
     1.47908) / 0.0192713)


Parameter Estimates

Parameter  Estimate  SE Estimate
Theta2        2.000            *
Theta1      110.000            *
Theta5        0.386     0.070056
Theta4        1.479     0.149592
Theta3        0.019     0.004137

Log (Suction) = LOGTEN((((Theta2 - Theta1) / (Resistivity - Theta1)) ^ (1 / Theta5) - 1) ^ (1
     / Theta4) / Theta3)
```

FRSCC parameters for Native Trail grass at 12-inch depth

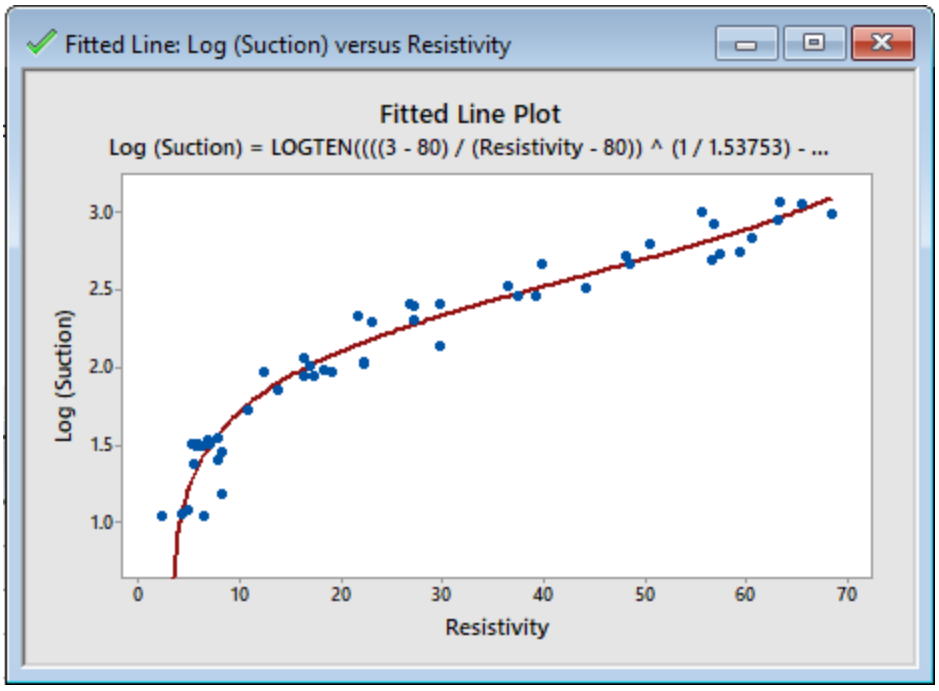

FRSCC for Switchgrass at 30-inch depth

```
Starting Values for Parameters

Parameter  Value
Theta2         3*
Theta1        80*
Theta5       0.4
Theta4       1.4
Theta3     0.029

* Locked.


Equation

Log (Suction) = LOGTEN((((3 - 80) / (Resistivity - 80)) ^ (1 / 1.53753) - 1) ^ (1 / 1.14519)
     / 0.00170932)


Parameter Estimates

Parameter  Estimate  SE Estimate
Theta2       3.0000            *
Theta1      80.0000            *
Theta5       1.5375     0.884939
Theta4       1.1452     0.085277
Theta3       0.0017     0.001187

Log (Suction) = LOGTEN((((Theta2 - Theta1) / (Resistivity - Theta1)) ^ (1 / Theta5) - 1) ^ (1
     / Theta4) / Theta3)
```

FRSCC parameters for Switchgrass at 30-inch depth

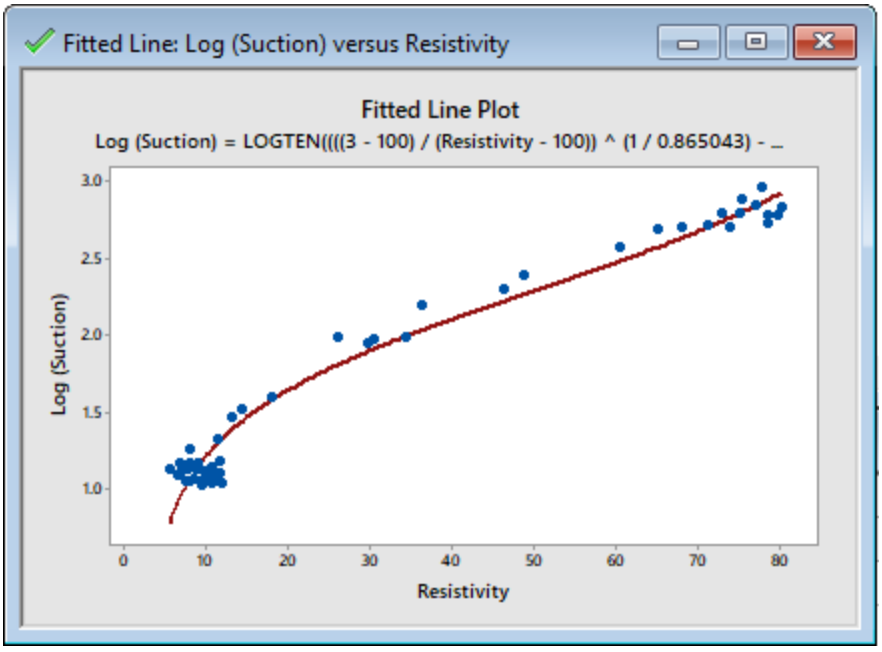

FRSCC for Switchgrass at 12-inch depth

```
Starting Values for Parameters

Parameter  Value
Theta2         3*
Theta1       100*
Theta5       0.4
Theta4     1.033*
Theta3     0.006

* Locked.


Equation

Log (Suction) = LOGTEN((((3 - 100) / (Resistivity - 100)) ^ (1 / 0.865043) - 1) ^ (1 / 1.033)
     / 0.00590791)


Parameter Estimates

Parameter  Estimate  SE Estimate
Theta2        3.000            *
Theta1      100.000            *
Theta5        0.865    0.0957714
Theta4        1.033            *
Theta3        0.006    0.0008718

Log (Suction) = LOGTEN((((Theta2 - Theta1) / (Resistivity - Theta1)) ^ (1 / Theta5) - 1) ^ (1
     / Theta4) / Theta3)
```

FRSCC parameters for Switchgrass at 12-inch depth

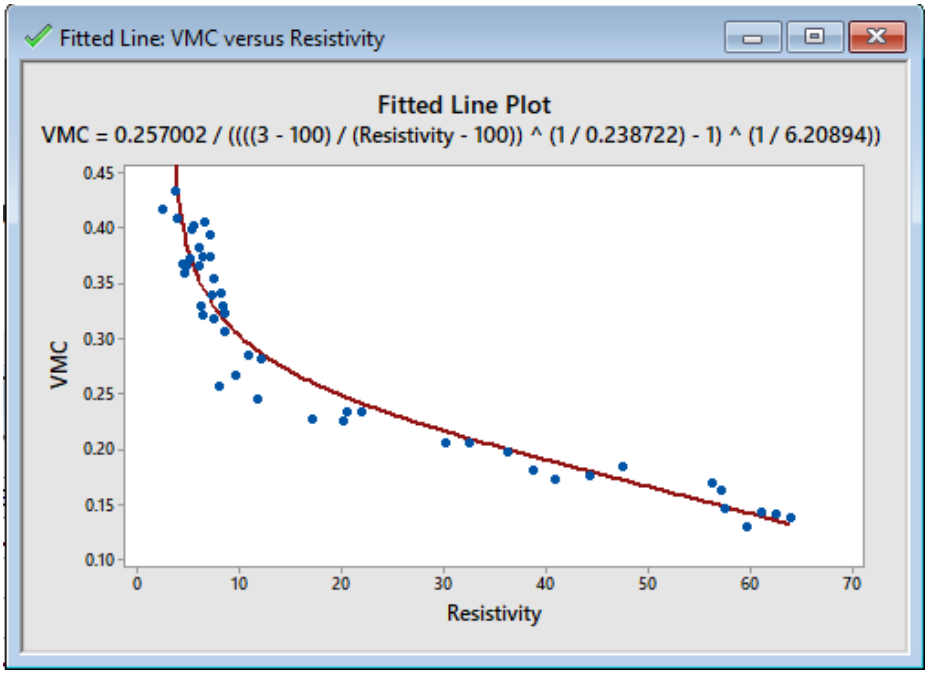

FRWCC for Bermuda grass at 30-inch depth

```
Starting Values for Parameters

Parameter  Value
Theta3      0.27
Theta2         3*
Theta1       100*
Theta5       0.3
Theta4       6.5

* Locked.


Equation

VMC = 0.257002 / ((((3 - 100) / (Resistivity - 100)) ^ (1 / 0.238722) - 1) ^ (1 / 6.20894))


Parameter Estimates

Parameter  Estimate  SE Estimate
Theta3        0.257     0.025186
Theta2        3.000             *
Theta1      100.000             *
Theta5        0.239     0.082347
Theta4        6.209     0.769419

VMC = Theta3 / ((((Theta2 - Theta1) / (Resistivity - Theta1)) ^ (1 / Theta5) - 1) ^ (1 /
     Theta4))
```

FRWCC parameters for Bermuda grass at 30-inch depth

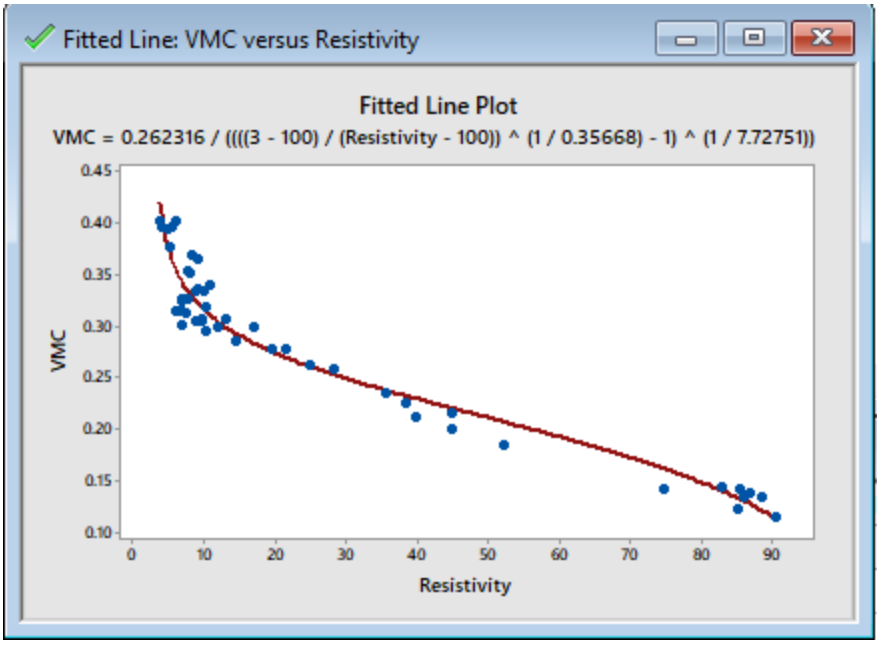

FRWCC for Bermuda grass at 12-inch depth

```
Starting Values for Parameters

Parameter  Value
Theta3      0.27
Theta2         3*
Theta1       100*
Theta5       0.3
Theta4       6.5

* Locked.


Equation

VMC = 0.262316 / ((((3 - 100) / (Resistivity - 100)) ^ (1 / 0.35668) - 1) ^ (1 / 7.72751))


Parameter Estimates

Parameter  Estimate  SE Estimate
Theta3        0.262     0.013630
Theta2        3.000             *
Theta1      100.000             *
Theta5        0.357     0.074207
Theta4        7.728     0.750385

VMC = Theta3 / ((((Theta2 - Theta1) / (Resistivity - Theta1)) ^ (1 / Theta5) - 1) ^ (1 /
     Theta4))
```

FRWCC parameters for Bermuda grass at 12-inch depth

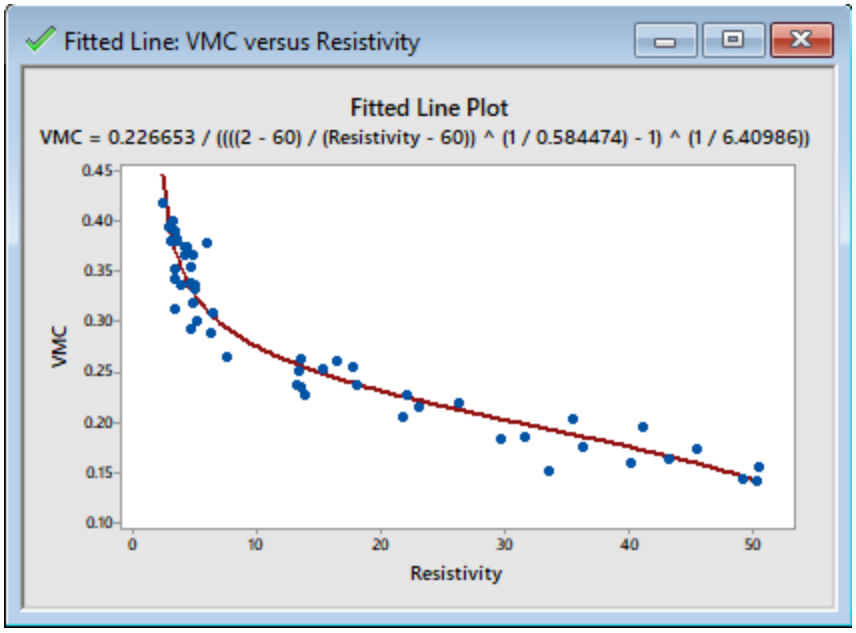

FRWCC for Native Trail grass at 30-inch depth

```
Starting Values for Parameters

Parameter  Value
Theta3      0.27
Theta2         2*
Theta1        60*
Theta5       0.3
Theta4     6.612

* Locked.


Equation

VMC = 0.226653 / ((((2 - 60) / (Resistivity - 60)) ^ (1 / 0.584474) - 1) ^ (1 / 6.40986))


Parameter Estimates

Parameter  Estimate  SE Estimate
Theta3       0.2267     0.022031
Theta2       2.0000             *
Theta1      60.0000             *
Theta5       0.5845     0.226041
Theta4       6.4099     0.576592

VMC = Theta3 / ((((Theta2 - Theta1) / (Resistivity - Theta1)) ^ (1 / Theta5) - 1) ^ (1 /
     Theta4))
```

FRWCC parameters for Native Trail grass at 30-inch depth

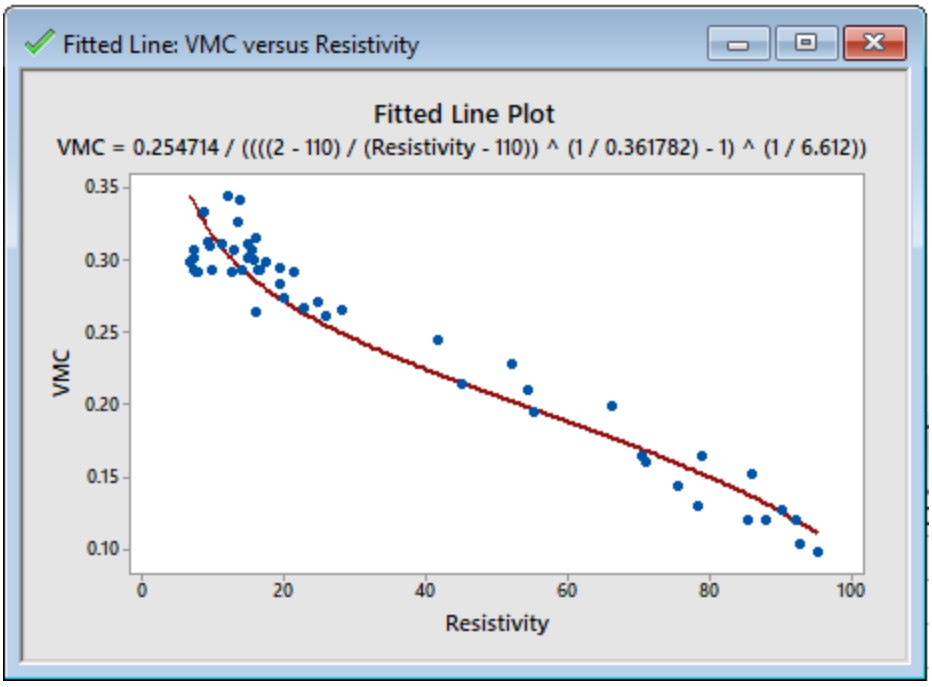

FRWCC for Native Trail grass at 12-inch depth

```
Starting Values for Parameters

Parameter  Value
Theta3      0.27
Theta2        2*
Theta1      110*
Theta5      0.3
Theta4    6.612*

* Locked.


Equation

VMC = 0.254714 / ((((2 - 110) / (Resistivity - 110)) ^ (1 / 0.361782) - 1) ^ (1 / 6.612))


Parameter Estimates

Parameter  Estimate  SE Estimate
Theta3        0.255    0.0065145
Theta2        2.000             *
Theta1      110.000             *
Theta5        0.362    0.0380473
Theta4        6.612             *

VMC = Theta3 / ((((Theta2 - Theta1) / (Resistivity - Theta1)) ^ (1 / Theta5) - 1) ^ (1 /
     Theta4))
```

FRWCC parameters for Native Trail grass at 12-inch depth

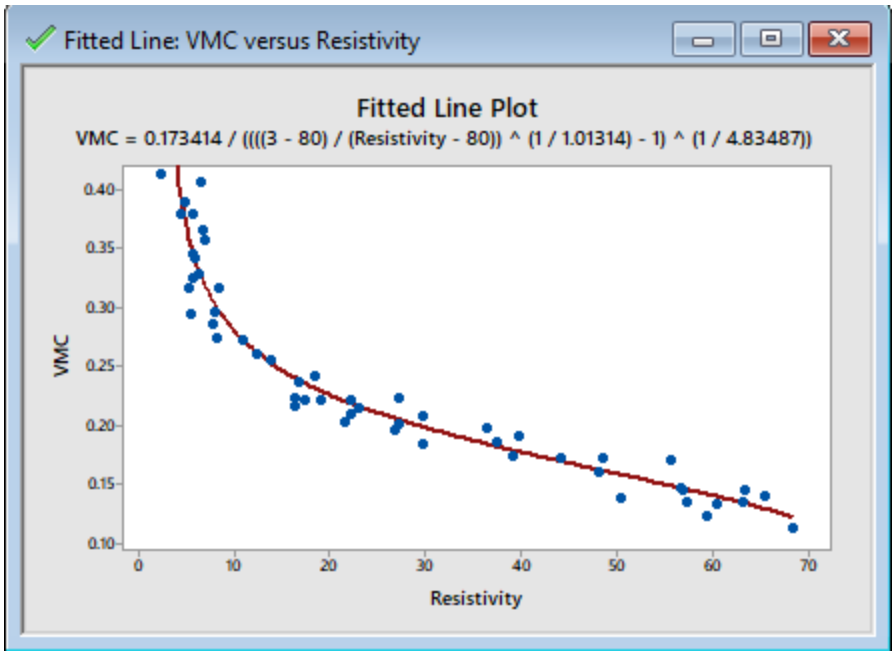

FRWCC for Switchgrass at 30-inch depth

```
Starting Values for Parameters

Parameter  Value
Theta3      0.27
Theta2         3*
Theta1        80*
Theta5       0.3
Theta4       6.5

* Locked.


Equation

VMC = 0.173414 / ((((3 - 80) / (Resistivity - 80)) ^ (1 / 1.01314) - 1) ^ (1 / 4.83487))


Parameter Estimates

Parameter  Estimate  SE Estimate
Theta3       0.1734     0.028557
Theta2       3.0000             *
Theta1      80.0000             *
Theta5       1.0131     0.564078
Theta4       4.8349     0.407313

VMC = Theta3 / ((((Theta2 - Theta1) / (Resistivity - Theta1)) ^ (1 / Theta5) - 1) ^ (1 /
     Theta4))
```

FRWCC parameters for Switchgrass at 30-inch depth

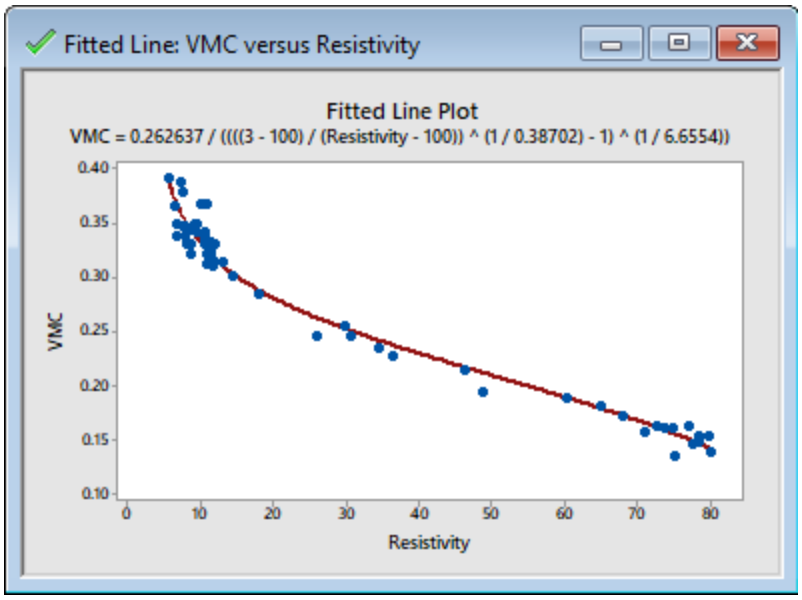

FRWCC for Switchgrass at 12-inch depth

```
Starting Values for Parameters

Parameter  Value
Theta3      0.27
Theta2         3*
Theta1       100*
Theta5       0.3
Theta4       6.5

* Locked.


Equation

VMC = 0.262637 / ((((3 - 100) / (Resistivity - 100)) ^ (1 / 0.38702) - 1) ^ (1 / 6.6554))


Parameter Estimates

Parameter  Estimate  SE Estimate
Theta3        0.263     0.015284
Theta2        3.000             *
Theta1      100.000             *
Theta5        0.387     0.082922
Theta4        6.655     0.631005

VMC = Theta3 / ((((Theta2 - Theta1) / (Resistivity - Theta1)) ^ (1 / Theta5) - 1) ^ (1 /
     Theta4))
```

FRWCC parameters for Switchgrass at 12-inch depth

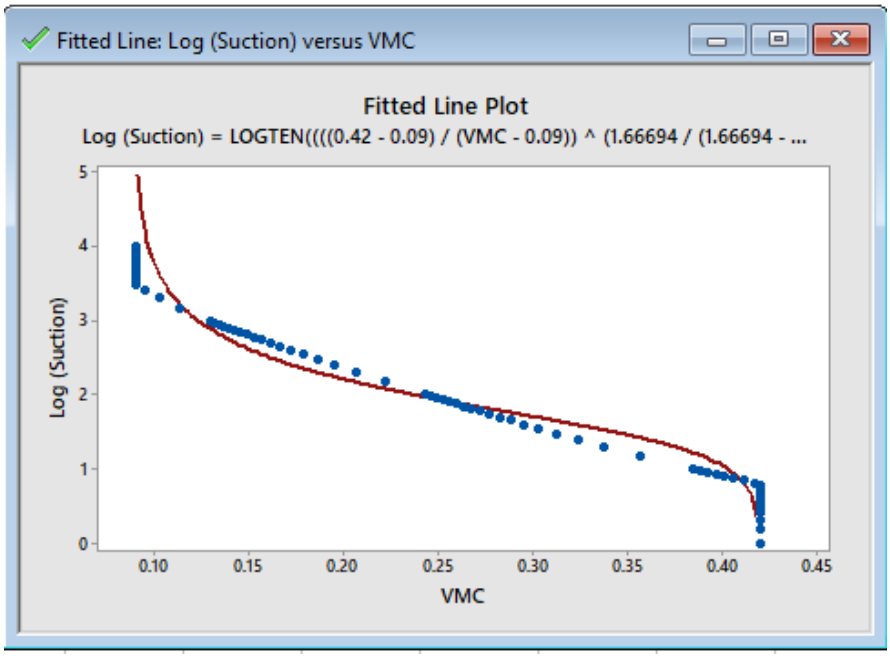

SWCC for Bermuda grass at 30-inch depth

```
Starting Values for Parameters

Parameter  Value
Theta2      0.42*
Thetal      0.09*
Theta4       1.9
Theta3      0.06

* Locked.


Equation

Log (Suction) = LOGTEN((((0.42 - 0.09) / (VMC - 0.09)) ^ (1.66694 / (1.66694 - 1)) - 1) ^ (1
     / 1.66694) / 0.0312434)


Parameter Estimates

Parameter  Estimate  SE Estimate
Theta2      0.42000            *
Thetal      0.09000            *
Theta4      1.66694    0.0320699
Theta3      0.03124    0.0031183

Log (Suction) = LOGTEN((((Theta2 - Thetal) / (VMC - Thetal)) ^ (Theta4 / (Theta4 - 1)) - 1) ^
     (1 / Theta4) / Theta3)
```

Estimated Statistical Parameters for Bermuda grass at 30-inch depth

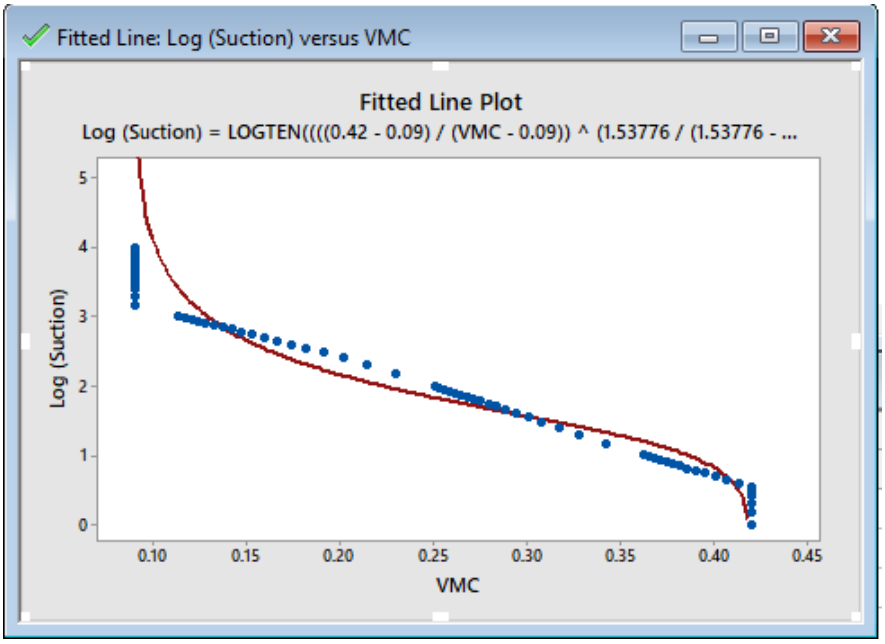

SWCC for Bermuda grass at 12-inch depth

```
Starting Values for Parameters

Parameter  Value
Theta2      0.42*
Theta1      0.09*
Theta4       1.9
Theta3      0.06

* Locked.


Equation

Log (Suction) = LOGTEN((((0.42 - 0.09) / (VMC - 0.09)) ^ (1.53776 / (1.53776 - 1)) - 1) ^ (1
     / 1.53776) / 0.0526127)


Parameter Estimates

Parameter  Estimate  SE Estimate
Theta2      0.42000            *
Theta1      0.09000            *
Theta4      1.53776    0.0223514
Theta3      0.05261    0.0047162

Log (Suction) = LOGTEN((((Theta2 - Theta1) / (VMC - Theta1)) ^ (Theta4 / (Theta4 - 1)) - 1) ^
     (1 / Theta4) / Theta3)
```

Estimated Statistical Parameters for Bermuda grass at 12-inch depth

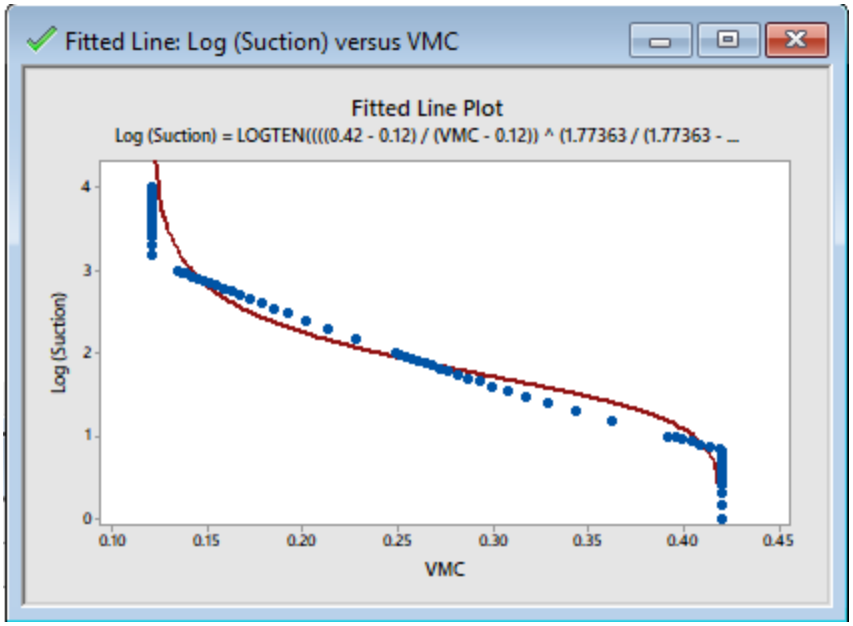

SWCC for Native trail grass at 30-inch depth

```
Starting Values for Parameters

Parameter  Value
Theta2      0.42*
Theta1      0.12*
Theta4       1.9
Theta3      0.06

* Locked.


Equation

Log (Suction) = LOGTEN((((0.42 - 0.12) / (VMC - 0.12)) ^ (1.77363 / (1.77363 - 1)) - 1) ^ (1
     / 1.77363) / 0.0307966)


Parameter Estimates

Parameter  Estimate  SE Estimate
Theta2      0.42000            *
Theta1      0.12000            *
Theta4      1.77363    0.0341433
Theta3      0.03080    0.0025510

Log (Suction) = LOGTEN((((Theta2 - Theta1) / (VMC - Theta1)) ^ (Theta4 / (Theta4 - 1)) - 1) ^
     (1 / Theta4) / Theta3)
```

Estimated Statistical Parameters for Native Trail grass at 30-inch depth

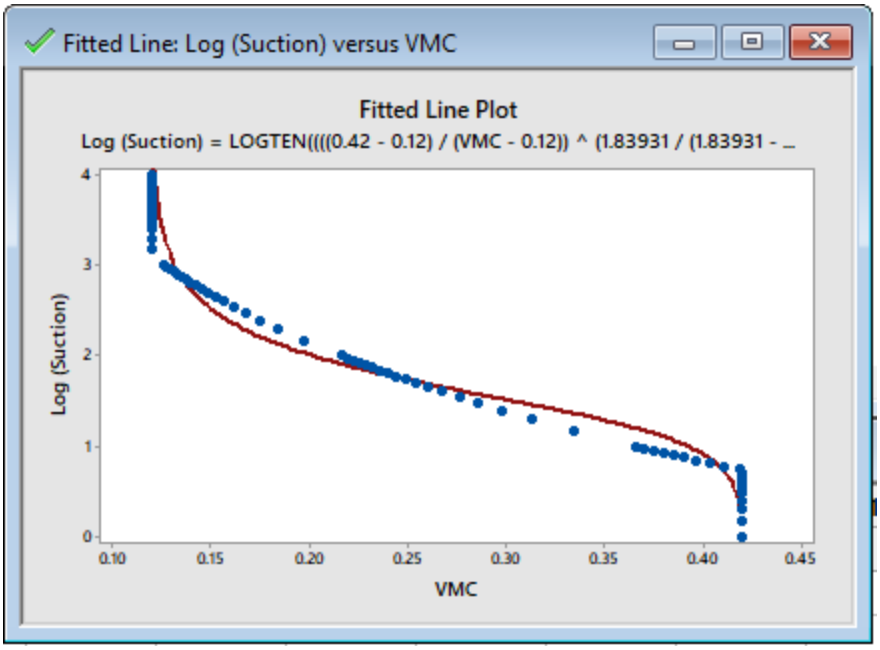

SWCC for Native trail grass at 12-inch depth

```
Starting Values for Parameters

Parameter  Value
Theta2      0.42*
Theta1      0.12*
Theta4       1.9
Theta3      0.06

* Locked.


Equation

Log (Suction) = LOGTEN((((0.42 - 0.12) / (VMC - 0.12)) ^ (1.83931 / (1.83931 - 1)) - 1) ^ (1
     / 1.83931) / 0.045926)


Parameter Estimates

Parameter  Estimate  SE Estimate
Theta2      0.42000            *
Theta1      0.12000            *
Theta4      1.83931    0.0319423
Theta3      0.04593    0.0036676

Log (Suction) = LOGTEN((((Theta2 - Theta1) / (VMC - Theta1)) ^ (Theta4 / (Theta4 - 1)) - 1) ^
     (1 / Theta4) / Theta3)
```

Estimated Statistical Parameters for Native Trail grass at 12-inch depth

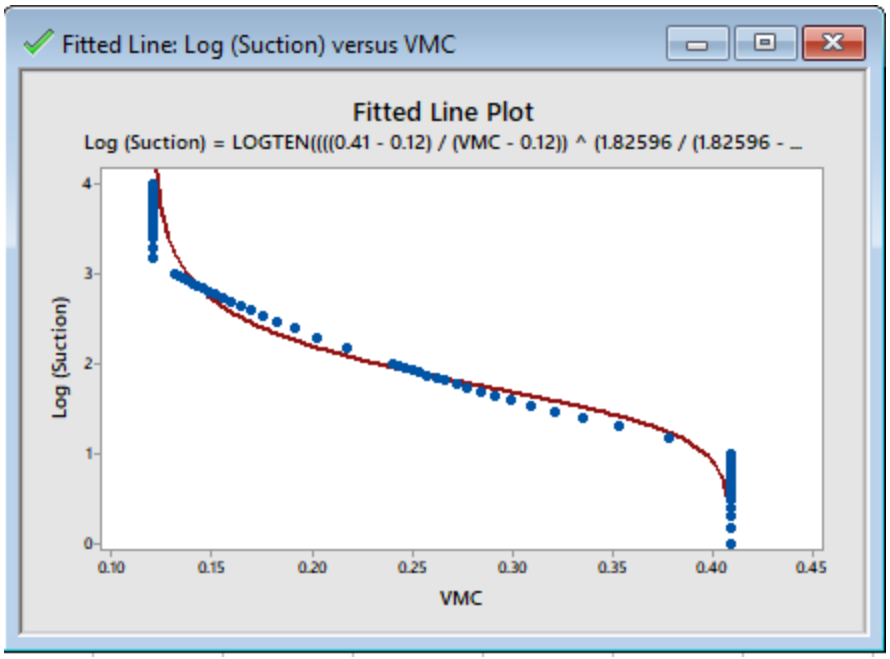

SWCC for Switchgrass grass at 30-inch depth

```
Starting Values for Parameters

Parameter  Value
Theta2      0.41*
Theta1      0.12*
Theta4       1.9
Theta3      0.06

* Locked.


Equation

Log (Suction) = LOGTEN((((0.41 - 0.12) / (VMC - 0.12)) ^ (1.82596 / (1.82596 - 1)) - 1) ^ (1
     / 1.82596) / 0.0293608)


Parameter Estimates

Parameter  Estimate  SE Estimate
Theta2      0.41000            *
Theta1      0.12000            *
Theta4      1.82596    0.0291540
Theta3      0.02936    0.0020983

Log (Suction) = LOGTEN((((Theta2 - Theta1) / (VMC - Theta1)) ^ (Theta4 / (Theta4 - 1)) - 1) ^
     (1 / Theta4) / Theta3)
```

Estimated Statistical Parameters for Switchgrass grass at 30-inch depth

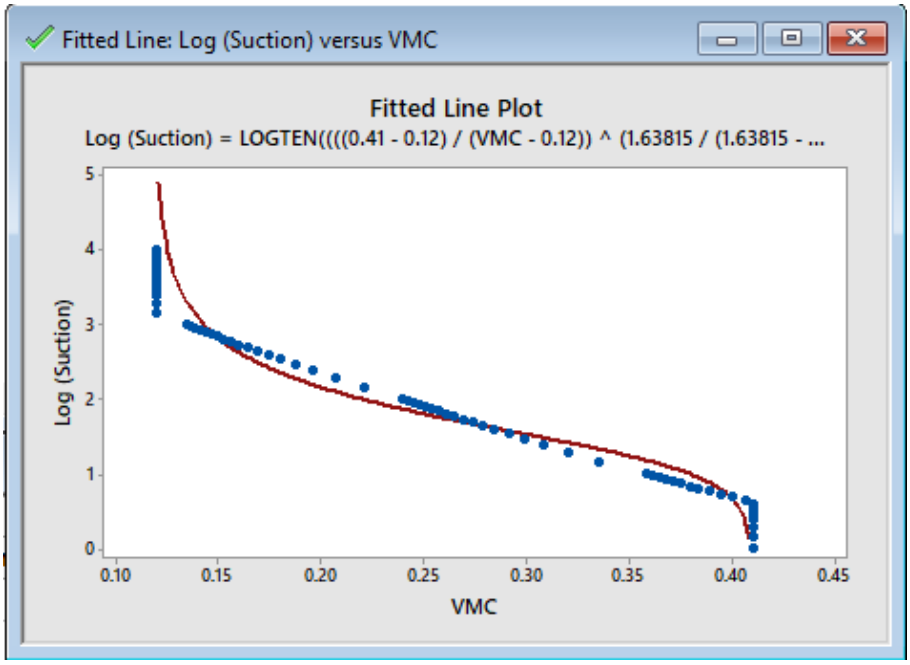

SWCC for Switchgrass grass at 12-inch depth

```
Starting Values for Parameters

Parameter  Value
Theta2      0.41*
Theta1      0.12*
Theta4       1.9
Theta3      0.06

* Locked.


Equation

Log (Suction) = LOGTEN((((0.41 - 0.12) / (VMC - 0.12)) ^ (1.63815 / (1.63815 - 1)) - 1) ^ (1
     / 1.63815) / 0.0508067)


Parameter Estimates

Parameter  Estimate  SE Estimate
Theta2      0.41000            *
Theta1      0.12000            *
Theta4      1.63815    0.0227783
Theta3      0.05081    0.0038921

Log (Suction) = LOGTEN((((Theta2 - Theta1) / (VMC - Theta1)) ^ (Theta4 / (Theta4 - 1)) - 1) ^
     (1 / Theta4) / Theta3)
```

Estimated Statistical Parameters for Switchgrass grass at 12-inch depth

References

Abu-Hassanein, Z. S., Benson, C. H., & Blotz, L. R. (1996). Electrical resistivity of compacted clays. Journal of geotechnical engineering, 122(5), 397-406.

Alam, M. J. B. (2017). Evaluation of Plant Root on the Performance of Evapotranspiration (ET) Cover System (Doctoral dissertation).

Alam, M. Z. (2016). Moisture Distribution Efficiency and Performance Evaluations of Bioreactor Landfill Operations (Doctoral dissertation).

Alam, M.J., Sarker, L., and Hossain, M.S. (2018). "Estimation of Field Scale Unsaturated Soil Behavior of Landfill Cover through Geophysical Testing and Instrumentation." Geocongress 2019. March 24-27, Philadelphia, Pennsylvania. (Under Review)

Albrecht, B. A., Benson, C. H., & Beuermann, S. (2003). Polymer capacitance sensors for measuring soil gas humidity in drier soils. Geotechnical Testing Journal, 26(1), 3-11.

Albright, W. H., Benson, C. H., Gee, G. W., Roesler, A. C., Abichou, T., Apiwantragoon, P., ... & Rock, S. A. (2004). Field water balance of landfill final covers. Journal of Environmental Quality, 33(6), 2317-2332.

Albright, W. H., Benson, C. H., & Waugh, W. J. (2010, August). Water balance covers for waste containment: principles and practice. American Society of Civil Engineers.

Assouline, S., & Or, D. (2014). The concept of field capacity revisited: Defining intrinsic static and dynamic criteria for soil internal drainage dynamics. Water Resources Research, 50(6), 4787-4802.

Bai, W., Kong, L., & Guo, A. (2013). Effects of physical properties on electrical conductivity of compacted lateritic soil. Journal of Rock Mechanics and Geotechnical Engineering, 5(5), 406-411.

Benson, C. H., Bohnhoff, G. L., Ogorzalek, A. S., Shackelford, C. D., Apiwantragoon, P., & Albright, W. H. (2005). Field data and model predictions for a monolithic alternative cover. In Waste containment and remediation (pp. 1-16).

Campbell, R.B., Bower, C.A., Richard, L.A., 1948. Change in electrical conductivity with temperature and the relation with osmotic pressure to electrical conductivity and ion concentration for soil extracts. Soil Sci. Soc. Am. Proc. 13, 33–69

De Vita, P., Di Maio, R., & Piegari, E. (2012). A study of the correlation between electrical resistivity and matric suction for unsaturated ash-fall pyroclastic soils in the Campania region (southern Italy). Environmental Earth Sciences, 67(3), 787-798.

Fredlund, D. G., Rahardjo, H., & Rahardjo, H. (1993). Soil mechanics for unsaturated soils. John Wiley & Sons.

Fredlund, D. G., & Xing, A. (1994). Equations for the soil-water characteristic curve. Canadian geotechnical journal, 31(4), 521-532.

Fredlund, M. D., Fredlund, D. G., & Wilson, G. W. (1997, April). Prediction of the soil-water characteristic curve from grain-size distribution and volume-mass properties. In Proc., 3rd Brazilian Symp. on Unsaturated Soils (Vol. 1, pp. 13-23). Rio de Janeiro.

Fredlund, D. G. (2002, March). Use of soil-water characteristic curves in the implementation of unsaturated soil mechanics. In Proceedings of the 3rd International Conference on Unsaturated Soils, Recife, Brazil (Vol. 3, pp. 887-902).

Fredlund, D. G., & Houston, S. L. (2013). Interpretation of soil-water characteristic curves when volume change occurs as soil suction is changed. Advances in unsaturated soils, 1, 15.

Gupta, S., & Larson, W. E. (1979). Estimating soil water retention characteristics from particle size distribution, organic matter percent, and bulk density. Water resources research, 15(6), 1633-1635.

Hong-jing, J., Shun-qun, L., & Lin, L. The Relationship between the Electrical Resistivity and Saturation of Unsaturated Soil.

Khire, M. V., Benson, C. H., & Bosscher, P. J. (2000). Capillary barriers: Design variables and water balance. Journal of Geotechnical and Geoenvironmental Engineering, 126(8), 695-708.

Kibria, G. (2011). Determination of geotechnical properties of clayey soil from resistivity imaging (RI).

Lane, K. S., Washburn, D. E., & Krynine, D. P. (1947). Capillarity tests by capillarimeter and by soil filled tubes. In Highway research board proceedings (Vol. 26).

Leong, E. C., Tripathy, S., & Rahardjo, H. (2003). Total suction measurement of unsaturated soils with a device using the chilled-mirror dew-point technique. Geotechnique, 53(2), 173-182.

Leung, A. K., Kamchoom, V., & Ng, C. W. W. (2016). Influences of root-induced soil suction and root geometry on slope stability: a centrifuge study. Canadian Geotechnical Journal, 54(3), 291-303.

Ley-Cooper, A. Y., Munday, T., Gilfedder, M., Ibrahimi, T., Annetts, D., & Cahill, K. (2015). Inversion of legacy airborne electromagnetic datasets to inform the hydrogeological understanding of the northern Eyre Peninsula, South Australia. Goyder Institute for Water Research Technical Report Series, (15/50).

Li, A. G., Yue, Z. Q., Tham, L. G., Lee, C. F., & Law, K. T. (2005). Field-monitored variations of soil moisture and matric suction in a saprolite slope. Canadian Geotechnical Journal, 42(1), 13-26.

Likos, W. J., & Lu, N. (2003). Automated humidity system for measuring total suction characteristics of clay. Geotechnical Testing Journal, 26(2), 179-190.

Malik, R. S., Kumar, S., & Malik, R. K. (1989). Maximal capillary rise flux as a function of height from the water table. Soil science, 148(5), 322-326.

Miller, R. W., & Donahue, R. L. (1995). Soils in our environment. Prentice hall.

Ng, C. W. W., Zhan, L. T, and Cui, Y. J. (2002). A new simple system for measuring volume changes in unsaturated soils." Canadian geotechnical Journal, 39, 757-764.

Pan, H., Qing, Y., & Pei-yong, L. (2010). Direct and indirect measurement of soil suction in the laboratory. Electronic Journal of Geotechnical Engineering, 15(3), 1-14.

Perera, Y. Y., & Padilla, J. M. (2004). Measurement of soil suction in situ using the Fredlund thermal conductivity sensor. Presentation material for mining and waste management short course, Vail, CO Google Scholar.

Piegari, E., & Di Maio, R. (2013). Estimating soil suction from electrical resistivity. Natural Hazards and Earth System Sciences, 13(9), 2369.

Richards, L. A. (1942). Soil moisture tensiometer materials and construction. Soil Sci, 53(4), 241-248.

Samouëlian, A., Cousin, I., Tabbagh, A., Bruand, A., & Richard, G. (2005). Electrical resistivity survey in soil science: a review. Soil and Tillage research, 83(2), 173-193.

Shihada, H. (2011). A non-invasive assessment of moisture content of municipal solid waste in a landfill using resistivity imaging.

Sposito, G., 1981, The Thermodynamics of Soil Solutions, Oxford Clarendon Press, London.

Tan, E., Marjerison, B., and Fredlund, D.G. (2003). Measurements and analysis of temperature and soil suction below thin membrane surface (TMS) in Saskatchewan. Proceedings of the 56th Canadian Geotechnical Conference, Winnipeg, Manitoba, Volume 2, pp 107-114. Sept. 29-Oct. 1.

Tan, E., Fredlund, D. G., & Gitirana Jr, G. F. N. (2004). Comparison of correction method for factors influencing thermal conductivity suction sensors. In Proceedings of the 5th Brazilian Symposium on Unsaturated Soils (pp. 127-132).

Tinjum, J. M., Benson, C. H., & Blotz, L. R. (1997). Soil-water characteristic curves for compacted clays. Journal of geotechnical and geoenvironmental engineering, 123(11), 1060-1069.

Van Genuchten, M. V., Leij, F. J., & Yates, S. R. (1991). The RETC code for quantifying the hydraulic functions of unsaturated soils.

Zhou, Q. Y., Shimada, J., & Sato, A. (2001). Three-dimensional spatial and temporal monitoring of soil water content using electrical resistivity tomography. Water Resources Research, 37(2), 273-285.

Zornberg, J. G., LaFountain, L., & Caldwell, J. A. (2003). Analysis and design of evapotranspirative cover for hazardous waste landfill. Journal of Geotechnical and Geoenvironmental Engineering, 129(5), 427-438.

Biographical Information

Linkan Sarker graduated with a Bachelor of Science in Civil Engineering from Bangladesh University of Engineering and Technology, Dhaka, Bangladesh in March 2016. After graduation, he started his career as an Assistant Engineer in Bangladesh Water Development Board in October 2016 and worked on "Haor Flood Management and Livelihood Improvement Project (HFM&LIP) – BD-P80". Linkan Sarker joined the University of Texas at Arlington in Fall 2017 for graduate studies. During his graduation period, he got the opportunity to work under Dr. Hossain as a graduate research assistant. The author's research interests include soil water storage properties of ET cover soil, sustainable waste management systems, deep and shallow foundation systems, numerical modeling, non-destructive testing and geophysical investigation.